PARALLEL SEPARATIONS ON MICROFLUIDIC CHIPS FOR HIGH
THROUGHPUT MONITORING OF INSULIN SECRETION FROM
SINGLE ISLETS OF LANGERHANS

by

John F. Dishinger

A dissertation submitted in partial fulfillment
of the requirements for the degree of
Doctor of Philosophy
(Chemistry)
in The University of Michigan
2008

Doctoral Committee:

      Professor Robert T. Kennedy, Chair
      Professor Mark E. Meyerhoff
      Professor Michael D. Morris
      Professor Edward L. Stuenkel

To Friends and Family

ACKNOWLEDGEMENTS

TABLE OF CONTENTS

LIST OF FIGURES

LIST OF ABBREVIATIONS

Ab	Antibody
AOD	Acousto-optical deflection
B/F	Bound-to-free ratio
β-GAL	β-galactosidase
BSA	Bovine serum albumen
BSS	Balanced salt solution
CAE	Capillary array electrophoresis
CCD	Charge-coupled device
CE	Capillary electrophoresis
CEC	Capillary electrochromatography
CZE	Capillary zone electrophoresis
DNA	Deoxyribonucleic acid
EDTA	Ethylenediaminetetraacetic acid
ELISA	Enzyme-linked immuno-sorbent assay
EOF	Electroosmotic flow
FFA	Free fatty acid
FITC	Fluorescein isothiocyanate
FMG	Fluorescein mono-β-D-galactopyranoside
GLP-1	Glucagon-like peptide-1

HFD	High fat diet
Hz	Hertz
kHz	Kilohertz
kV	Kilovolt(s)
LIF	Laser-induced fluorescence
LOD	Limit of detection
mM	Millimolar
μg	Microgram
μL	Microliter
μM	Micromolar
NA	Numerical aperture
NBD	4-chloro-7-ni-trobenz-2-oxa-1,3-diazole
nM	Nanomolar
OPA	o-phthaldialdehyde
PCR	Polymerase chain reaction
PDMS	Poly(dimethylsiloxane)
PETG	Phenylethyl β-D-thio-galactoside
PTEN	Phosphatase and tensin homolog
pL	Picoliter
pM	Picomolar
PMT	Photomultiplier tube

RFU	Relative fluorescence units
RIA	Radioimmunoassay
RSD	Relative standard deviation
SD	Standard deviation
SEM	Standard error of the mean
S/N	Signal-to-noise ratio
TNT	2,4,6-trinitrotoluene
UV	Ultraviolet
V	Volt(s)

ABSTRACT

Microfluidic devices for the simultaneous characterization of insulin release from four and 15 isolated pancreatic islets were developed. Quantification of released insulin from islet samples was performed using parallel immunoassays coupled to capillary electrophoresis with fluorescence detection. Assays for insulin were completed in a serial fashion on each channel every 6 – 10 s, giving fast temporal resolution used for investigations into insulin secretion dynamics. Assay limits of detection were between 0.5 – 10 nM insulin.

Individual islets were housed on the chips while perfusion streams carrying glucose or other secretagogues were used to induce insulin release. Secreted insulin was then mixed with fluorescently-labeled insulin and anti-insulin antibody in reaction channels for a competitive immunoassay. Portions of the continuously flowing reaction streams were injected onto separation channels where bound fluorescent insulin:antibody and free fluorescent insulin complexes were separated electrophoretically and detected via fluorescence. Relative amounts of these products were used to determine the amount of released insulin.

The 15-islet microchip was used to investigate possible roles of leptin signaling on insulin secretion. Through a collaborative effort, islets from mice lacking leptin receptors only in the pancreas were compared to control islets through insulin release

studies. Specifically, the effects of leptin, glibenclamide, glucagon-like peptide-1, and palmitic acid on glucose-stimulated insulin secretion were investigated. It was observed that leptin produces an inhibitory effect on insulin release and that lack of leptin signaling in islets enhances insulin release stimulated with glucose.

Modifications were made to the 15-islet chip to ensure more uniform sampling of insulin from islets. The new islet sampling method was used to characterize oscillatory insulin release under various conditions. It was found that when treated appropriately, islets from individual mice displayed similar insulin secretion and Ca^{2+} flux oscillation frequencies. These frequencies were shown to be different from mouse to mouse, complementing previous studies. Additionally, the effects of free fatty acid-induced liptoxicity on pulsatile insulin release were investigated. Results from these experiments demonstrate the usefulness of single islet data not previously available at this level of throughput.

CHAPTER 1

INTRODUCTION

The development towards lab-on-a-chip devices has been greatly advanced since the first introduction of microfluidics for chemical analysis,[1,2] with much progress being made in the area of chemical separations.[3-6] The attractiveness of microfluidics-based separations to analytical chemists owes to its ability to routinely perform rapid and sensitive experiments on a small footprint with minimal use of sample and reagents. Additionally, microfluidic technology facilitates the fabrication of devices with integrated functions,[7-9] an advantage which has led to a multitude of microdevices for pertinent biochemical assays. The success of microchips in basic research has led to the birth of specialized commercial devices for multiple bioanalytical applications.[10-12] It is clear that recent advancements made with these tools have placed the use of microchips on the frontier of research in cell biology, genetics, pharmacology, and other biomedical fields.

Many advances with microfluidic devices highlighted above were demonstrated on "single-sample" chips capable of performing only one analysis at a time. An additional advantage of microfluidics is the ease of fabricating several analysis manifolds on a single device, thus potentially increasing throughput while keeping the cost of fabrication essentially the same. Research using such parallel separations will help to realize the continued advancement of microdevices used for real-world applications.

Advances in high-throughput techniques have already shown importance to many fields with conventional multiplexing instrumentation for drug discovery,[13] protein characterization,[14] and DNA analysis.[15] Clearly, the time and cost savings that these high-throughput methods offer can be increased by utilizing the short analysis times and small reagent volumes associated with micro-scale systems. However, several challenges in developing parallel analysis microchips must be overcome. These challenges include: (i) organizing multiple channel networks on a single device with a small footprint, (ii) coupling multiplexed chips to peripheral equipment (e.g. power supplies, pumping devices), (iii) developing multi-channel detection methods, and (iv) achieving reproducible analyses across parallel channels.

Over the past decade, we have seen the addressing of these concerns with numerous reports of parallel separations on microchips. The majority of this introduction will serve as a brief review of recent technological advances towards realizing high-throughput microfluidic devices using parallel separations. Though microchip channel organization and operation are critical to performance, design details are commonly influenced by chosen parallel detection methods. As detection is a crucial part of performing parallel separations on microchips, a discussion of various methods of multiplexed detection, consisting mainly of fluorescence techniques, will precede review of recently developed microchips for parallel analysis of biomolecules, affinity assays, and DNA analysis.

Multiplexed Detection Methods

One important aspect considered in the development of a microfluidic system with multiple separation channels is how detection will be performed because most detectors are designed for single point detection. Although there have been a multitude of reports using single separation microchips and detectors for measuring low quantities of analyte,[16,17] the development of a multi-channel instrument capable of highly sensitive detection of numerous channels is challenging. Several research groups have developed specialized detectors for use with their own custom-designed microchips that use specific technology providing either high sensitivity, high sampling rates, or ease of use. In broad terms, three basic methods of detecting simultaneous separations on multiple channels have been utilized: i) moving a single point detector across the chip at a frequency high enough to adequately detect separated bands in each channel (e.g. scanning laser-induced fluorescence (LIF)), ii) having a single detector that can continuously monitor all separations while maintaining channel-to-channel resolution (e.g. fluorescence imaging), and iii) assigning independent detectors to each channel on the device (e.g. parallel electrochemical detection).

Scanning LIF. Fluorescence detection is commonly used with microchips owing to its high sensitivity and ease of use with micrometer-dimensioned channels.[18] Lasers are commonly used for excitation on these devices; however, coupling laser excitation to multiple detection points has been a challenge requiring unique solutions. Rather than using multiple stationary laser spots for excitation, requiring many complicated optical alignments to be made for proper excitation and detection, the majority of research has focused on scanning a single laser spot across several channels. Numerous methods of

scanning LIF detection have been demonstrated, ranging from relatively simple stage translation devices for use with a stationary laser to detectors based on a mobile objective lens.

Translation Stage. The basis of translation stage-driven multiplexed LIF detection is moving a microchip over a fixed detection point so that the multiple channels on a device can be sampled. The advantage in using this approach is that detection can be performed on parallel aligned channels without moving any components of the optical train. The first reported scanner of this type, albeit not used for detection with microchips, was reported as an approach to high-throughput DNA sequencing using capillary array electrophoresis (CAE).[19] This same stage translation detection scheme was later demonstrated for use with parallel separation chips.[20] In this report, the translation stage detector was used for monitoring multiple DNA separations on a chip with 14 parallel channels (12 channels for separations and two for optical alignment). Parallel epi-fluorescence detection was performed using a stationary 20x objective lens while scanning the microchip a distance of 1.2 mm at a speed of 1.0 cm s^{-1}, allowing an overall sampling rate of 3.3 Hz.

A more recent study also shows the use of stage translation for fluorescence detection of parallel capillary electrophoresis (CE) separations.[21] In this report, the advantage of having a non-moving optical train has been exploited to facilitate optical gating for sample introduction in parallel channels. Optical gating, previously shown to be compatible with microchips in a study performed by this same group,[22] uses high intensity laser light to continuously photobleach sample flowing though a separation channel. An analysis is made by temporarily blocking the laser and letting a fluorescent

sample plug separate by CE. Experiments were performed by scanning a five-channel CE microchip across two laser spots (gating and probe beams) which were offset by 400 μm to allow simultaneous detection on one channel and gating on another. A voice coil actuator, which can provide accurate placement from micrometer to centimeter distances, was used to drive the translation stage. It was found that moving the stage at a frequency of greater than 10 Hz produced significant vibrations that increased experimental noise, illustrating a drawback of using this detector for monitoring fast separations.

Scanning Mirror. As translation stage detectors cannot offer the needed speed for detection of fast parallel separations, a drive towards the development of faster scanning detectors led to coupling mirror-based laser scanning with microchip separations. Unlike translation stages, scanning mirror systems raster a laser spot across channels on a stationary chip. The use of galvo-mirrors for scanning laser spots across a short distance has been previously demonstrated by many commercial scanning confocal imaging systems.[23] Some of the scanning mirrors used in these instruments can scan at kHz frequencies, holding potential for improvement over the approximate 10 Hz limit of translation stage detection. However, mirror-driven parallel detection on microchips with kHz rates has yet to be demonstrated.

The earliest mirror-driven laser scanning detectors were built for monitoring simultaneous DNA separations.[24,25] One study gives a brief description of the laser scanning device, stating that a 5-μm laser spot was scanned across a 48 channel microchip (a distance of 7.4 mm) at rate of 40 Hz.[24] Fluorescence was collected through a stationary objective and detected with a PMT to generate 16-bit images from which

parallel electropherograms were extracted. The reported limit of detection (LOD) using this detector was 1 molecule Cy3 dye per 100 μm^2.

Details of another homemade mirror-based scanning detector were described in a later study.[26] Juxtaposing the previous galvo-mirror detector that was described as scanning at a constant rate across a microchip, the mirror used in this study behaved similarly to a stepping motor allowing fast transitions between channels and longer integration times for a single detection point. This laser scanning technique is advantageous as it increases the duty cycle of the detector yielding higher sensitivity detection. A specific duty cycle of 71% was reported for this detector when scanning over an eight-channel microchip (six channels for separations, two for alignment) at a rate of 7.1 Hz for each channel. An LOD of 30 pM fluorescein was reported using this detector.

Acousto-optical Deflection. Though mirror scanning detectors can achieve high sampling rates and increased duty cycles, they are still mechanically dependent on moving parts. The use of any mechanically controlled scanner is going to inhibit achieving ultrafast scanning rates due to issues with mechanical noise and the distortion of signal.[27] The Landers group has done much work[27-29] towards eliminating the need for mechanically controlled instrumentation in parallel microchip detectors by employing laser scanning technology based on acousto-optical deflection (AOD). The principles of AOD are centered on laser light diffracting though an optically transparent medium at an angle that is dependent upon both the wavelength of light and the frequency of acoustic waves traveling though the device. The angle of light diffraction can be changed by manipulating the acoustic wave frequency via a piezoelectric transducer. The advantage

of using such a device for laser scanning includes the elimination of mechanical noise while achieving fast scan rates (kHz range). The developed detector has been used with a variety of microchips with an on-chip scanning distance of up to 2.4 cm, longer than the highest reported mirror-driven chip scanning distance of 10 mm. Figure 1.1 shows a series of CCD images illustrating the scanning of a laser spot across an eight-channel chip. For these studies, fluorescence emission from sample bands was collected though a non-moving objective directed onto a PMT. An additional advantage in using this method of laser scanning is the ability to randomly address microchannels with channel-to-channel transition times down to 11.3 μs. One disadvantage, however, is that the diffraction of light through this device is wavelength dependent, making descanning and epi-fluorescence detection difficult to perform.[23]
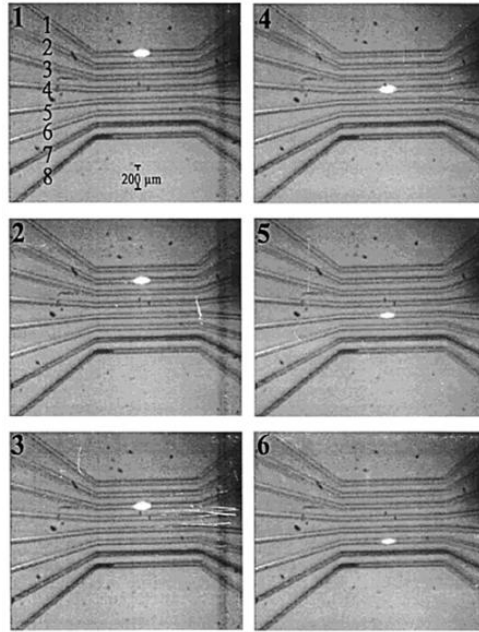
Figure 1.1. Six CCD images showing the positioning of a laser spot (white dot in the images) scanned across eight microfluidic channels using AOD. For this laser scanning technique, the laser passes through an optically transparent diffractive medium before reaching the chip surface. The angle of diffraction through the medium can be controlled by applying acoustic waves to the device. Altering the frequency of acoustic waves changes the angle of light diffraction, thus allowing accurate positioning and scanning of a laser spot across parallel running channels. This type of laser scanner was used to monitor parallel separations on a microchip, however, detection was performed with a PMT rather than CCD imaging as shown. Reproduced from reference 27.

Rotary Confocal. Attempts to maximize the number of microfluidic channels fabricated on a single device have led to the exploration of new channel organization methods. One design that has been proven useful for the arrangement of hundreds of channels on a single device is the radial alignment of separation channels in which fluidic reservoirs are situated close to the outside edge of a circular chip and separation channels converge to a common waste reservoir in the center. The Mathies group, responsible for the introduction of this parallel network design, has also developed a detector suitable for use with radially aligned channels.[30] Detection with this device, continually improved upon to allow use with higher channel densities from 96 to 384,[31,32] is based on rotating an objective lens around an off-center axis for laser-excited confocal fluorescence in a

8

circular path. For this device, the larger mechanically-based movements of the optical train have allowed dramatic increases in the number of channels on which detection can be performed. The detector uses a hollow stepping motor shaft with a rhombic prism and objective lens placed atop to allow displacement of laser light traveling up a vertical axis (orthogonal to the microchip surface) by 1 cm. The prism and objective are then rotated resulting in a scanning path of a 2 cm diameter circle. Fluorescence is collected though the same objective and directed towards a four-color confocal detector. It has been reported that sampling frequencies as high as 20 Hz can be used with a spatial resolution of ~12.6 μm, however, lower rotational speed is typically reported for experiments with this detector. LODs as low as ~1 pM (S/N = 2) have been reported using this device.

Fluorescence Imaging Detectors. CCDs and other imaging detectors have been used in conjunction with the scanning laser instruments featured above; however, mostly for the purpose of detector characterization and alignment rather than for detection in actual separation experiments. In cases when highly sensitive detection is not required, it may be advantageous to use an imaging detector due to the near 100% duty cycle capabilities, commercial availability, lack of moving parts, and relative ease of use. Indeed, parallel fluorescence detection of multiple separations on a microchip has been performed on standard commercially available fluorescence microscopes using arc lamp excitation and CCD camera detection.[33,34] Commercially available CCD cameras attain frame collection rates up to hundreds of frames per second making them useful for detection of fast separations. Additionally, the use of commercial imaging detectors requires little optical alignment. Disadvantages of an imaging detector include the risk of channel crosstalk (controlled by proximity of channels in the detection region and image

resolution) and a defined imaging area that may be difficult to manipulate if a specific image magnification is required.

Several groups have demonstrated laser-induced excitation with CCD detection.[35-39] In these studies, laser light was shaped into a line using a cylindrical lens and directed across all sample channels on a chip, exciting sample plugs passing through it. Laser light was directed at an angle (typically around 45°) towards the chip surface while fluorescence was collected through perpendicular optics that focused an image of the detection region onto a CCD chip. Parallel separation data were then produced by plotting fluorescence intensities versus time from several regions of the images that corresponded to microfluidic channels. This detection scheme was used to monitor up to 10 parallel channels with a sampling frequency of 30 Hz.[36] An interesting modified version of this detector was demonstrated by a system that positioned a laser directed across parallel channels though the side of the microchip (perpendicular and in the same plane as channels).[40] Imaging detection from 48 samples across a 140 mm width was completed with a CCD.

Electrochemical Detection. Electrochemical detection is another method for monitoring separations that has been used for parallel analysis on microchips owing to the ease of microfabricating detection electrodes on the same scale as microchannels. Although detection limits are not as low as have been achieved with fluorescence detection, electrochemical monitoring does offer reasonable LODs while requiring relatively simple instrumental setups. Electrochemical detection for parallel microchips has recently been demonstrated.[41] In this study, parallel electrochemical detection was performed with a contact conductivity array used to monitor simultaneous separations

performed in 16 channels on a microchip. In contrast to other electrochemical techniques such as amperometry, conductivity detection does not require the analyte to be electroactive,[42] suggesting that this device can be used with a wide variety of native samples.   Detection at each channel was controlled by independent pairs of microfabricated gold electrodes (60 μm wide with a 5 μm space) and electrical circuits (16 circuits in total). Parallel separations were monitored using a bipolar pulse voltage waveform with an amplitude of ±0.6 V and frequency of 6 kHz. An image of the system is shown in Figure 1.2A. LODs as low as 1.6 μM were reported from using this detector with separations of peptides.
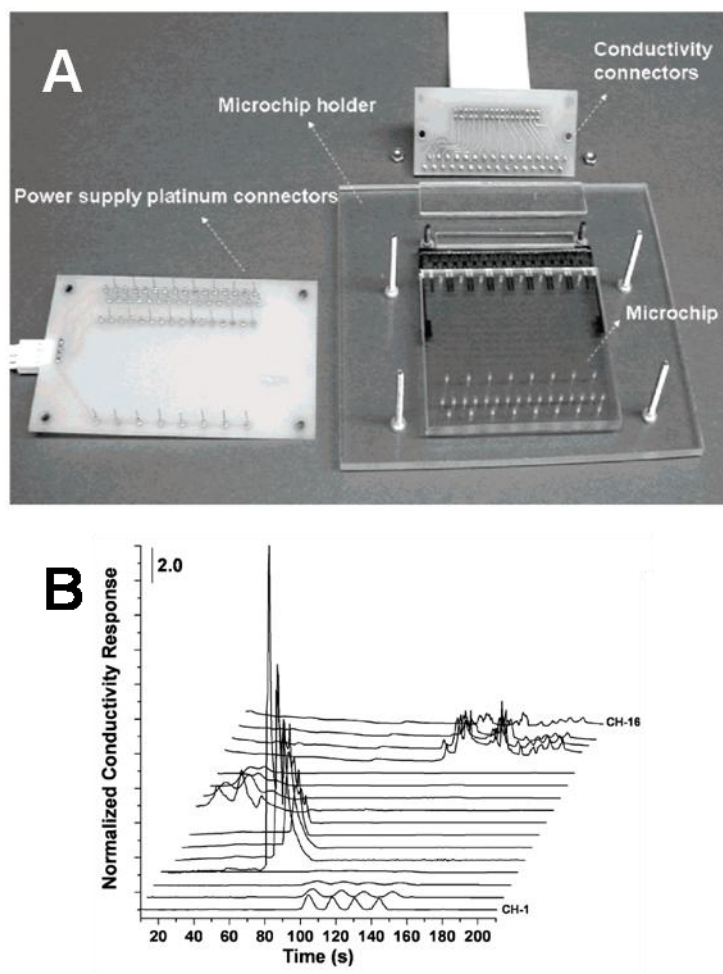
Figure 1.2. (A) Illustration of a workstation consisting of a microfluidic chip, chip holder, and necessary electrical connection devices for parallel CE separations and electrochemical detection. The device, fabricated from polycarbonate, allowed 16 parallel separations of amino acids, peptides, proteins, and DNA fragments. Electropherograms, staggered for clarity, are shown in (B). **(B)** CZE separations of amino acids, peptides, and proteins are shown in channels 1 – 4 (bottom 4 separations), channels 5 – 8, and channels 9 – 12, respectively. Channels 13 – 16 (top four) were used for CEC separations of oligonucleotides. Separations of all sample types were performed simultaneously. Reproduced from reference 41.

Parallel Microchip Applications

The multi-channel detectors reviewed have been used with a wide variety of parallel microchips, with most applications involving parallel chemical separations. Specific designs of parallel microchips have ranged from simple arrays of CE channels to more complicated systems including devices for parallel single cell lysing and separation[43] and on-chip PCR coupled to CE analysis.[44] This section will highlight

advances towards microchips for parallel separations of biomolecules, affinity assays, and DNA analysis.

Separation of Biomolecules. One of the earliest examples of parallel amino acid separations on a microchip was performed on the previously described optical gating translation stage multiplexed detector.[21,45] The nature of optical gating allowed chip designs to consist of parallel-aligned straight channels with no integrated injectors. In these studies, parallel separations of NBD-labeled amino acids (arginine, phenylalanine, glycine, and glutamic acid) were performed on a five-channel microchip with a 750 V cm^{-1} field strength and 5 mm separation distance. Reported detection limits for these separations were 1 mM, 500 μM, 500 μM, and 3.3 mM for arginine, phenylalanine, glycine, and glutamic acid, respectively. Additionally, parallel separation of DNA fragments was performed by this group using a similar chip design and detector.[45]

Another microchip for parallel CE separations of biomolecules has been reported more recently.[46] This chip, while performing separations on only four parallel channels, required a more complicated design to allow for electrokinetic injections to be made using four single-tee injectors. Injections and separations on a single device were controlled by a high voltage power supply consisting of six high voltage modules and 12 high voltage relays. This study reported separations of FITC-labeled glycine, arginine, phenylalanine, and lysine in a separation field of 400 V cm^{-1} over a distance of 40 mm. The same chip was used to separate myoglobulin, ovalbumin, BSA, and conalbumin using similar experimental procedures (same separation field and distance). In an additional study by this group, a similar parallel chip and detector were used for multi-channel chiral separations.[38]

Further increasing the number of parallel separations of biomolecules performed on a single device, a 16-channel polycarbonate chip has been used to separate amino acids, peptides, proteins, and DNA fragments in a single experiment.[41] The 16 channels on the device were arranged into eight pairs of independent channels, allowing simultaneous separations of multiple sample types to be performed with relatively different experimental conditions. The chip performance was evaluated by performing CZE analysis of amino acids (alanine, valine, glutamine, tryptophan), peptides (leucine enkephalin, methionine enkephalin, oxytocin), and proteins (chymotrypsinogen A, cytochrome C, BSA) and CEC separations of an oligonucleotide ladder. Electropherograms from these separations are illustrated in Figure 1.2B. Separations of all analytes were completed in less than 4 minutes in a field of 90 V cm^{-1} yielding detection limits as low as 7.1 μM, 1.6 μM, 3.3 μM, and 0.09 μg/μL for amino acids, peptides, proteins, and oligonucleotides, respectively.

Although it has been shown that radial organization of channels allows hundreds of parallel separations to be conducted on a single chip,[31] the parallel organization of channels on a device can still be advantageous due to its compatibility with several detector types, ease of sample loading,[41] and simple design that facilitates integrated electrodes for CE control. The latter advantage was demonstrated through a device that used a unique 12-channel parallel design for separations of DNA fragments.[34] The chip used I-shaped microchannels fabricated in PDMS (tapered at the injection point to act as a passive stop valve) to perform injections of sample and CE separations in a channel with only two fluidic reservoirs. The elimination of reservoirs used for sample injections facilitated the fabrication of parallel microchannels with integrated electrodes by

14

allowing the close proximity of parallel networks. Functionality of the device was tested by performing parallel separations of 10 fragments of a 100 – 1000 bp DNA ladder.

Affinity Assays. The versatile organization of channel layouts offered by microfluidics makes the technique attractive for use with biochemical and affinity assays. For this reason, microchips have been frequently used in studies of protein and enzyme interactions.[47] Though microchips offer an increase in analysis speed for a single sample, the overall speed of multiple assay completion on a single sample device is still lower compared to the multiplexing abilities of standard larger-scale methods such as plate-readers or gels with multiple lanes. The creation of microdevices for parallel affinity assays increases the overall throughput of homogeneous assays in microchip format, making rate of completion comparable with standard assay techniques.

Immunoassays. The first microfluidic device for the parallel completion of CE-based immunoassays was characterized with direct assays for ovalbumin and anti-estradiol.[26] The device, illustrated in Figure 1.3, consisted of eight separate channel manifolds, two for detector alignment and six capable of supporting online mixing of immunoassay reagents and CE-LIF analysis. Mixing of reagents, reaction, and separation of products was completed within 60 s for all experiments and within 30 s in optimized conditions, demonstrating the potential of high-speed parallel immunoassays on a chip. Detection was performed with a scanning LIF instrument built in-house. The chip was used to demonstrate both simultaneous immunoassays of a single sample and simultaneous calibration and analysis in a single experiment, allowing a complete calibrated assay to be performed within 30 s. Detection limits reported for an anti-

estradiol assay were 4.3 nM in any single channel and 6.4 nM for the cross-channel calibration mode.
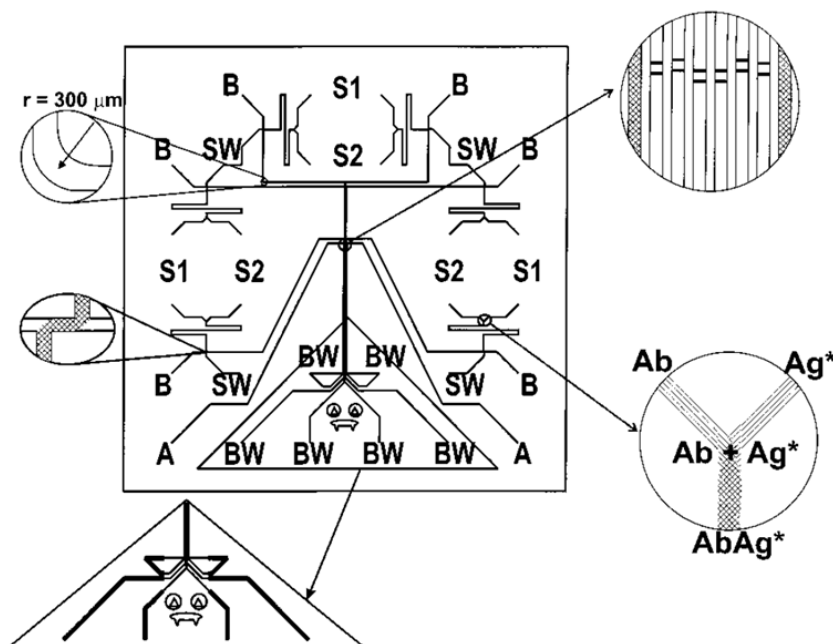
Figure 1.3. Illustration of a microchip design for six simultaneous CE-based immunoassays. Each of six channel manifolds on the device is capable of online mixing of immunoassay reagents (lower right expansion) from reservoirs S1 and S2. Additional fluidic reservoirs shown in the figure include running buffer (B), sample waste (SW), and buffer waste (BW). After mixing, portions of the immunoassay mixtures were then injected onto parallel CE separation channels using a double-tee injector (lower left expansion). Parallel CE separations of the immunoassay mixture were performed on multiple separation channels arranged parallel (upper right expansion) before passing through the detection point. The most outer two channels were used for optical alignment of detection equipment. The device was used for assays of ovalbumin and anti-estradiol. Reproduced from reference 26.

A dramatic increase in the number of simultaneous CE-based immunoassays performed on a microchip was demonstrated with a 48-channel device.[48] While offering an increased rate of immunoassay product separation and detection, this device was comprised of only electrophoretic injection and separation channels and lacked the ability for on-chip mixing of reagents and calibration. Sample preparation was performed completely off-chip and consisted of a 45 minute incubated reaction. The chip was used for a TNT assay with a reported 1 ng mL^{-1} LOD and dynamic range of 1 – 300 ng mL^{-1}.

A recently developed chip has demonstrated the use of parallel immunoassays for the monitoring of cellular secretions from multiple independent biological samples housed on the device.[49] With this device, insulin secretion was continuously sampled from four separate pancreatic islets and quantified every 6.25 s using online mixing and reacting of immunoassay reagents coupled to parallel CE-LIF analysis. Over 700 assays were completed in a 20 min experiment, noting a significant decrease in immunoassay reagent costs compared to typical insulin ELISA kits. Parallel fluorescence detection was performed using a commercial scanning confocal microscope operated in line scan mode. An LOD for insulin was reported as 7 nM.

Additional parallel immunoassays, though not utilizing CE, have been developed for sandwich-based assays.[50,51] One report examined a polymer CD-shaped chip that utilized centrifugal force for mixing and dispensing immunoassay reagents in precisely defined volumes.[50] The chip, when rotated at sufficient speed, would introduce solutions of biotinylated antibodies against a target molecule into 104 parallel on-chip microcolumns packed with streptavidin-coated particles. Solutions of sample and then fluorescently labeled detection antibody were then introduced in a similar manner after which fluorescence of the packed beds was used to determine sample binding. Assays for α-fetoprotein, interleukin-6, and carcinoembryonic antigen with reported LODs of 0.15, 1.25, and 1.31 pM, respectively, were performed at speeds up to 104 immunoassays in 50 min.

Enzyme Assays. A parallel microchip for enzyme assays was reported[52] that used a similar chip design and translation stage optical gating detector from previous work.[21,45] To monitor multiple enzymatic reactions, continuous serial injections of an

enzyme/substrate mixture were made into parallel microchannels for CE-LIF analyses. The chip was used for monitoring the hydrolysis of fluorescein mono-β-D-galactopyranoside (FMG) by β-galactosidase (β-Gal) with and without phenylethyl β-D-thio-galactoside (PETG), a competitive inhibitor. The separation of enzyme reaction products was performed in a separation field of 500 V cm^{-1} with 30 s temporal resolution. Results from the parallel studies were used to calculate K_m values from Lineweaver-Burk plots. Additionally, the simultaneous monitoring of the hydrolysis of FMG with different inhibitors (no inhibitor, lactose, and PETG) was performed by testing each inhibitor on a different channel. The results from this study illustrate the potential for microfluidics-based high-throughput screening of drug candidates for potential activity.

Recently, microchips with 16 and 32 parallel electrophoresis units were used to investigate G protein GTPase activity.[53] Utility of the 16-channel design was demonstrated by extracting kinetic information from serial assays performed in parallel every 20 s. The 32-channel design was used at a slightly lower temporal resolution (assays every 30 s), but still allowed an overall throughput of 4,320 assays per hour. Separations on both devices were reproducible showing normalized peak area RSDs of 5% and 11% for the 16-channel and 32-channel devices, respectively.

DNA Analysis and Integrated Devices. To address the needs of the human genome project, many researchers strived for the development of methods to improve the speed, cost-effectiveness, and throughput of DNA sequencing.[54] The developments of capillary array gel electrophoresis have offered techniques equaling the high-number DNA sample processing capabilities of conventional slab gel electrophoresis, making it commonly used for DNA analysis. Owing to the simple, low cost fabrication of

microfluidic devices and potential for high speed separations, it has not been surprising to see rapid development of microchips for parallel DNA separations and sequencing. The capabilities of the first parallel chip for DNA analysis were tested by performing 12 simultaneous separations of pBR322 DNA samples and also by genotyping HLA-H.[20] While this device was not able to provide higher throughput than the current CAE techniques, it demonstrated potential for multiplexed genetic analysis on chips.

The ease of fabricating parallel channels in microfluidic devices has allowed rapid improvements to this 12-channel design to be made over the past decade. There are several reviews available that include a discussion on the development of these devices.[32,54-56] The Mathies group has pioneered much progress towards high-throughput genetic analysis on microchips by developing 48-,[24] 96-,[30,57] and 384-lane[31] devices for DNA separations. The development of these chips was a significant advancement as the throughput of DNA microdevices was improved while the cost of fabrication did not increase substantially. Potential applications of parallel DNA chips have been demonstrated through single nucleotide polymorphism genotyping,[58,59] single-strand conformation polymorphism analysis,[60] and short tandem repeat typing.[61]

Additionally, a recent paper has reported a system with 768 parallel channels for high throughput DNA sequencing.[62] This system consisted of two 25 cm x 50 cm microfabricated plates, one illustrated in Figure 1.4, with 384 separation channels each. Analysis was performed on an automated custom-built instrument for sample loading, separation, detection, and plate regeneration (one plate was prepared for experiments while another was used for analysis). A scanning epi-fluorescence detector rotating at 3 Hz, compatible with the 384 lanes of a single chip, was used for single plate detection.

Once the separations were completed on one chip, the laser was then relocated to the adjacent chip for a second analysis.
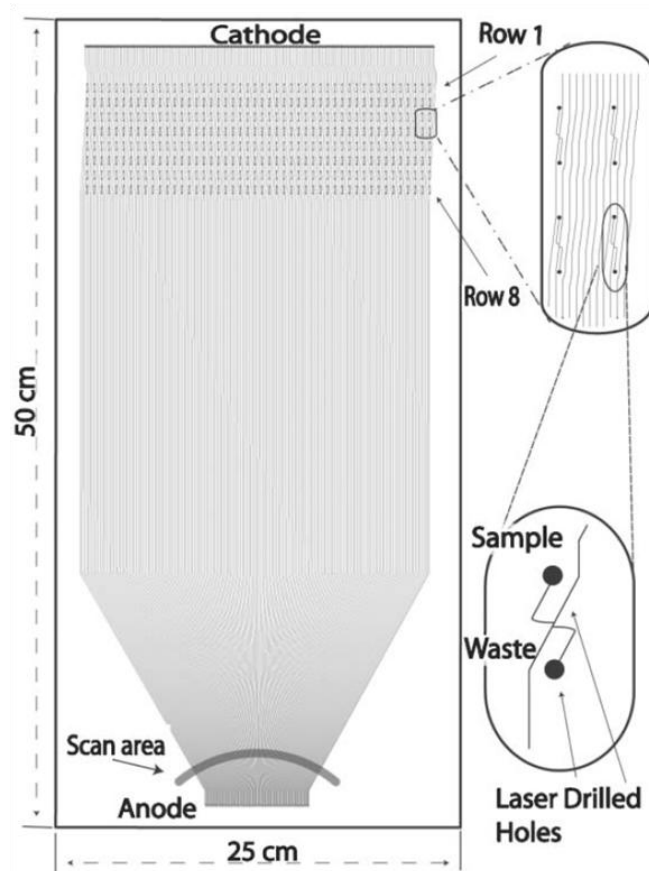
Figure 1.4. One of two microfabricated plates used in a 768-lane system for DNA sequencing. Each plate consists of 384 parallel channels for separations, with the spacing between channels narrowing upon reaching the anode to facilitate scanning laser detection. Separation and detection was performed on one plate while another was prepared for experimentation. On this chip, 384 samples were loaded into laser-drilled access ports arranged into eight rows (each containing 48 cross injectors), illustrated by the expansions in the figure. Fluidic reservoirs for the device were fabricated using a fiberglass board that was affixed to the plate. Reproduced from reference 62.

While these devices show unprecedented capabilities for performing hundreds of separations simultaneously, they are comprised of only simple injection and separation channels and have no other integrated function capabilities. Recent advances in integrated parallel DNA analysis on microchips include devices for PCR amplification of samples and CE separations.[44,63] On these chips, precise temperature of four parallel

nanoliter sized PCR chambers was controlled with resistance temperature detectors and heaters integrated into the devices. Flow through these chambers and onto separation channels were controlled by PDMS valves. Though these reports present a down-sizing of the number of parallel analyses compared to previous DNA microchips, there exists potential for an increase in throughput through the addition of microchannel networks and heating elements.

Concluding Remarks on Parallel Microchips. The research devoted to developing lab-on-a-chip devices for multiplexed analysis along with complimentary detection instrumentation has yielded a number of exceptional systems that exemplify the potential for their widespread use. Work towards this goal is still needed; however, preliminary success in this field has shown outstanding results. Widespread use of parallel microchips is beginning to be realized through the commercial development of high-throughput microdevices by several companies. Future work in this direction should focus on the integration of sensitive detectors on parallel analysis chips, eliminating the need for specialized instrumentation and facilitating portability and use in clinical, environmental, and research lab locations. The advancements outlined in this chapter lead the way for a greater transition from microchips being used only in basic research labs to their specialized design and use for real-world situations.

Analysis of Living Cells on Microfluidic Chips

The ability to create devices for performing sophisticated physiological experiments on cells has made the use of microfluidic chips attractive for the analysis of biological samples. The first microchips developed specifically for cellular studies

focused on cell sorting[64,65] and cytometry.[66,67] Analysis of cellular components with these devices could be performed with on-chip cell lysing.[68,69] Later, the development of cell trapping and perfusion methods for maintaining cell viability allowed the on-chip culturing of samples for long-term analysis.[70,71] Many of these devices made use of advances in fabrication technology that allowed decreases in microchip volumes. Small channel volumes compatible with the sizes of cells allow for rapid exchange of cell media and reagents, which can be critical in experiments requiring fast stimulation and monitoring of cells.

Recent work in developing microdevices for the analysis of cells has produced a number of devices for examining cellular physiology. The ease of fabricating and integrating electrodes into microchips has allowed the creation of chips for electrophysiological patch clamp experiments[72,73] as well as electrochemical detection of cellular secretions.[74] Microfluidic substrates are commonly optically transparent (e.g., glass or PDMS) allowing cells trapped on a chip can be probed by spectroscopic methods, for example, using Ca^{2+} sensitive dyes to measure intracellular Ca^{2+} levels.[75] Recently, the ability to design elaborate microchannel networks has been used to produce a device for high throughput screening of cell-cell communication in an array format.[76] These examples show various microchip techniques used for the analysis of cells and demonstrate the versatility afforded by microfluidic tools for studying a variety of biological systems on the cellular level.

Pancreatic Islets of Langerhans

The endocrine pancreas, responsible for producing and secreting hormones controlling blood glucose levels,[77] is made up of clusters of 2,000 – 4,000 cells known as islets of Langerhans. The cells that comprise islets are classified by their hormonal component: α-cells, producing glucagon; β-cells, producing insulin; δ-cells, producing somatostatin; and PP cells, producing pancreatic polypeptide.[78] Insulin released from islets is a primary regulator of fuel metabolism promoting glucose uptake by target tissues and storage of this fuel as glycogen.[79] Dysfunction of islets, causing decreased insulin production and secretion as well as impaired glucose sensing and cell turnover,[80] can lead to lost control of blood glucose levels and development toward the disease diabetes.

Diabetes mellitus, a disease characterized by hyperglycemia, affects 23.6 million people in the U.S. alone.[81] There are two major classes of diabetes: type 1, characterized by autoimmune destruction of β-cells and type 2, characterized by insulin resistance of target tissues and the inability of islets to overcome this resistance with sufficient insulin secretion.[82] Typical treatments for the disease include administration of insulin as well as drugs that stimulate insulin release from existing islets or treat insulin resistance; however, recent work involving gene therapy,[83] stem cells,[84] and cellular[85] and islet transplantation[86] have also been gaining attention.

The development of new treatments for diabetes is facilitated by research into the underlying causes of the disease, often requiring methods for measuring insulin release from islets. In typical batch islet experiments, groups of islets are perfused with an insulin secretagogue after which fractions of perfusate are collected and analyzed for

insulin content. Analysis of single islet secretion has been performed using similar techniques;[87] however, the offline nature of fraction analysis makes these methods time and labor consuming and not amenable for certain applications. For example, characterization of islets for transplantation requires rapid determination of islet health before implantation into a patient.[88] Additionally, batch islet experiments hamper the ability to measure secretion kinetics on the single islet level since groups of islets may have varying secretion phases.

Tools for rapid analysis of insulin release from single islets have been developed.[89,90] The rapid nature of these methods owes to using an electrophoresis-based immunoassay for insulin,[91] allowing solution-phase mixing of immunoassay reagents for favorable kinetics. In this assay, solutions of fluorescently-tagged insulin, anti-insulin antibody, and sampled insulin are mixed and allowed to react after which the formation of immunoassay products is measured by CE-LIF. Recent advances in these tools have made use of microfluidics for quantitative insulin release measurements from single islets.[92,93] However, the single-sample nature of these devices makes throughput lower than conventional batch islet perfusion techniques, and thus not amenable for research requiring large sample sets. Research presented in this dissertation is aimed at the development of microchips for parallel analysis of single islets capable of producing high throughput data that can be used to analyze single islet secretion dynamics was well as produce averaged plots commonly used in comparative studies.

Dissertation Overview

Chapter 2 describes the development of a microfluidic chip for monitoring insulin release from four isolated pancreatic islets in parallel. The device uses parallel CE-based immunoassays to quantify insulin release from islets, a technique previously developed in our lab. On the chip, multiplexed fluorescence detection of parallel aligned separation channels was performed using a scanning confocal microscope operated in line scan mode. Insulin monitoring ability was demonstrated by characterizing secretions from islets stimulated with a step change glucose concentration (3 mM to 11 mM). Data and results from this chapter were originally published in *Analytical Chemistry*.[49]

Chapter 3 presents a further multiplexed islet secretion monitoring chip, capable of analyzing 15 islets simultaneously. The developed chip made use of a radial alignment of microfluidic networks in which CE separation channels converged at a common point for multiplexed detection via fluorescence imaging. The outer portion of the chip was used for islet housing and mixing of immunoassay reagents. The chip was used to successfully characterize glucose-stimulated insulin release from 15 islets in parallel.

Results from a study investigating the effects of leptin signaling on insulin release using the 15-sample device are presented in Chapter 4. This work was done in collaboration with Dr. Rohit N. Kulkarni and Dr. Tomoaki Morioka of the Joslin Diabetes Center at Harvard Medical School who developed a pancreas-specific leptin receptor knockout mouse model. Work performed by the author was limited to testing single islets for insulin release under various conditions. Data presented in this chapter

were either originally published in *The Journal of Clinical Investigation*[94] or are in preparation for submission.

Chapter 5 deals with improving the insulin sampling portion of the 15-islet microchip to allow more uniform sampling of islet secretions. Fluid flow through the improved microchip was characterized, and data showing biphasic and pulsatile insulin release from single islets is presented. This chapter includes results from preliminary investigations into pulsatile insulin release properties including: i) characterization of oscillatory secretion frequencies of islets from individual animals and ii) studying the effects of chronic free fatty acid exposure on oscillatory insulin secretion. Results presented in this chapter are in preparation for submission.

CHAPTER 2

SERIAL IMMUNOASSAYS IN PARALLEL ON A MICROFLUIDIC CHIP FOR
MONITORING INSULIN RELEASE FROM FOUR PANCREATIC ISLETS

Introduction

Microfluidics offers a versatile platform for growing, manipulating, monitoring, and analyzing cells because it enables precise control of cellular environment, automation, and integration of analytical functions. Microfluidic devices have been used for analyzing both lysed cells[69,95,96] and for monitoring activity of living cells. Examples of the latter application include chips for monitoring oxygen consumption response to drugs,[97] patch-clamp analysis,[98] and the capture and chemical activation of single cells.[99]

Pancreatic islets, which comprise the endocrine portion of the pancreas, are cell clusters that contain 2,000-4,000 cells each and control blood glucose levels through secretion of the peptide hormones glucagon and insulin.[100] The secretion of insulin from an islet is regulated primarily by the metabolism of glucose.[101] Exposing islets to step increases in glucose concentration initiates complex insulin release dynamics consisting of a "first phase" burst of insulin secretion followed in a few minutes by a "second phase" of sustained lower rate of release.[102,103] Impaired glucose-stimulated insulin release is a hallmark of type 2 diabetes;[104] therefore, considerable effort is devoted to studying characteristics of insulin secretion to better understand the development of

this disease. Most secretion studies are performed by using radioimmunoassay or ELISA to analyze insulin content in fractions collected from groups of islets. Although powerful, these methods are cumbersome, expensive, and not amenable to high throughput experiments on single islets. Because of these limitations and the importance of studying insulin release, improvements upon methods of insulin secretion measurement are of interest.

Our lab has previously developed a microfluidic chip that can be used to monitor insulin secretion from single islets.[93] In this device, cells on the chip are continuously perfused with physiological media or buffer. A small fraction of the perfusate is continuously sampled by electroosmotic flow and assayed for insulin by serial electrophoresis-based competitive immunoassays. Rapid chemical separations on the chip enable assays to be performed every few seconds, allowing the dynamics of secretion to be monitored. The chip-based device was a useful advance because it automated the monitoring of secretion and provided sufficient sensitivity to allow detection at high temporal resolution from single islets.[92,93] Indeed, the device has already been used to assay the effects of gene knockouts on insulin secretion.[105] Although this chip is high throughput in the sense that many immunoassays can be performed on a single biological entity, it only allows one sample to be monitored at a time.

An additional advantage of using microfluidic techniques for investigation into biological systems is the facilitation in creating high throughput tools. Microfluidic devices for parallel separations have been developed for genetic analysis,[20,25,31,45] isoelectricfocusing,[28] immunoassays,[26,48,51] enzyme assays,[52] and single-cell capillary

electrophoresis (CE).[43] The basic principle underlying these devices is the multiplexing of microfluidic channels or manifolds, each capable of analyzing an individual sample, on one microchip. In this work, a new device will be described that allows serial immunoassays to be performed in parallel for monitoring insulin release from multiple independent islets.

Experimental Section

Chemicals and Reagents. Fluorescein isothiocyanate-labeled insulin (FITC-ins) was purchased from Molecular Probes (Eugene, OR), and monoclonal antibody (Ab) to human insulin was from Biodesign International (Saco, ME). Collagenase type XI, insulin, ethylenediaminetetraacetic acid (EDTA), and Tween 20 were purchased from Sigma (St. Louis, MO). Tricine, electrophoresis grade, was from MP Biomedicals (Aurora, OH). Cell culture reagents were obtained from Invitrogen (Carlsbad, CA). All other chemicals were purchased from Fisher (Pittsburgh, PA). All solutions were made using Milli-Q (Millipore, Bedford, MA) 18-MΩ deionized water and filtered using 0.2-µm nylon syringe filters (Fisher). Stock antibody solution was stored at 4 °C in the manufacturer-provided phosphate-buffered saline. Stock FITC-ins was diluted to 166 µM using the immunoassay reagent buffer and stored at -32 °C until use.

Several different solutions were used as physiological, electrophoresis, and reagent buffers. Balanced salt solution (BSS) consisted of 125 mM NaCl, 5.9 mM KCl, 1.2 mM $MgCl_2$, 2.4 mM $CaCl_2$, 25 mM tricine, and 0.7 mg mL^{-1} bovine serum albumin

(BSA), adjusted to pH 7.4. Immunoassay reagent buffer consisted of 50 mM NaCl, 1 mM EDTA, 20 mM tricine, 0.1% (w/v) Tween 20, and 0.7 mg mL^{-1} BSA, adjusted to pH 7.4. Separation buffer consisted of 20 mM NaCl and 150 mM tricine, adjusted to pH 7.4.

Microfluidic Chip Fabrication and Preparation. The developed microfluidic chip consists of four independent channel networks, each capable of performing online immunoassays. The number of channel networks on the device was limited at four due to spatial restrictions (fluidic reservoir placement) and detection limitations (line scan distance), which are discussed later in more detail. Figure 2.1 illustrates the layout for an individual microfluidic channel network and the entire parallel system. The networks have equivalent electrical impedance (channels are of the same length) in order to minimize bias that nonuniform channel networks would have on assay performance.
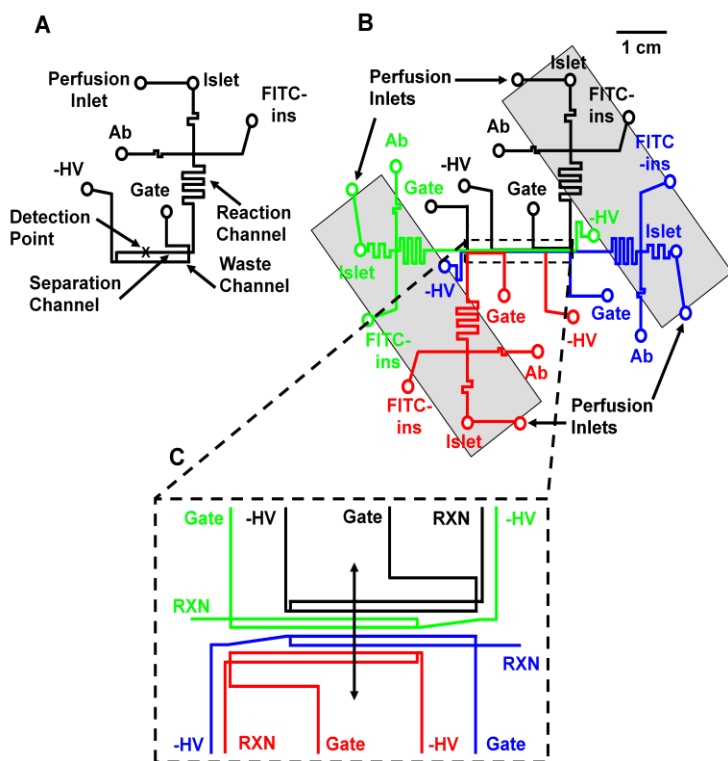
Figure 2.1. Channel layout of a microfluidic device for monitoring insulin secretion from four islets. Each color indicates a single independent channel network. (A) A single fluidic network from the device. Solid lines indicate microfluidic channels, and circles represent fluidic reservoirs and access holes to the channel networks. Some features of the design have been exaggerated to help demonstrate chip function (e.g. spacing between separation and waste channels). All channels were 9 μm deep. Operation of the chip is described in the Experimental Section. (B) The complete chip design (drawn to scale). Shaded regions represent heating strips applied to underside of chip. (C) Close-up of the gating/detection region (not to scale). All of the separation channels run parallel to each other, allowing for a scanning laser spot (path indicated by black arrows) to be used for LIF detection.

The device was fabricated using a previously described method.[106] Briefly, 76 mm x 76 mm borofloat glass photomask blanks (0.7 mm thick) were purchased from Telic Co. (Santa Monica, CA). Each blank had a 530 nm layer of AZ1518 positive photoresist on a 120 nm layer of chrome. The blanks were exposed to UV light for 2 s at 26 mW cm^{-2} through a custom-made photomask with the pattern shown in Figure 2.1B (Digidat, Pasadena, CA). They were then exposed to AZ915 MIF photoresist developer (Clariant Corp., Summerville, NJ) and then CEP-200 chrome etchant (Microchrome Technologies, Inc., San Jose, CA). The exposed glass regions were etched in 14:20:66

(v/v/v) $HNO_3/HF/H_2O$ for 15 min resulting in 9 µm deep channels. Channel access holes were drilled at the points indicated in Figure 2.1B with diamond-tipped 360 µm diameter drill bits (Tartan Tool Co., Troy, MI). Piranha solution (3:1 v/v H_2SO_4/H_2O_2) was used to clean the etched blanks and cover plates, which were then exposed to RCA solution (5:1:1 v/v/v $H_2O/NH_4OH/H_2O_2$) for 40 min at 60 °C. The etched and cover plates were sandwiched between two 3" diameter MACOR plates (Astro Met, Inc., Cincinnati, OH), placed under a 400 g stainless steel mass, and bonded at 610 °C for 8 h in a Neytech Centurian Qex furnace (Pacific Combustion, Los Angeles, CA). Once bonding was completed, microfluidic reservoirs (Upchurch Scientific, Oak Harbor, WA) were attached to the device over the access holes.

Electrical connections to the 20 fluidic reservoirs were made with a chip-electrode interface built in-house. Islet, Ab, and FITC-ins reservoirs were at ground. Gate reservoirs were connected to either ground or a high-voltage power supply (CZE1000R, Spellman High Voltage Electronics, Hauppauge, NY) through a single high-voltage relay (Kilovac, Santa Barbara, CA). Negative high voltage (-HV) reservoirs were connected to a single high-voltage power supply. Two thin-film heating strips (Minco, Minneapolis, MN) attached to the underside of the chip allowed for the heating of all four islet reservoirs and reaction channels to 37 °C. Heating of the chip was necessary in order to sustain islet health and decrease the time needed for the reacting of the immunoassay reagents. Each perfusion inlet on the chip was connected via fused-silica capillary (150 µm i.d., 360 µm o.d.) to a five-port manifold (Upchurch Scientific) and then to a reservoir containing perfusion solution pressurized with He to 170 kPa. This system provided a flow of 0.6 µL min^{-1} into each islet reservoir.

Prior to daily use, chips were flushed with pressure-driven flow of deionized water by applying vacuum to the -HV reservoirs and then islet reservoirs for 5 min each (40 min total). Chips were then conditioned by electroosmotically pumping 0.1 M NaOH through all channels followed by deionized water and then experimental solutions. For this last step, FITC-ins and Ab (both 250 nM in immunoassay reagent buffer) were placed in the FITC-ins and Ab reservoirs, respectively. Separation buffer was placed in the gate and -HV reservoirs. For islet measurements, a single islet was placed in each drilled access hole in the islet reservoirs and perfused with BSS. The flow in the perfusion system did not result in significant hydrodynamic flow throughout the channel network because the islet reservoir was open to atmosphere at the top of the chip, which allowed buffer from the perfusion inlet to exit the chip into a larger reservoir on the chip surface.

Microfluidic Chip Operation. The operation of the device is similar to that previously described for a single-islet immunoassay system. To perform measurements, -5 kV was applied to the -HV reservoirs causing electroosmotic flow from the FITC-ins, Ab, and islet reservoirs into the reaction channel where immunocomplexes were formed. With the gate reservoirs at ground, the flow from the reaction channels was normally diverted to waste. Actuation of the high-voltage relay switched the gate reservoirs from ground to -4.5 kV for 1.25 s, allowing short plugs of solution from the reaction channels to be loaded onto the separation channels where the Ab bound and free FITC-ins were separated by electrophoresis. A single relay actuated all of the gates simultaneously. During normal operation, injections and separations were performed at 6.25 s intervals. Analyte zones were detected 1 cm from the injection crosses using a scanning confocal

fluorescence microscope described below. The relative peak heights were used to quantify the insulin in the islet reservoirs according to a competitive immunoassay calibration curve collected prior to the islet measurements. For calibration, insulin was pumped directly into the islet reservoirs using the perfusion system without islets present. For islet measurements, the islets were perfused with BSS containing different concentrations of glucose.

Multiplexed Laser-induced Fluorescence and Data Analysis. LIF detection of multiple separation channels was accomplished using a laser-scanning confocal microscope (RCM 8000, Nikon, Melville, NY) operated in line scan mode. To facilitate detection, the chip was designed so that the detection point 1 cm downstream from the injection cross was aligned for all four networks. The microscope, when operated in line scan mode, scans a laser spot from the 488 nm line of a water-cooled Ar+ laser (Coherent, Santa Clara, CA) bidirectionally across a sample surface at 15.75 kHz.[23] In order to achieve scanning across the entire detection region of the chip, a 10x (0.3 numerical aperture (NA)) microscope objective (Nikon, Melville, NY), allowing an estimated scanning distance of 470 µm, was used to focus on the detection points. The chip detection region (Figure 2.1C) was designed to fit within this scan distance. With this field of view, eight channels (23 µm wide at the top with 35-µm edge-to-edge gaps between each) could be probed with each scan. Four of the channels running across the detection line are separation channels while the others are waste channels (a consequence from using the flow gate injection design). The passing of the waste channels (through which fluorescent solution was continuously flowing) across the detection zone

facilitated alignment of the device in the z-axis. Alignment marks on the chip allowed reproducible placement of the detection zones for each channel on the laser scan line.

Line scan data were collected and recorded on optical disk cartridges (TQ-FH332, Panasonic, Secaucus, NJ) using an optical disk recorder (TQ-3038F, Panasonic). Each frame of data on an optical disk (containing 525 line scans) was averaged to a single data point to produce an overall 30 Hz sampling rate. Electropherograms were constructed by plotting the fluorescence intensity from fixed points within the line scans using MetaMorph software (Universal Imaging, Downingtown, PA). The resulting parallel electropherograms were subjected to a seven-point moving average smooth before being analyzed using software written in-house.[107]

Islet Isolation Protocol. Pancreatic islets were isolated from 20 to 30 g male CD-1 mice using a previously described method.[108] Briefly, mice were sacrificed by cervical dislocation before collagenase type XI was injected into the pancreas via the main pancreatic duct. The pancreas was removed and exposed to a collagenase solution at 37 °C. A Ficoll gradient was then used to separate islets from exocrine tissue. Islets that were selected for experiments had a diameter of 100 to 200 μm, an intact islet membrane, and an oblong to spherical shape. The islets were incubated in RPMI 1640 cell culture media with 10% fetal bovine serum, 100 units mL^{-1} penicillin, and 100 μg mL^{-1} streptomycin at 37 °C and 5% CO_2. Islets were used 1-6 days after isolation.

Results and Discussion

Continuous Parallel Measurements. Typical electropherograms obtained in parallel with online mixing of the Ab and FITC-ins reagents are shown in Figure 2.2,

illustrating the completion of 20 immunoassays in 30 s. Each separation consists of a FITC-ins:Ab complex zone that is detected before a free FITC-ins zone. Migration time relative standard deviations (RSDs) for the single channel networks are less than 1% for five consecutive injections and slightly larger (2%) for migration times over all four channels. RSDs of this magnitude were typical for all experiments performed with this chip design. These low values suggest good reproducibility of glass surface properties and resulting EOF between separation channels. This reproducibility also suggests that the electric fields across each of the four channel networks are of similar magnitude, indicating little or no current leakage between channels. It is possible that the migration times could have been affected by both the alignment and wobble associated with the laser scan line, but judging from the achieved precision, these aspects of the instrumental setup seem to have little effect. Good reproducibility is important because a single relay is used to control the injections. If migration times drifted, or were significantly different, then the injections could only be performed at the rate of the slowest migration time.
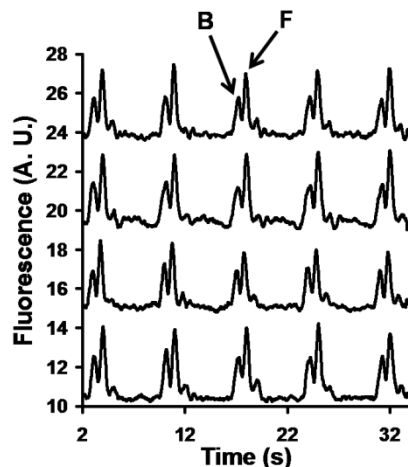
Figure 2.2. Typical series of parallel electropherograms obtained from online mixing of reagents. Solutions of 250 nM FITC-ins, 250 nM Ab, and 100 nM insulin standard were continuously mixed online while CE-LIF analyses were made every 6.25 s. Bound (B) and free (F) peaks are indicated by arrows. Fluorescence signal is in arbitrary units (AU) and offset for clarity.

The separation potential used for the separations in Figure 2.2 was -5 kV. As the separation channel is electrically coupled to the reaction channel, it was necessary to determine an appropriate potential that allowed for fast separations but still gave an adequate reaction time for the competitive immunoassay. It was observed that the application of -5 kV to the waste reservoirs, yielding a separation field of 600 V cm^{-1}, allowed for the separation of the bound and free zones in less than 5 s while giving a 60 s reaction time for the immunoassay. This reaction time was deemed adequate for these experiments given that it was found to produce easily detectable B/F values.[109]

Rapid serial injections after online reaction, necessary for continuous monitoring of insulin release from islets, was made possible through the use of a microfluidic flow gate style injection. This style of injector, as opposed to most double-tee[110] or pinched[111] injection designs, facilitates the continuous monitoring of a sample with online reactions because the field strength in the separation channel remains similar during injection and separation, allowing for continuous flow through the reaction channel during both modes.

In contrast to previous designs of parallel immunoassay chips that required the stopping or reversal of flow during a separation,[26] this design can perform serial immunoassays that allow continuous monitoring of the sample chamber. However, one disadvantage with this design is that waste channels must pass through the detection area, limiting the space available for additional separation channels. It is also possible to obtain continuous monitoring by using a modification of the pinched injection mode. This design may allow more channels in the detection zone and would have the added advantage of less electrophoretic discrimination in the injection.[112]

Calibration. Calibration of the device was performed by perfusing standard insulin solutions into the islet reservoir of the chip with no islets present. Figure 2.3 represents a typical calibration curve for a microchip, obtained using standards between 1 and 500 nM insulin. (All standards were dissolved in BSS to replicate conditions used for living islet experiments.) The calibration curves for each channel network all show a similar dose-response function that is characteristic of antigen-antibody binding; however, some variation is seen from network to network. Previous studies using parallel CE-based immunoassay chips also showed irregularity between data collected from multiple manifolds on a single device, which was partially attributed to nonuniform surface characteristics across a single glass wafer.[26] Results from experiments discussed in future chapters support this theory. Regardless of the origin, the fluctuation of performance is not a concern as long as calibration of each individual channel network is performed, rather than using one calibration curve for all networks.
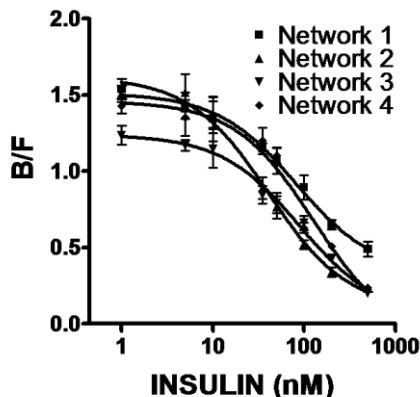
Figure 2.3. Calibration curves obtained with the four-islet chip. The curves were obtained while perfusing insulin standards (1 – 500 nM) into the islet reservoirs with no islet present. Data points are averages of five consecutive electropherograms. Error bars are ± 1 standard deviation.

Data points in Figure 2.3 are the average of five electropherograms collected in series. The average RSDs for data points from each single network range between 8 and 9% (corresponding to 6 – 100 nM insulin depending on location in standard curve). LODs for the channel networks, calculated as the concentration of analyte required to produce a change in B/F that is greater than 3 times the standard deviation of the background B/F, were 10 nM insulin for networks 1, 3, and 4 and 7 nM insulin for network 2. These LODs are roughly 10-fold worse than those reported with the previous single islet microchip (0.8 nM insulin).

The increase in detection limit is ultimately a result of using a scanning detector, which lessens the time available for the analysis of a single detection point. In the detector used here, the laser spot is continuously moving across the sample surface, and as a result, spends much time focused on regions of the chip that do not generate signal. Furthermore, the objective magnification was reduced to 10x and 0.3 NA compared to 40x and 0.6 NA used for single-islet chip studies. This change gave a wider field of

view, allowing multiple channels to be detected, but it also decreased the light collection. Because of these limitations, it was necessary to increase the concentrations of immunoassay reagents (Ab and FITC-ins) used for islet experiments from 50 nM each (point detection) to 250 nM each in order to maintain a detectable signal. The higher reagent concentrations decreased the sensitivity of the immunoassay.[113] Although this increase in immunoassay reagent concentration ultimately produced a less sensitive system, it was still sufficient for the detection of insulin release from single islets. Presumably a more sophisticated detector design[30] would be beneficial in these circumstances by allowing longer data acquisition times, increased instrumental sensitivity, and lower reagent concentrations.

In addition to increasing reagent concentration, the injection volume for each separation was increased (when compared to the single islet microchip with point detection) to help compensate for the decreased detector sensitivity. Increased injection times resulted in poorer resolution of the bound and free peaks than what was previously obtained with the single islet chip. It was found that an injection time of 1.25 s, yielding 315 pL of injected sample, allowed for adequate responsivity of the detection system while retaining sufficient resolution for a peak height ratio analysis.

Although the use of microfluidics offers the expediency of disposable devices, it is convenient to fabricate chips that can be reused throughout a series of experiments. Figure 2.4 illustrates channel network calibration drift of a single device over a period of two weeks. During these two weeks, the microchip was conditioned and used daily. The figure shows typical three-point "daily" calibration curves, fitted from the linear portion of the full dose-response curves. All of the plots show little drift in calibration after three

days of use. Some of the networks, however, show significant drift after 14 days of use, necessitating recalibration of the device before this time. The calibration plots used for islet studies were performed daily and collected immediately before each experiment.
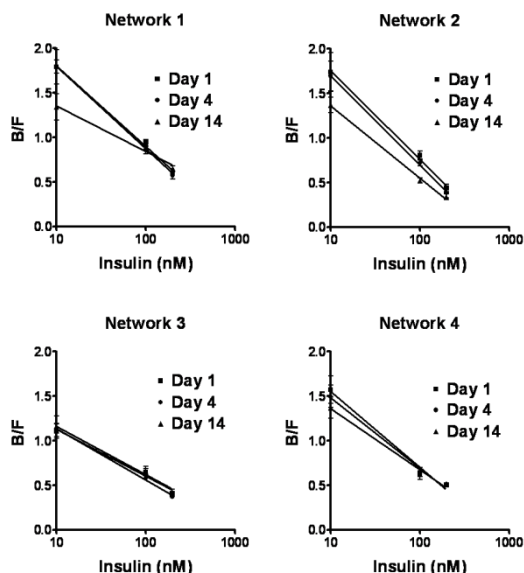
Figure 2.4. Calibrations obtained on each channel network over a two week period of continuous use. Standard insulin solution concentrations used were 10, 100, and 200 nM. Data points are the average of five consecutive electropherograms. Error bars are ± 1 standard deviation.

Characterization of Insulin Secretion from Multiple Pancreatic Islets. The ability of the microchip to continuously monitor the extracellular environment from multiple independent living biological entities was tested by detecting glucose-stimulated insulin secretion from islets of Langerhans. These experiments were performed by placing a single islet in each of the islet reservoir access holes and serially analyzing perfusate for insulin as the glucose concentration was altered in the perfusion fluid. Panels A-D in Figure 2.5 show insulin secretion from four islets monitored simultaneously on a single chip. All the islets show an increase in insulin secretion with the perfusion of 11 mM glucose and a decrease to basal levels with return to 3 mM glucose as expected. Despite the similarities in overall levels and response, the temporal

41

patterns show variability that illustrates the classical patterns of insulin release from individual islets. The secretion pattern in Figure 2.5A shows an initial burst or "first phase" of insulin secretion at ~3 min after the perfusion of 11 mM glucose BSS. It is also known that some islets will give rise to oscillatory secretion, as illustrated by the data in Figure 2.5B-D.[87,114,115] The period of oscillations observed here is in good agreement with previous observations of 2 and 3 min periods for isolated islets. The variability of single islet data is common and illustrates the need to collect data from multiple individuals to gain insight into the overall response.
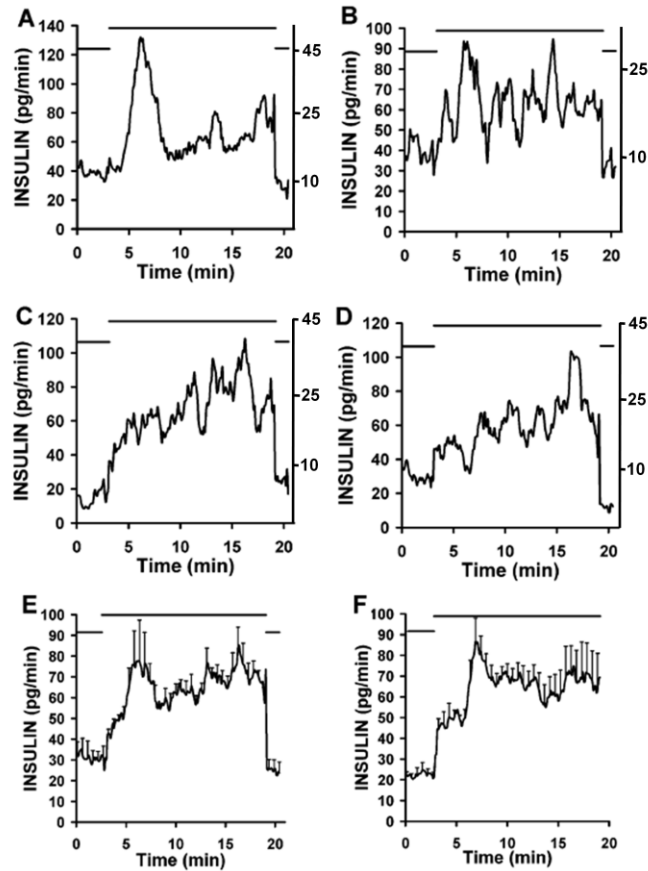
Figure 2.5. Insulin release from islets of Langerhans measured on a multiplexed microfluidic chip. Error bars (± standard error of the mean) are placed every five data points for clarity. Bars placed above plots indicate step changes of glucose concentration in perfusion buffer (low bar 3 mM glucose, high bar 11 mM glucose). Scales on right side of panels A – D indicate concentration of insulin (nM). Detected insulin secretion from four islets (A – D) on a single chip is shown. Averaged insulin secretion from (A – D) is shown in (E), and from a second four-islet experiment in (F).

42

Figure 2.5E represents the averaged insulin secretion data from Figure 2.5A-D, and Figure 2.5F shows the average of another set of four islets. A comparison of the data from (E) and (F) reveals the similarity of averaged responses from different experiments. Despite individual variations, the plots show that the averaged basal secretion, peak secretion, time to peak, and sustained level after peak are all similar to each other, illustrating the reproducibility of the method and averaged islet behavior.

For all eight islets tested, the average rate of insulin release was 27.0 (1.6 pg min^{-1} per islet under basal conditions (perfusion of 3 mM glucose BSS)). Secretion increased by an average of 350% to just under 100 pg min^{-1} per islet after stimulation with 11 mM glucose BSS. The percent increase and absolute level are in good agreement with other studies performed under similar conditions that used either single islets or groups of islets and monitored release using ELISA or RIA. Recently, a study monitoring insulin release rates from mouse islets showed secretion at or below ~100 pg min^{-1} per islet resulting from a step change from perfused 3 to 15 mM glucose.[116]

Advantages of Parallel Islet Analysis. These results illustrate that the microchip can be used to simultaneously quantify chemical secretions from four islets, giving a four-fold increase in throughput over the single islet chip. The ability to operate individual biological experiments in parallel, even those requiring complicated measurements such as serial immunoassays, offers important savings in time and cost. In islet experiments, as in any biological experiment, it is necessary to perform numerous replications to determine the statistical significance of differences due to experimental manipulations. Such replications can be time-consuming when studies are performed at the single-entity level. For example, the throughput of single islet secretion experiments

is typically just 1-3 islets per day. Therefore, although 70 islets can typically be isolated from a single mouse, only a fraction can be used for experiments because islets are stable in culture for just few days. As a result, multiple mice must be sacrificed and numerous islet isolations performed to obtain enough samples for replicate experiments. Given the high costs of labor and animal models, especially genetic knockout mice, low throughput becomes expensive. Another significant cost savings is in the assay itself. The data in panels E and F in Figure 2.5 represent over 1450 immunoassays. Performing a similar number of assays using conventional immunoassay technology (which would be difficult because of the sensitivity required) would cost ~$8200, just for reagents at typical prices of ELISA kits. In contrast, the reagents used for these assays cost under $60.

An increase in the number of networks in parallel would be desirable in order to further capitalize on cost and time savings. As use of this line scan detector limits the size of the detection window to a slit that is ~470 µm long (when using a 10x objective), it may be possible to increase channel density through the detection window by decreasing the spacing between channels. This approach could possibly double the number of channels detected, provided the resulting interchannel space is thick enough to maintain electrical isolation. While this design change would allow higher sample capacity, it is likely this would also result in a lower duty cycle and ultimately higher detection limits.

In the present design, only half of the channels that pass through the detection window are separation channels. A change in the microfluidic configuration, such as a modified pinch injector, may allow all of the channels passing through the detection window to be separation channels and thus double the number of islets simultaneously

monitored without any loss of sensitivity. The use of scanning detectors that allows larger areas or different shapes to be observed, such as a laser-excited rotary confocal scanner, would allow a further increase in number of channels that can be monitored. Scanning over ever larger areas, however, may ultimately be limited by decreases in signal-to-noise ratio because of the reduced duty cycle. This problem is especially acute for the rapid separations used in this application because they require fast scan rates for adequate data sampling. The use of imaging detectors as opposed to scanning detectors may be useful for fast separations because they would allow continuous observation of all points in the detector window, thus lessening geometric constraint and allowing more channels to be detected simultaneously.

Conclusions

A microfluidic device capable of performing serial immunoassays in parallel for chemical monitoring of the environment around living cells was developed. The 4-fold higher throughput results in substantial time and cost savings over a single-sample device for physiological experiments. Although the LOD is ~10-fold higher than the single-channel device, it was still sufficient for monitoring insulin secretion at 6.25 s intervals from single islets. Future directions will involve an increase in throughput and improved assay sensitivity comparable to what was obtained with the single-sample chip.

CHAPTER 3

MICROFLUIDIC CHIP FOR PARALLEL MONITORING OF INSULIN RELEASE
FROM FIFTEEN PANCREATIC ISLETS

Introduction

Insulin secreted from pancreatic islets helps to maintain glucose homeostasis through actions at the insulin receptor in target tissues including liver, muscle, and brain.[117] Impaired insulin secretion is a hallmark of diabetes which is a prevalent and growing health problem. Type 1 diabetes is characterized by autoimmune destruction of β-cells. Islet transplant[118] and development of insulin-secreting cells derived from stem cells[84] are receiving active research interest as possible treatments for this disease. Type 2 diabetes is characterized by insulin resistance (i.e., poor response to insulin by target tissues) and insufficient insulin release from β-cells to overcome this resistance.[104] Research into the causes and treatments of diabetes routinely requires measurement of insulin secretion. The long analysis time of traditional secretion measurement methods utilizing ELISA or RIA hampers the use for certain clinical applications such as evaluating the quality of islets prior to transplant. Additionally, these types of experiments are of interest for studying the kinetics of insulin secretion, and so methods for measuring insulin release from single islets with fast temporal resolution are of significant biomedical interest.

Microdevices developed in our lab have greatly simplified measuring insulin secretion from single islets at high temporal resolution. In these devices, insulin release from single islets is detected at 5 to 10 s intervals with an electrophoretic immunoassay.[92,93] While useful, these devices suffer from a practical problem in that they have a low throughput for islet experiments. To increase throughput, a four-islet system was developed.[49] While an improvement, the detection system had relatively poor sensitivity and the improved throughput was not sufficient to justify the compromise in performance. The goal for the work presented here was to develop an easy-to-use parallel system that would further increase throughput for islet experiments without compromise on immunoassay sensitivity.

A key design consideration for microfluidic devices with parallel separation systems is the arrangement of the detection zones as this has a large impact on the number of separation channels that can be incorporated as well as the complexity of the detector. In our previous on-line parallel immunoassay system,[49] and with most other parallel systems on chips, the detection zones are arranged along a line with separation channels running parallel to each other. Such an arrangement allows relatively simple optics, either an excitation source shaped to a line or linear scanning of a laser (readily available on commercial microscopes), to be used for fluorescence detection.

It has been demonstrated that substantial improvements in parallel operation can be achieved by using a radial channel design.[30] In this design, sample preparation and injection zones are arranged in a circle on the outside rim of the chip while the separation zones converge towards a common outlet at the center. This design uses the space on a chip more efficiently because the detection zones are confined to a small space at the

center of the device while the multiple reservoirs and inlets required for sample manipulation are placed along the outer rim of the chip with more area. Radial designs have allowed multiplexing of 96 and 384 electrophoresis channel arrays.[30,31] Sensitive fluorescence detection on these devices has been performed using a custom-built rotary scanning confocal detector. While this has been shown to be an effective detector, the use of charge-coupled device (CCD) cameras for imaging detection on multiplexed chips[33,37,46,51] suggests the potential for high throughput analysis with microfluidic devices using a less complicated detector.

In this work we have adapted a radial design to parallel, online, serial immunoassay for cellular monitoring. To simplify detection, we utilize a commercially available fluorescence imaging microscope with an electron-multiplying CCD for detection. We show that this detector, while not as sensitive as the scanning confocal design, has adequate sensitivity for the insulin immunoassay as well as sufficient speed for monitoring the rapid separations used here. With this detector and radial design, we were able to successfully operate 15 channel networks in parallel and simultaneously monitor insulin secretion from 15 islets.

Experimental Section

Chemicals and Reagents. Balanced salt solution (BSS) used as a physiological buffer for islets experiments consisted of 125 mM NaCl, 5.9 mM KCl, 1.2 mM $MgCl_2$, 2.4 mM $CaCl_2$, 25 mM tricine, and 0.7 mg mL^{-1} bovine serum albumin (BSA), adjusted to pH 7.4 with NaOH. Buffer for immunoassay reagents was 50 mM NaCl, 1 mM ethylenediaminetetraacetic acid (EDTA), 20 mM tricine, 0.1% (w/v) Tween 20, and 0.7

mg mL^{-1} BSA, adjusted to pH 7.4. Separation buffer consisted of 20 mM NaCl and 150 mM tricine, adjusted to pH 7.4.

Tricine, electrophoresis grade, was purchased from MP Biomedicals (Aurora, OH). Collagenase type XI, insulin, EDTA, fluorescein, and Tween 20 were from Sigma (St. Louis, MO). Cell culture reagents were from Invitrogen (Carlsbad, CA). Fluorescein isothiocyanate-labeled insulin (FITC-ins) was obtained from Molecular Probes (Eugene, OR), and monoclonal antibody (Ab) to human insulin was from Biodesign International (Saco, ME). All other reagents were from Fisher (Pittsburgh, PA). All solutions were made with 18-MΩ deionized water from a Millipore (Bedford, MA) Milli-Q filtration system and filtered with 0.2 μm nylon syringe filters (Fisher).

Stock FITC-ins was diluted to 166 μM using the immunoassay reagent buffer (without Tween 20) and stored at -32 °C until use. Stock Ab solution was stored at 4 °C following the manufacturer's instructions.

Microfluidic Chip Fabrication. The microfluidic device illustrated in Figure 3.1A was fabricated from borofloat glass using previously described wet-chemical etching techniques.[49] Channels were etched to 15 μm deep with a hydrofluoric acid etching solution. Access holes to the microchannels were drilled with 360 μm diameter drill bits (Tartan Tool Co., Troy, MI). The four perfusion inlet connectors were from Upchurch Scientific (Oak Harbor, WA). The remaining fluidic reservoirs were made in-house from polytetrafluoroethylene (PTFE) tubing obtained from McMaster-Carr (Aurora, OH) and attached to the chip with epoxy (E-6000, Eclectic Products, Inc., Pineville, LA). Epoxy was allowed to cure for 24 hours before chips were used.
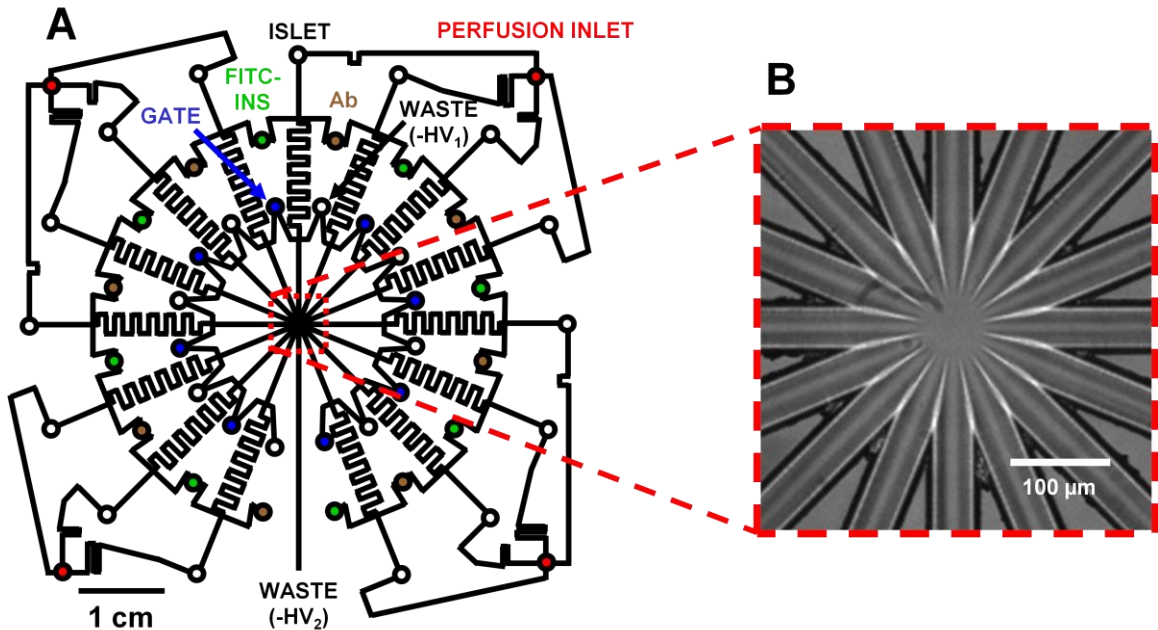
Figure 3.1. Channel layout of a radially designed microfluidic chip for monitoring insulin secretion from 15 independent islets. (A) The channel network of the entire device. Microfluidic channels are indicated by solid black lines, and circles represent fluidic reservoirs. Each type of fluidic reservoir (holding a different solution) is color-coded for clarity. Operation of the chip is described in the Experimental Section. (B) Brightfield image of the detection area taken with the CCD camera.

Microfluidic Chip Preparation and Operation. The microfluidic chip design in Figure 3.1A consists of 15 channel networks, each capable of continuously monitoring insulin levels using an online competitive immunoassay coupled to capillary electrophoresis (CE) separation with fluorescence detection. Flow through the separation channels converges at a common point for fluorescence detection and then continues into a single waste channel.

Electrical connections to 48 of the fluidic reservoirs were made with a chip-electrode interface built in-house. Two separate high voltage power supplies (CZE1000R, Spellman High Voltage Electronics, Hauppauge, NY) were used to apply potential to the waste reservoirs (-HV$_1$ and -HV$_2$) and a single high-voltage relay

(Kilovac, Santa Barbara, CA), controlled by a LabVIEW program, connected the gate reservoirs to ground.

Prior to daily use, channels were rinsed with deionized water by applying vacuum to the common waste ($-HV_2$) reservoir for ~5 min. Chips were then conditioned in a similar fashion with 0.1 M NaOH. After conditioning with pressure-driven flow, electroosmotic pumping of NaOH solution was used to condition channels individually by applying a negative high voltage to the common waste ($-HV_2$) reservoir and grounding the other reservoirs one or two at a time. Using electroosmotic pumping to condition all channel networks simultaneously was not feasible as this produced an electrical current higher than the maximum rating of the power supplies used. Electroosmotic pumping of NaOH in every channel yielded uniform conditioning of the parallel networks and was found to help reduce the variability of flow across the entire chip. After conditioning with NaOH, the chip was flushed again with deionized water and finally with buffer solutions.

For islet experiments, single islets were placed in each islet reservoir access hole with BSS and perfused with a glucose solution. A thin film heating strip (Minco, Minneapolis, MN) was attached to the underside of the chip to maintain islet viability during the experiment by heating the access holes to 37 °C. Solutions of 50 nM FITC-ins and 40 nM Ab (both in immunoassay reagent buffer) were placed in FITC-ins and Ab reservoirs, respectively. Separation buffer was placed in the remaining fluidic reservoirs.

Perfusion of the islets with physiological buffer was accomplished by connecting the perfusion inlets on the chip to a five-port manifold (Upchurch Scientific) with fused-silica capillary (250 μm i.d., 360 μm o.d.) and then to a vial of perfusion solution

contained in a pressurized stainless steel reservoir. This setup allowed the perfusion of 15 independent islets using a single solution. Application of 125 kPa to the reservoir provided a flow of 0.6 μL min^{-1} to each islet. The pressure-driven flow from the perfusion system did not result in any significant hydrodynamic flow within the rest of the microchip because the islet perfusion chambers were open to atmosphere, allowing the majority of flow to exit into the fluidic reservoirs positioned over the islets.

Insulin that was secreted from the islet was sampled electrophoretically by grounding the islet reservoir and applying -4 kV to the common waste ($-HV_2$) reservoir. FITC-ins and Ab reservoirs were also grounded allowing the sampled insulin to mix and react with the immunoassay reagents while flowing through the reaction channels. A potential of $<$-1 kV was applied to the gating waste ($-HV_1$) reservoirs, diverting flow from the reaction channels towards the gating waste ($-HV_1$) reservoirs while the gate reservoirs were at ground. A single high-voltage relay was used to switch all the gate reservoirs from ground to float (open circuit) which allowed small plugs of the reaction mixture to enter the 15 separation channels. Injections of 0.5 s were performed at 10 s intervals. After the gate reservoirs were returned to ground, flow from the reaction channels was again diverted by separation buffer and the sample plugs in the separation channels were separated by CE. Fluorescence detection was performed at the point of separation channel convergence, yielding an effective separation distance of 1 cm.

Separation of the two fluorescent products (bound FITC-ins:Ab and free FITC-ins) allowed comparison of peak heights to be used to quantify the amount of insulin introduced to each channel network. Calibration of the microchip was performed by operating the device while perfusing insulin standards into the chip without the presence

of islets. This allowed specific bound FITC-ins:Ab and free FITC-ins peak height ratios to be assigned to insulin concentrations.

Fluorescence Detection and Data Analysis.   Simultaneous fluorescence detection of all separation channels was accomplished by collecting time-lapse intervals of fluorescence images using an inverted epi-fluorescence microscope (IX71, Olympus America, Inc., Melville, NY). Fluorescence excitation light was from a 300 W Xe arc lamp (LB-LS/30, Sutter Instrument Company, Novato, CA) and passed through a FITC filter cube (Semrock, Rochester, NY) before being focused on the chip detection region with an objective lens (Olympus America Inc., Melville, NY). Emitted fluorescence was collected with the same objective and detected using an electron-multiplying CCD camera (C9100-13, Hamamatsu Photonic Systems, Bridgewater, NJ). In order to image the entire detection region of the chip with the highest light gathering efficiency, a 20x objective lens (0.75 numerical aperture) that allowed for the collecting of 400 x 400 μm^2 images was selected for fluorescence detection. A sample brightfield image taken using this objective (Figure 3.1B) shows all 15 separation channels and the common waste channel within the detection region.

Images were collected at ~28 Hz (to allow for adequate sampling of electrophoresis separations), stored, and analyzed with SlideBook software (Intelligent Imaging Innovations, Inc., Denver, CO). Fluorescence intensities from 35 μm diameter regions of interest that corresponded to each separation channel were extracted to produce parallel electropherograms that were analyzed using software written in-house.[107]

Isolation of Murine Islets. Pancreatic islets were isolated from 20 to 30 g male CD-1 mice as previously described.[108] After isolation, islets were incubated at 37 °C and 5% CO_2 in RPMI cell culture media supplemented with 10% fetal bovine serum, 100 units mL^{-1} penicillin, and 100 μg mL^{-1} streptomycin. Islets were used 1 – 6 days after isolation. Islets chosen for experiments were of average size (100 – 200 μm diameter) and with an intact membrane.

Results and Discussion

Multiplexed Detection with an Electron-Multiplying CCD Camera. By arranging 15 separation channels in a radial fashion, with all flow leading to a common point before exiting through a common waste channel (Figure 3.1), fluorescence detection of all networks could be accomplished using standard fluorescence microscopy with an imaging detector. The detection limit of the system was tested by injecting 8 nM fluorescein for 0.5 s (yielding the introduction of 250 pL of sample) at 10 s intervals while imaging at 28 frames per second. As shown by the electropherograms in Figure 3.2, a reasonable signal to noise ratio was obtained and the limit of detection (LOD) was ~600 pM. LODs as low as 10 pM fluorescein have been reported from the use of scanning laser detection systems with parallel chip designs;[30] however, this value was obtained by continuously flowing fluorescein through separation channels. When a similar experiment was performed with the microdevice and detector used in this study, an LOD of 160 pM was obtained. In contrast, previous reports of groups using fluorescence imaging detection have reported higher LODs (30 nM for 6-carboxy-fluorescein (FAM)).[33]
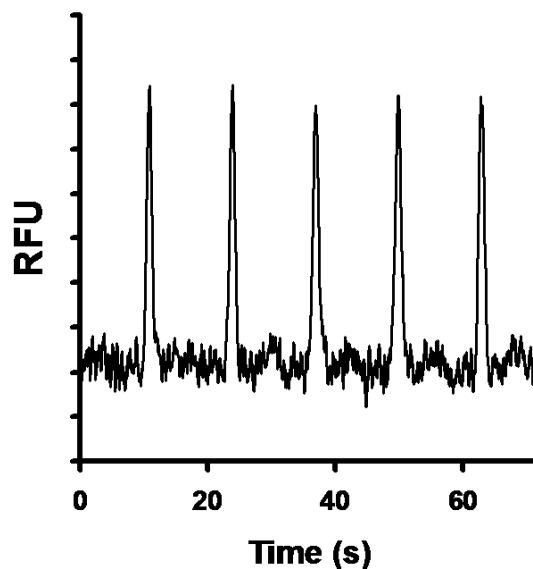
Figure 3.2. Electropherograms obtained by making serial injections of 8 nM fluorescein. Injections and separations were performed in parallel on the device; however, only data from a single network are shown. Data are shown in relative fluorescence units (RFU).

The dynamic range (i.e., concentration window that will yield a change in bound-to-free ratio, B/F) and LOD of a competitive immunoassay are determined in part by the concentration of antibody and labeled antigen used in the assay.[113] For immunoassay dynamic range and LOD comparable to what was previously obtained with the single sample device,[93] it was necessary to use 50 nM FITC-ins (higher concentrations can be useful but give worse sensitivity). Therefore, even though the LOD for fluorescein obtained using the CCD camera on this chip is worse than that achieved with custom-built laser scanning detectors, it is sufficient for achieving detection limits in the immunoassay that are comparable to our previous work. The simplicity and commercial availability of the CCD system for detection make it an attractive alternative for this application.

Microfluidic Chip Design and Performance. After determining that the LOD for the system was adequate, device operation was tested by the collection of serial

immunoassays with online reagent mixing on this system. Typical serial electropherograms collected after mixing FITC-ins, Ab, and insulin online in each channel network are illustrated in Figure 3.3A and B. Each panel shows five separations consisting of a peak for the FITC-ins:Ab complex (bound) and the slower migrating FITC-ins (free). The separations shown in the figure were performed on the same channel but with 1 and 100 nM insulin in the sample respectively. The change in peak heights observed in panels 3.1A and 3.1B was caused by the addition of insulin which shifted the ratio of bound and free FITC-ins through a competitive binding reaction. Relative standard deviation (RSD) for migration times on a single microfluidic network/separation channel are less than 1% (n = 5 separations). RSDs for single channel B/F were less than 3.5% for n = 5 separations with 100 nM insulin. Over 20 min of continuous operation (120 assays) the RSD was slightly larger at ~6%, correlating to ~10 nM insulin.
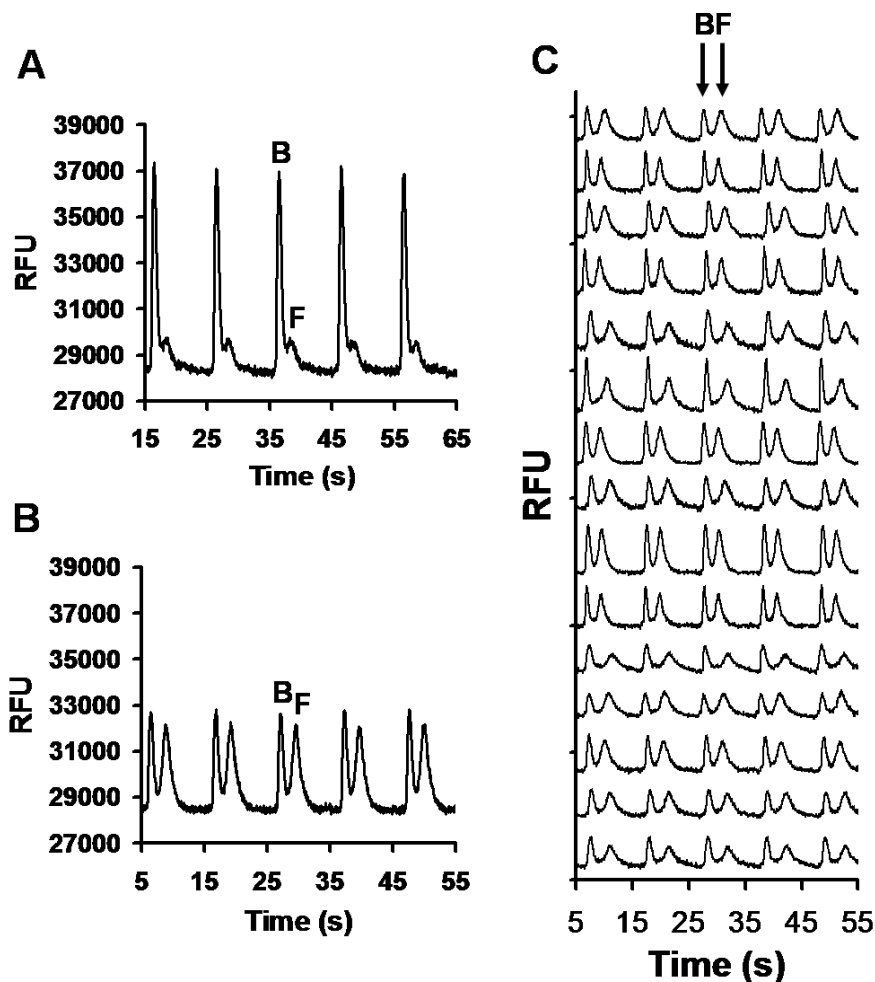
Figure 3.3. Typical serial and parallel electropherograms obtained with online mixing of immunoassay reagents. Injections were made every 10 s. FITC-ins bound complex [B] and free FITC-ins [F] are labeled accordingly. (A) Serial electropherograms collected when mixing 50 nM FITC-ins, 40 nM Ab, and 1 nM insulin standard. (B) Electropherograms collected after the introduction of 100 nM insulin standard into the same channel used in (A). RFU values are shown in (A) and (B) to allow peak height comparisons. (C) Serial electropherograms collected in parallel after introduction of 100 nM insulin standard using all 15 channel networks. Traces are offset for clarity.

Figure 3.3C illustrates serial electropherograms collected in parallel using all 15 networks on the device. Migration time RSD across the entire chip is less than 6%. Although this is an increase from the previous four-sample chip (migration time RSD = 2%), it is acceptable as a variation of this magnitude does not significantly slow the rate at which immunoassays can be completed. Good reproducibility between networks is

important for separations in parallel using a single relay for injections because serial analyses can only be performed as fast as separations occur on the slowest channel. The averaged B/F RSD across all 15 channels was 11.7%.

Application of -4 kV to the common waste ($-HV_2$) reservoir yielded electrical current that was close to the maximum rating of the power supply. Thus, the power available limited the electric field to ~400 V cm^{-1}, which was 1/3 lower than previous chips, producing slower separations and reducing temporal resolution from 6 s to 10 s. Although lower, 10 s injection frequency is still adequate for the characterization of single islet insulin secretion dynamics. It is feasible that a power supply with a higher power rating can be used for faster separations. It is also possible to reduce the channel depth to yield lower current and faster separations, but we found that this decreased detection sensitivity; therefore a channel depth of 15 μm was used as the best compromise with this power supply and detector.

Calibration. The device was calibrated by perfusing insulin standards (dissolved in BSS) into the islet reservoir while monitoring B/F by online immunoassay. Typical calibration curves for all 15 networks collected simultaneously are shown in Figure 3.4. While the curves vary slightly in shape and slope, all have the expected dose-response shape characteristic of competitive immunoassays.[113] The reason for variation in dose response curves among the different channels is not clear. Reports of other parallel microfluidic chips have discussed non-uniform flow characteristics across a single device,[26,30,48] and it is possible that the variations observed in curve shape are due to slightly different FITC-ins and Ab mixing ratios resulting from non uniform channel surfaces properties. To ensure that the variation between calibration curves did not affect

the calculated insulin levels in any particular network, each network was calibrated before an islet experiment.
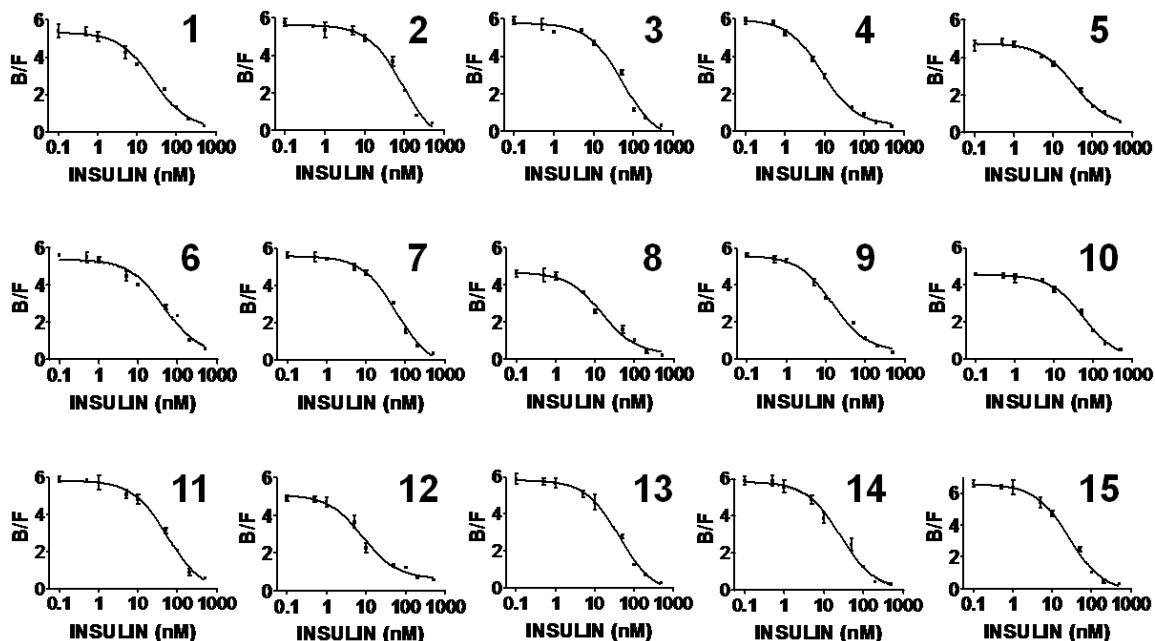
Figure 3.4. Calibration curves for all 15 networks obtained with insulin standards (0.1 nM – 500 nM) and the online immunoassay. Numbers in upper right corner of each plot indicates channel network number. Error bars are ±1 standard deviation. Data points are averages of five consecutive electropherograms.

Although the curves are variable enough to require individual calibration of each channel, the dynamic range in each curve was consistently useful for single islet experiments. Calibration curves ranging from 5 to 200 nM insulin (corresponding to B/F ratios typically observed from an islet) were collected each day before an experiment. The LODs (calculated as the concentration of analyte required to produce a change in B/F that is greater than 3 times the standard deviation of the background B/F) from the calibration curves in Figure 3.4 were between 0.5 and 1 nM insulin.

Comparison to Four-sample Parallel Microchip. The 15-sample microchip offers several significant advantages over the previously developed four-sample device.[49]

The increase in throughput is a result of both the inclusion of a radial design of channel networks and the modification of the microfluidic flow-gate injector that was used on the four-sample chip. The type of flow-gate injector used on these chips allows for periodic sampling from the continuously flowing reaction mixtures. The previously used injector type was designed to minimize the number of power supplies needed for analysis;[119] however, this necessitated waste channels running parallel to separation channels to also pass through the detection area, ultimately decreasing the number of parallel analyses that can be performed. In contrast, the design used here has flow-gate injectors with decoupled waste channels controlled by a second power supply, eliminating the need for waste channels to run parallel to separation channels and allowing for increased separation channel density within the detection area.

In addition to the increase in throughput, LOD was improved 10-fold in comparison to the four-sample chip that used a commercial scanning confocal detector. This improvement in LOD can be attributed to the increased sensitivity of the detection scheme which has allowed for a decrease in immunoassay reagent concentrations (currently 50 nM FITC-ins and 40 nM Ab, previously 250 nM FITC-ins and 250 nM Ab). This improved LOD is significant as it allows for quantification of lower amounts of insulin that are secreted from an islet in low glucose conditions. The previous four-sample chip had an LOD of 10 nM insulin which corresponds to 35 pg min^{-1} at 0.6 μL min^{-1} islet perfusion. Because observed average secretion rates from islets perfused at 3 mM glucose are close to this value, this detection limit was barely sufficient to detect this lower level of release. The 15-sample chip has an LOD of less than 7 pg min^{-1} using the

same perfusion conditions meaning that basal secretion can be routinely detected and quantified with this device.

Parallel Measurement of Insulin Release from Pancreatic Islets. Functionality of the 15-sample microchip was tested by simultaneously monitoring insulin secretion from 15 individual islets stimulated with glucose. Figure 3.5A represents 15 insulin secretion profiles from independent islets stimulated with a 3 mM to 11 mM glucose step change. A variety of secretion dynamics that are typical of isolated islets are seen among the 15 profiles including pronounced 1st phase "bursts" and oscillatory secretions.[87,120] An averaged plot of all 15 profiles (illustrated in Figure 3.5B) shows a biphasic insulin secretion profile that is characteristic of pancreatic endocrine tissue stimulated with elevated glucose.[103,121] These results demonstrate the usefulness of a high throughput single islet monitoring system by showing the capability of obtaining information on the single entity level as well as data that can be made into averaged plots (commonly used for islet comparisons between islet types). Single islet data is important because it gives information pertaining to the dynamics of insulin secretion, which can be just as critical as the amount of insulin released.[122]
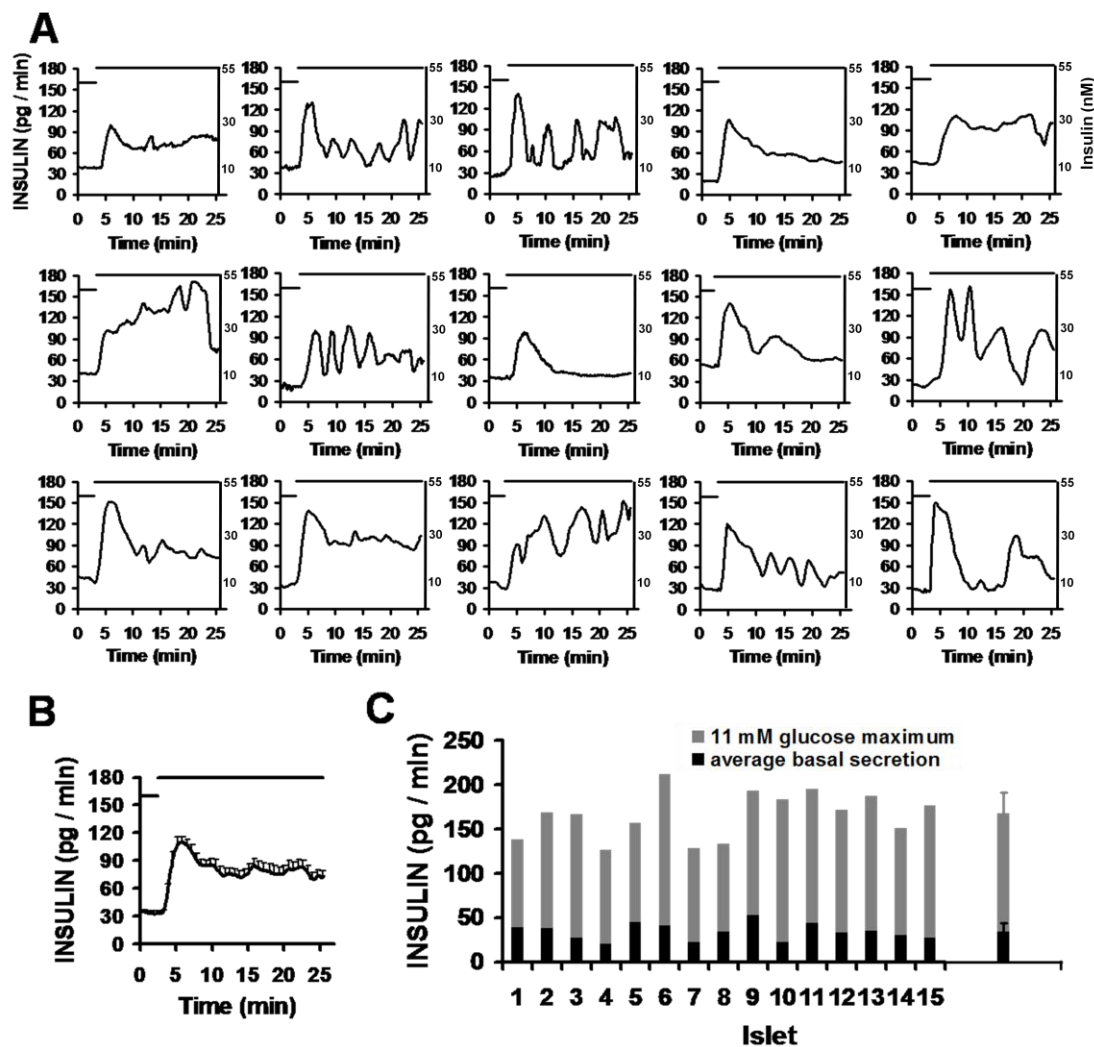
Figure 3.5. (A) Plots showing insulin release rates from single islets collected in parallel using the 15-sample device. Perfusion glucose concentration is indicated by bars placed above plots (low bar = 3 mM, high bar = 11 mM). **(B)** Plot showing average insulin secretion rate from the 15 islets in (A). Error bars are ± standard error of the mean and placed every other data point for clarity. **(C)** Comparison of average basal secretion rates (3 mM glucose) and maximum insulin release rates after 11 mM glucose stimulation of all 15 islets. Average bars (error bars ±1 standard deviation) show good reproducibility between basal and stimulated insulin secretion rates.

The results obtained from the 15-sample system agree well with previous observations. The measured basal rates of insulin secretion (34 pg min^{-1} at 3 mM glucose) are similar to what has been previously observed in our lab (27 pg min^{-1} with the four-sample design and 47 pg min^{-1} with the single sample chip). This value is also comparable to basal secretion rates at 3 mM glucose reported by other groups (20 – 26 pg

min^{-1}) using islet perfusion techniques.[123] As shown by Figure 3.5B and C, the basal and peak rate of secretion across individual islets is similar in magnitude. These results suggest good reproducibility of the perfusion method as well as the sampling of insulin across all 15 networks on the device.

Of the 15 islets reported here, approximately 40% showed oscillations over the 17 min period of elevated glucose. Oscillations observed in the single islet plots range in duration from 3 to 5 min, agreeing with what has been noted in previous studies that have monitored insulin secretion and Ca^{2+} flux (increase in intracellular Ca^{2+} concentration triggers insulin exocytosis)[124] in isolated mouse islets.[114,125,126]

The averaged insulin secretion plot in Figure 3.5B required 2200 immunoassays collected continuously at a rate of 90 per minute. This high throughput made the experiments shown here possible and illustrates the potential of microfluidic devices for automating complex cellular measurements. This system also has a significant cost savings as the cost of reagents used was ~$0.01 per assay, less than the approximate $0.04 per assay using the four-sample chip and $0.15 per assay with the single sample device for experiments of the same length. Clearly, these devices illustrate a vast improvement over typical insulin immunoassay kits that may cost over $5 per assay.

Conclusions

We have developed a high throughput microchip for monitoring cellular secretions from 15 independent biological samples using a radial alignment of separation channels that is compatible for detection using an epi-fluorescence microscope and CCD camera. Testing of the device was accomplished by continuously monitoring insulin

secretion from 15 individual pancreatic islets in parallel at 10 s intervals. While the sensitivity of this camera based method is not as good as what has been reported with specially built scanning laser-induced fluorescence detectors, it has been shown to be adequate for monitoring insulin secretion from islets and shows promise for use in other types of assays.

Further scale up of the number of parallel systems is feasible. Important factors affecting the number of channel networks that can be placed on a device with a radial design include network complexity, detection area size, and imaging resolution. Complex networks that allow for integrated functioning (such as precolumn reactors and multiple perfusion lines in this chip with their associated reservoirs) occupy more area on the chip surface than simple CE designs, thus limiting the number of networks that can be incorporated. Detection area can also become limiting because the detection zones for all channels must fit within the field of view of the camera. Using smaller channel widths can offset this problem somewhat. Use of lower magnification objectives can also be used to allow for a larger detection region, but this may decrease sensitivity as a result of using a lower numerical aperture for collection of fluorescence. Image resolution is also an important consideration in the number of channels that can be incorporated. In order to prevent cross-talk between networks, the collected fluorescence images must be of high enough resolution to completely resolve adjacent channels on the chip.

CHAPTER 4

INVESTIGATION OF LEPTIN SIGNALING IN PANCREATIC ISLETS USING HIGH THROUGHPUT SINGLE ISLET SECRETION MEASURMENTS PERFORMED ON A MICROFLUIDIC CHIP

Introduction

The hormone leptin, secreted from adipose tissue, is known to regulate stored energy in the body through interactions at the hypothalamus controlling appetite and energy expenditure.[127-129] While these actions have been well characterized, the ability of leptin to lower high circulating levels of insulin in ob/ob mice (lacking the ability to produce leptin)[130] and the discovery of leptin receptors on pancreatic cells[131,132] has suggested a direct effect of leptin on endocrine pancreas function. Indeed, several studies have reported leptin having an inhibitory effect on insulin secretion from isolated pancreatic islets and β-cells,[133-135] supporting the presence of a proposed insulin/leptin feedback loop.[135] Levels of leptin in the body are proportional to fat mass, and according to the proposed feedback loop, an increase in adiposity and thus leptin would reduce insulin production and direct less energy to the formation of adipose tissue. This mechanism is hypothesized to assist in maintaining nutrient balance, and disruption would contribute to obesity and hyperinsulinemia associated with diabetes. However, it must be stated that some studies have shown leptin to either enhance[136] or not affect[137] insulin release, and that the function of the adipoinsular axis described above is still debated.

Research in this field has lead to a number of proposed leptin action mechanisms on β-cells, summarized in Figure 4.1. It is thought that leptin signaling in islets directly affects insulin production and secretion. Investigating leptin signaling often utilizes mutated mice that lack functional leptin receptors throughout the body (db/db). However, as these mice have receptor defects in various tissues, it is difficult to correlate observed results with specific effects of leptin on the pancreas. In an effort to probe the direct effects of leptin on the endocrine pancreas, the Kulkarni Lab has developed a mouse model lacking leptin receptors (ObR) only in the pancreas using the Cre-*loxP* technique.[94]
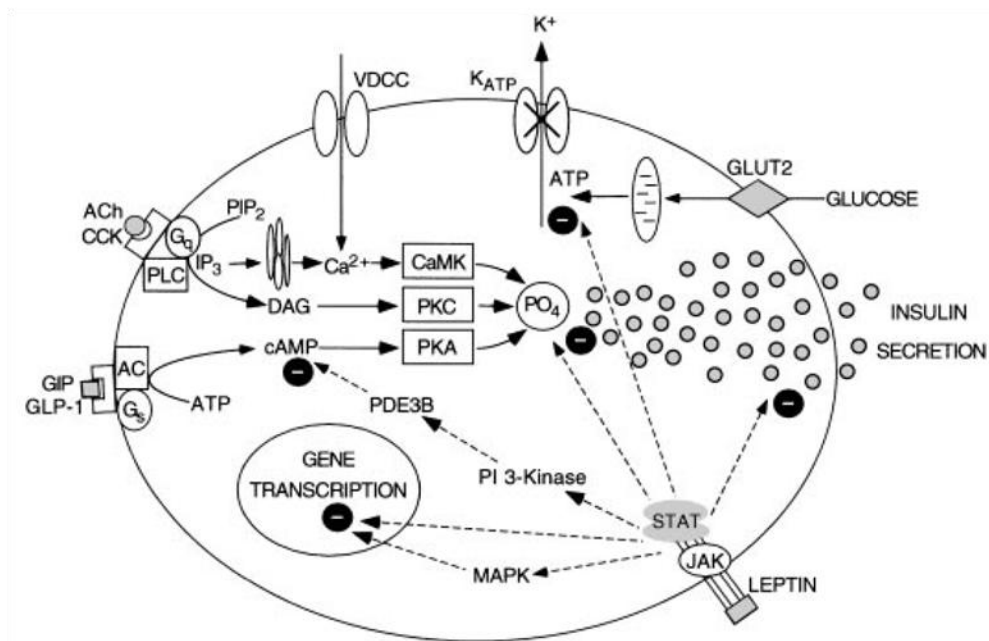
Figure 4.1. Proposed effects of leptin signaling on the pancreatic β-cell. The binding of leptin to cell receptors may activate the janus kinase/signal transducer pathway (JAK/STAT), eventually leading to inhibition of preproinsulin gene transcription. Several other leptin action possibilities, for example involving phosphoinositide 3-kinase and cyclic AMP, are hypothesized that ultimately lead to the inhibition of insulin secretion through various pathways. Reproduced from reference 135.

In a collaborative study, the 15-sample microchip for parallel monitoring of insulin secretion (described in Chapter 3) was used to perform in vitro analyses on islets

from pancreas-specific leptin ObR knockout mice (KO) and control (ObRlox) animals. In addition to probing potential leptin action pathways in islets by monitoring insulin release from islets stimulated under various conditions, these experiments served as an evaluation of the device for real islet studies involving a variety of experimental protocols. Presentation of in vitro secretion data is accompanied by comparisons to results from in vivo experiments (e.g. live animal insulin secretion assays and glucose tolerance tests) performed by collaborating research groups for investigations into potential mechanisms involving in leptin signaling.

Experimental Section

Chemicals and Reagents. Unless otherwise noted, all reagents were from Fisher (Pittsburgh, PA). Cell culture reagents were from Invitrogen (Carlsbad, CA). Tricine, electrophoresis grade, was purchased from MP Biomedicals (Aurora, OH). Collagenase type XI, insulin, ethylenediaminetetraacetic acid (EDTA), Tween 20, mouse recombinant leptin, glibenclamide, fatty acid-free bovine serum albumen (BSA), and palmitic acid were from Sigma (St. Louis, MO). Fluorescein isothiocyanate-labeled insulin (FITC-ins) and Fura-2 calcium dye were obtained from Molecular Probes (Eugene, OR), and monoclonal antibody (Ab) to human insulin was from Biodesign International (Saco, ME). Glucagon-like peptide-1 (7-36) amide (GLP-1) was from Bachem (Torrance, CA). All solutions were made with 18-MΩ deionized water from a Millipore (Bedford, MA) Milli-Q filtration system and filtered with 0.2 μm nylon syringe filters.

Buffer Preparation. Balanced salt solution (BSS) consisted of 125 mM NaCl, 5.9 mM KCl, 1.2 mM $MgCl_2$, 2.4 mM $CaCl_2$, and 25 mM tricine. Krebs ringer buffer

(KRB) was 118 mM NaCl, 5.4 mM KCl, 2.4 mM $CaCl_2$, 1.2 mM $MgSO_4$, 1.2 mM KH_2PO_4, and 20 mM HEPES. Buffer for immunoassay reagents was 50 mM NaCl, 1 mM EDTA, 20 mM tricine, 0.1% (w/v) Tween 20, and 0.7 mg mL^{-1} BSA. Separation buffer consisted of 20 mM NaCl and 150 mM tricine. All buffers were adjusted to pH 7.4 with NaOH.

Animal and Islet Preparation.   Experiments were performed using a mouse model that was deficient in leptin receptors only in the pancreas.   Mice were developed by the Kulkarni Lab using the Cre-*loxP* technique as previously described.[94,138]   All animals were housed in specific pathogen free facilities, had free access to food and water, and were maintained on a 12 hr light/dark cycle. Islets were isolated from the animals using previously described methods.[108] Size-matched islets used in experiments had a spherical shape and smooth surface indicative of an intact membrane.

Parallel Microfluidic Assay for Insulin.   Insulin release from single islets was measured in parallel using a 15-sample microfluidic chip. The design and function of this microdevice was based on previous secretion monitoring techniques developed in our lab.[49,93]   Briefly, 15 single islets were loaded onto the device and perfused with BSS containing various amounts of glucose, leptin, palmitic acid, glibenclamide, or GLP-1. Portions of the islet perfusate streams were reacted with 50 nM FITC-ins and 40 nM Ab on the chip for a competitive immunoassay for insulin. Immunoassay products were separated and detected every 10 s with parallel capillary electrophoresis and multiplexed fluorescence detection.   Parallel electropherograms were produced with Slidebook software (Intelligent Imaging Innovations, Inc., Denver, CO) and analyzed using Cutter software.[107]

Intracellular Calcium Flux Measurements. Intracellular calcium levels in islets were measured with Fura-2 using methods based on previously described techniques.[139,140] Briefly, islets were loaded with 2 μM Fura-2 dye for 45 min at 37ºC prior to experiments. Islets were washed in KRB, loaded into a microfluidic perfusion chamber and perfused with glucose and various drugs of interest. Once perfused, the dye was excited by 340 nM (Ca^{2+} complex) and 380 nM (free dye) light and the emission at 510 nM was collected, ratioed, and converted to Ca^{2+} concentration.

Results

Effects of Leptin on Glucose-stimulated Insulin Release. Isolated islets from pancreas-specific leptin receptor knockout (KO) and control (ObRlox) mice were tested for insulin release and Ca^{2+} flux (a precursor to insulin release) while stimulated using glucose with or without the presence of leptin. Results, illustrated with averaged plots, are shown in Figure 4.2. KO islets showed significantly higher levels of both Ca^{2+} flux and insulin release compared to ObRlox islets (statistical analysis, performed here and throughout this chapter by comparing the averaged areas under the curve with an unpaired 2-tailed Student's *t* test, gave $P < 0.05$), suggesting that inhibition of leptin signaling in islets from lean animals may enhance pathways leading to glucose-stimulated insulin secretion. Additionally, control ObRlox islets showed noticeably inhibited insulin release when perfused with elevated glucose and 10 nM leptin compared to those perfused with only glucose ($P < 0.05$). Traces from KO islets with and without leptin were not significantly different from each other in either insulin or Ca^{2+} plots.
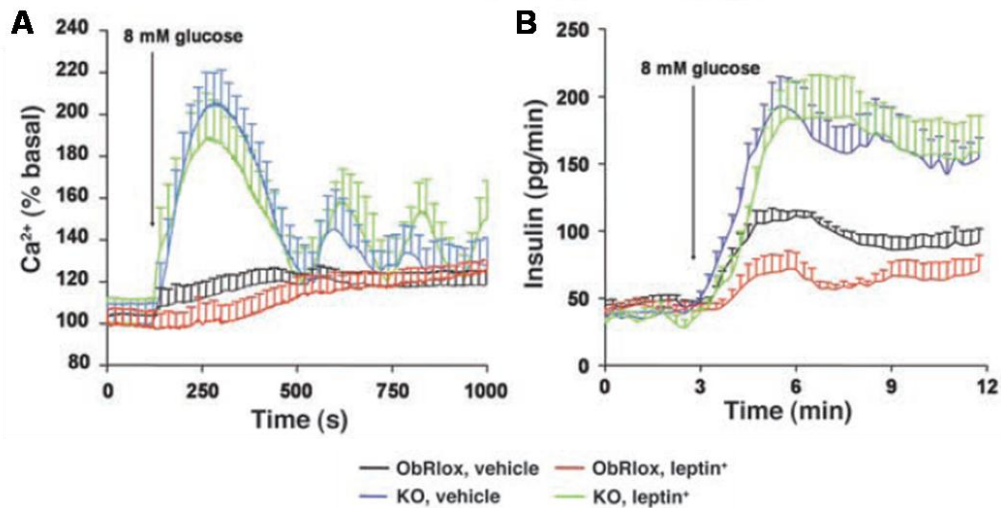
Figure 4.2. Representative traces of intracellular Ca^{2+} flux (A) and insulin secretion (B) measured in primary size-matched islets isolated from 6-month-old male ObRlox and KO mice with or without 100 (A) or 10 nM leptin (B). Error bars, placed every other point for clarity, are ± standard error of the mean (SEM). Each data set is n = 6 islets. Reproduced from reference 94.

Acute and Chronic Exposure to Fatty Acid. Acute free fatty acid (FFA) exposure experiments were performed by assaying insulin release while perfusing islets with glucose and 0.5 mM palmitic acid (±10 nM leptin). Results are shown in Figure 4.3. In both islet types, acute stimulation with FFA and no leptin yielded increases in insulin release, though only significant ($P < 0.05$) in 15 mM glucose regions. However, perfusion of ObRlox islets with 10 nM leptin resulted in no significant ($P > 0.05$) decrease in insulin release compared to traces collected with no leptin either in the presence or absence of FFA. It is thought that the previously observed inhibitory effect of leptin (Figure 4.2) may have been masked by the presence of bovine serum albumin (BSA) in perfusion buffer (present for appropriate FFA action on cells). Previous studies have also noticed this effect.[133] A large proportion of plasma leptin (up to 98% in lean humans) is thought to be bound to serum proteins,[141] suggesting that the effects of endogenous leptin may be diminished in the presence of BSA.
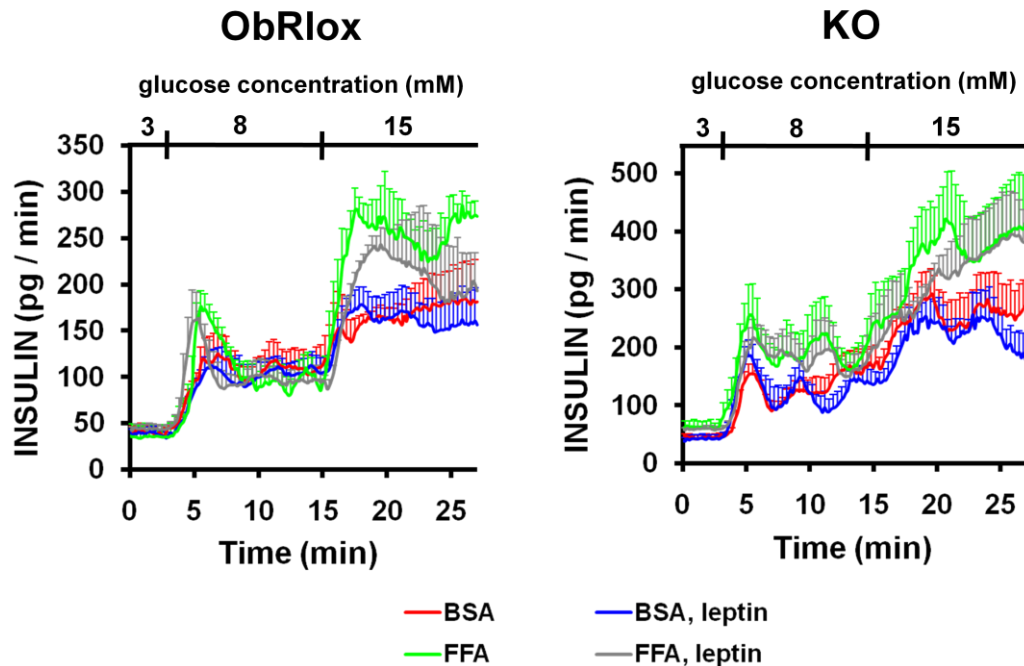
Figure 4.3. Effects of acute FFA exposure on ObRlox (left) and KO (right) islets. Data sets are from islets perfused with glucose solution (± 10 nM leptin) containing 0.5 mM palmitic acid (FFA) or FFA-free BSA (BSA). Error bars are ± SEM. For all sets, n ≥ 5.

Chronic exposure of islets to FFA has been shown to inhibit glucose stimulated insulin release through proposed mechanisms involving β-cell metabolism,[142,143] signal transduction,[144] and gene transcription.[145,146] As illustrated in Figure 4.4, both islet types showed a decrease in insulin release after a 48 hr incubation in RPMI media supplemented with 0.5 mM palmitic acid compared to incubation with FFA-free BSA. ObRlox islets treated with FFA showed a significant decrease ($P < 0.05$) in released insulin compared to BSA treatment only after perfusion with 15 mM glucose. KO islets with these treatments, however, showed significant decreases in both 8 and 15 mM glucose regions of the plot compared to control experiments. While administration of leptin to KO islets showed no effect as expected, ObRlox islets secreted less insulin during perfusion of 10 nM leptin compared to only glucose for both BSA and FFA treatments.
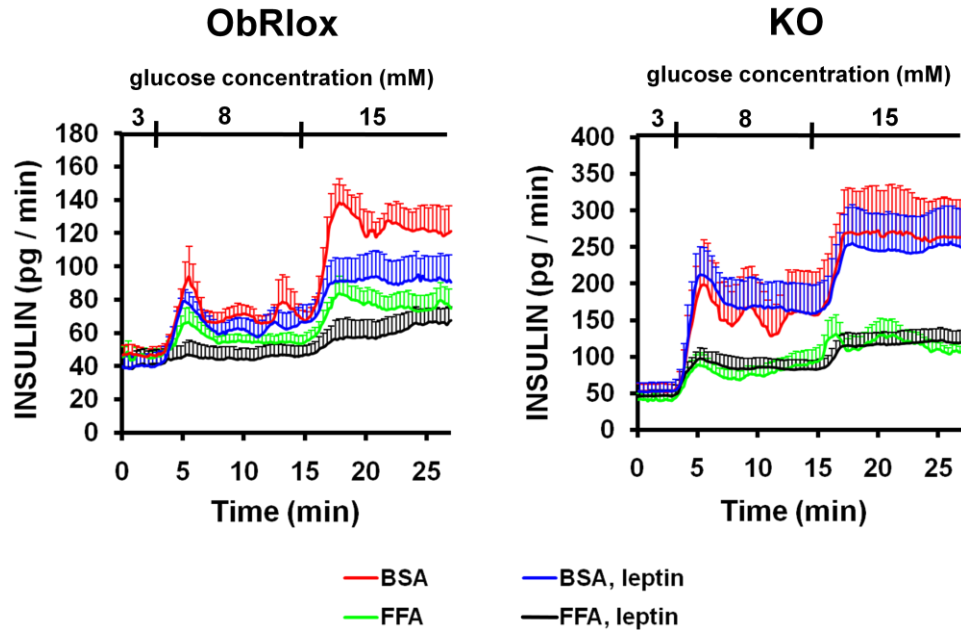
Figure 4.4. Effects of chronic FFA exposure on ObRlox (left) and KO (right) islets. Data sets are from islets incubated for 48 hrs in either 0.5 mM palmitic acid (FFA) or control cell media (BSA), and then perfused with 8 and then 15 mM glucose (± 10 nM leptin). Error bars are ± SEM. Each data set is n ≥ 5 islets.

Stimulation of Islets with Sulfonylurea. To assess the possible interaction of leptin signaling pathways and K_{ATP} channel-independent secretion, insulin release was measured from control ObRlox and KO islets stimulated with glibenclamide in either 3 mM or 8 mM glucose with or without the presence of 10 nM leptin. Results are presented in Figure 4.5. KO islets show significantly higher release ($P < 0.05$) compared to control ObRlox islets in glibenclamide and 8 mM glucose. Additionally, while no effect of leptin on KO islets was observed, it seemed to have a mild, though not significant, inhibitory effect on secretion from ObRlox islets in the presence of 8 mM glucose. Ca^{2+} flux measurements using the same protocol (data not shown) showed no difference in intracellular Ca^{2+} levels between both types of islets with or without leptin, suggesting the differences in observed secretion levels are not due to enhanced Ca^{2+} permeability of cells.

72
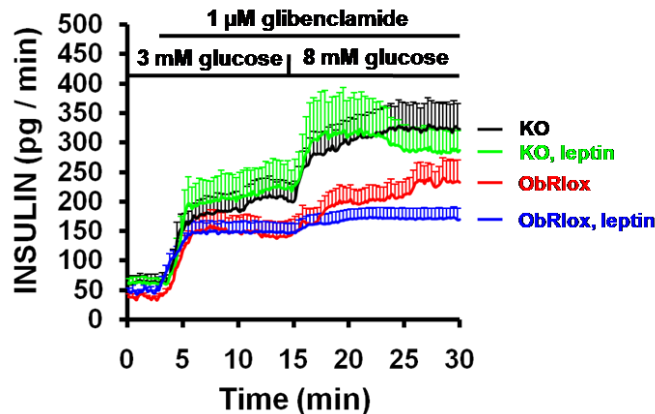
Figure 4.5. Insulin release from ObRlox and KO islets stimulated with glibenclamide with or without 8 mM glucose or 10 nM leptin. Error bars are ± SEM, all data sets are n ≥ 7.

Effects of GLP-1 and Leptin on Insulin Secretion. A final series of experiments investigated potential leptin interaction with GLP-1 signaling. ObRlox and KO islets were stimulated with glucose and GLP-1 in the presence or absence of leptin. Results, illustrated in Figure 4.6, show a number of interesting trends. For both types of islets, the addition of GLP-1 (red traces) yielded significantly ($P < 0.05$) higher rates of insulin secretion compared to islets perfused with glucose only (black traces), agreeing with previous studies showing GLP-1 to enhance glucose-stimulated insulin release.[147] Additionally, leptin is shown to produce a significant ($P < 0.05$) inhibitory effect on secretion from ObRlox islets both with and without the presence of GLP-1 (red trace vs. green trace and black vs. blue in Figure 4.6). Interestingly, there is no significant difference between secretion from ObRlox islets stimulated with glucose, GLP-1, and leptin compared to glucose only, suggesting leptin-inhibited insulin release from control islets is reversed upon the addition of GLP-1. These results are consistent with leptin signaling interacting with GLP-1 pathways in islets, though, further islet functionality studies as well as investigations into expression of known GLP-1 signaling intermediates are needed to probe signaling pathways involved with these findings.
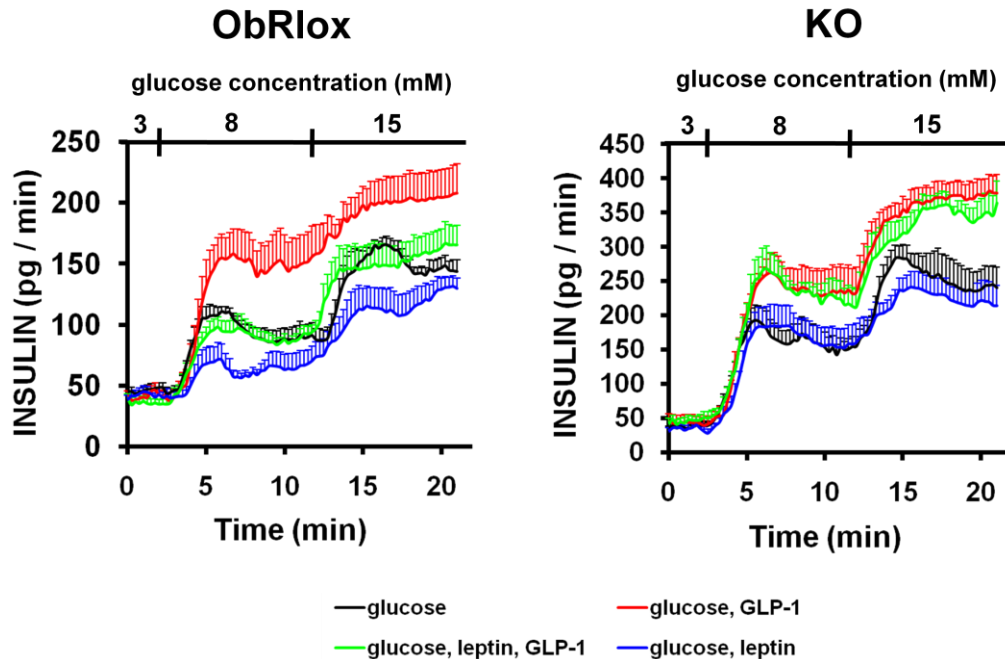
Figure 4.6. Insulin release from ObRlox (left) and KO (right) islets perfused with glucose with or without the presence of either 10 nM leptin or 10 nM GLP-1. Perfusion of leptin and GLP-1 was in 8 and 15 mM glucose only. Error bars are ± SEM and all data sets are n ≥ 5.

Discussion

Comparison with in vivo Observations. Data showing enhanced insulin secretion resulting from the removal of leptin receptors from islets (Figure 4.2) complements observations from experiments on living animal models. The effects of pancreas-specific ObR removal on in vivo β-cell secretory function were investigated by collaborating labs through a collaborative effort by monitoring glucose-stimulated insulin secretion in live animals.[94] KO animals of both sexes showed enhanced insulin release two minutes after an i.p. glucose challenge compared to control (Figure 4.7A). Additionally, KO mice showed lower glucose excursion after i.p. injection of glucose, consistent with increased glucose tolerance (Figure 4.7B). The results are consistent with inhibition of leptin signaling leading to enhanced insulin release.
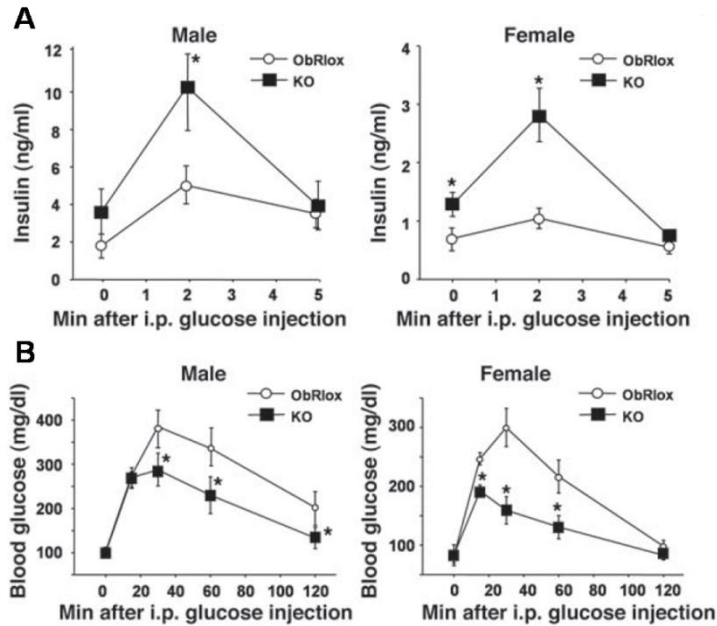
Figure 4.7. Early-phase insulin release and glucose tolerance were improved in pancreas ObR-KO mice compared to ObRlox controls. (A) Plasma insulin levels after injection of glucose (3 g kg^{-1} body weight) in 6-month old mice of both types. (B) Blood glucose levels after injection of glucose (2 g kg^{-1} body weight). For all plots, *P < 0.05 compared to ObRlox controls and n ≥ 6. Error bars are ± SEM. Reproduced from reference 94.

To assess if the observed increase in acute insulin release (Figure 4.7A and Figure 4.2) and improved glucose tolerance (Figure 4.7B) in KOs could provide protection from the effects of diet induced obesity, mouse types were fed with a high fat diet (HFD). After 12 weeks on HFD, both mouse types showed similar weight gain and insulin resistance compared to control groups on normal chow (data not shown). Interestingly, KO animals showed impaired glucose tolerance resulting from decreased acute in vivo insulin response to glucose compared to ObRlox controls (Figure 4.8A & B). Additionally, KO animals showed significantly reduced islet mass compared to controls after HFD (Figure 4.8C). These results suggest that KO animals may be more susceptible to lipotoxic effects.
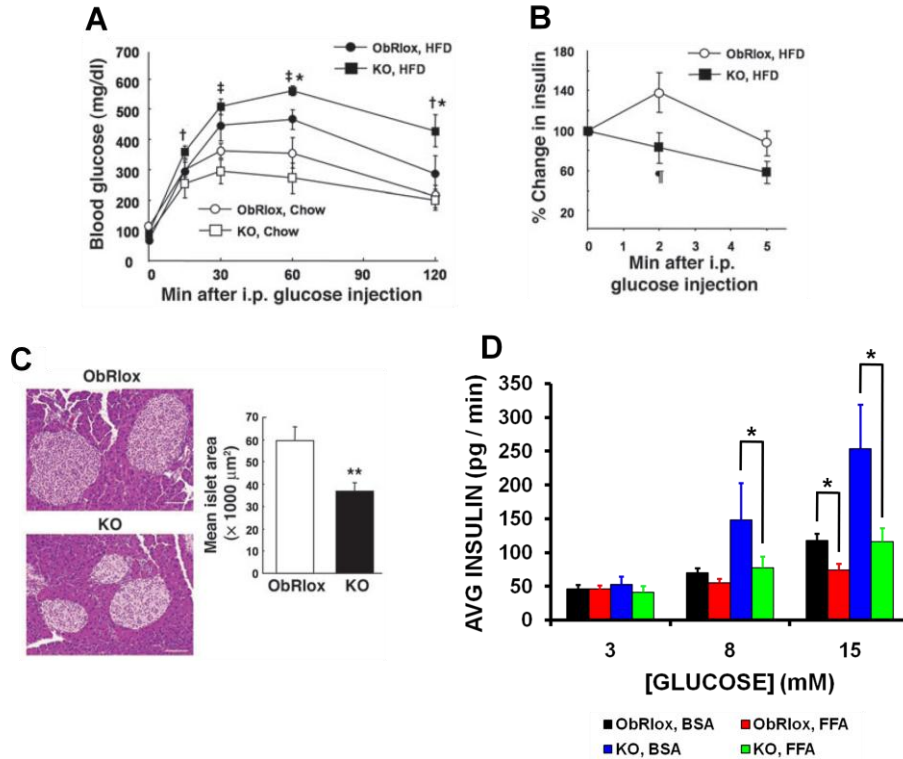
Figure 4.8. Effects of diet-induced obesity on islet function and size. (A) Glucose tolerance test results for 4-month-old male mice of both types on regular chow (Chow) or high fat diet (HFD) for 12 weeks. *P < 0.05 for KO versus ObRlox mice both on HFD, n = 5; †P < 0.05, ‡P < 0.01 for KO mice on HFD versus KO mice on Chow, n = 5 (KO) or 3 (Chow). (B) Change in insulin levels after glucose injection (3 g kg^{-1} body weight) in mice on HFD for 12 weeks. ¶P = 0.07; n = 4. (C) Left: Hematoxylin and eosin staining in representative pancreas sections of mice on HFD for 12 weeks. Scale bars = 100 μm. Right: Mean islet area from ≥ 10 islets from 5 mice for each genotype. Error bars are SEM. **P < 0.01 versus ObRlox. (D) Plot comparing averaged insulin secretion rates from islet data presented in Figure 4.4 (only treatments without the presence of leptin). *P < 0.05. Error bars are ± SEM. (A), (B), and (C) are reproduced from reference 94.

Results from isolated islet FFA incubation experiments complement these observations. A plot comparing average insulin release (from data presented in Figure 4.4) from each islet type for BSA and FFA incubations is shown in Figure 4.8D. Insulin release from KO islets decreased by 48% and 54% for 8 and 15 mM glucose stimulations, respectively, after FFA incubation. In comparison, ObRlox control islets decreased by only 21% and 37%, suggesting that islets from animals with pancreas ObR deletion may be more susceptible to FFA incubation-induced effects. These results indicate that islets developed without leptin signaling may have inferior lipid regulation mechanisms

76

compared to control islets and thus are more susceptible to FFA-induced lipotoxic effects.

Proposed Mechanisms of Leptin Effects on Islets. Islet types were investigated with immunohistochemical analysis (by collaborating researchers) to probe if disruption of leptin signaling affects islet morphology. KO islets were found to have a 2-fold increase in β-cell mass secondary to an increase in size, but unlikely due to enhanced mitosis or altered β-cell apoptosis (data not shown). Western-blotting analysis of islet lysates showed increased phosphorylation of PKB/Akt at Ser473 (p-Akt), p70 S6 kinase at Thr389 (p-p70S6K), and FoxO1 at Ser256 (p-FoxO1) in KO islets by 2.1-, 1.3-, and 4.3-fold, respectively, compared to ObRlox islets (Figure 4.9A). p70S6K and PKB/Akt are important for determining β-cell size and survival, respectively,[148-150] suggesting that absence of leptin action improves β-cell growth via these pathways.
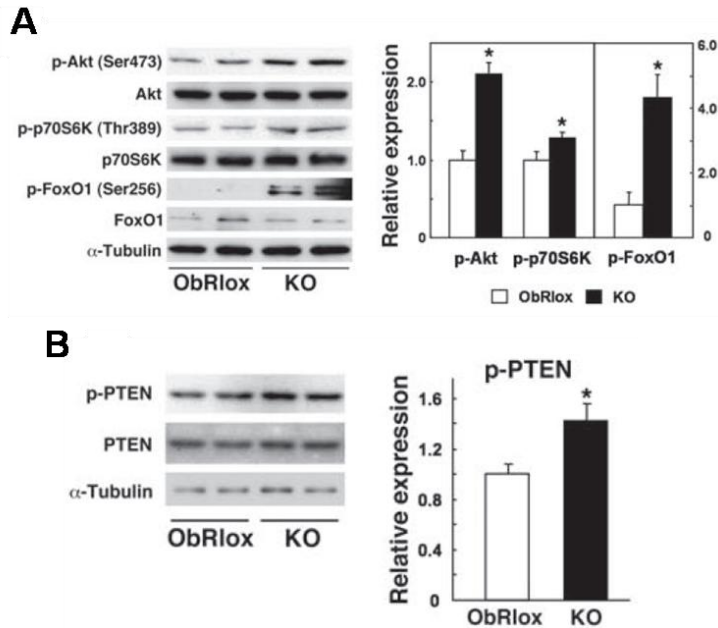
Figure 4.9. Increased expression of insulin signaling proteins in islets from KO mice. (A) Western blot analysis of islet lysates for p-Akt (Ser473), Akt, p-p70S6K (Thr389), p70S6K, p-FoxO1 (Ser256), FoxO1, and α-tubulin as a control. The relative expression of p-Akt, p-p70S6K, and p-FoxO1 normalized to each total protein is shown in the plot on the right. *P < 0.05 versus ObRlox; n ≥ 4. (B) Western blot analysis for p-PTEN, PTEN, and α-tubulin. The relative expression of p-PTEN in KO and ObRlox islets is shown in the graph. *P < 0.05 versus ObRlox; n = 4. Reproduced from reference 94.

A recent report showed phosphatase and tensin homolog (PTEN), a negative regulator of the PI3K/Akt pathway, to be regulated by leptin in pancreatic β-cells.[151] To investigate the effects of inhibited leptin signaling on phosphatase activity, western-blotting analysis for PTEN was performed on islet lysates. Results in Figure 4.9B show a mild upregulation of PTEN phosphorylation (p-PTEN) in KOs compared to ObRlox controls with no difference in total PTEN expression. This enhanced PTEN phosphorylation in KOs may indirectly increase signaling in the PI3K/Akt pathway in islets (shown in Figure 4.9A) since phosphorylation of PTEN leads to inactivation of its phosphatase activity.

In addition to these proposed roles in islet growth and development, leptin is thought to protect islets from lipid overload and nonoxidative metabolic products of fatty acids by increasing β-oxidative metabolism of surplus fatty acids and reducing lipogensis.[152,153] Prior studies showing that expression of ObRs in islets of Zucker diabetic fatty rats decreased accumulation of lipid content illustrate this potential role for leptin in lipid metabolism and storage.[152] The islet secretion results shown in Figure 4.4 and in vivo results from Figure 4.8 also suggest a role for leptin in regulating lipid metabolism in islets. It is appealing to hypothesize that the decreased in vivo secretory response and islet size in KO animals after HFD is due to secondary effects of lipid overload caused by inhibited leptin signaling. An outline summarizing this possibility is illustrated in Figure 4.10. However, further investigation into specific connections between leptin signaling, lipid metabolism, and islet growth factors are needed.
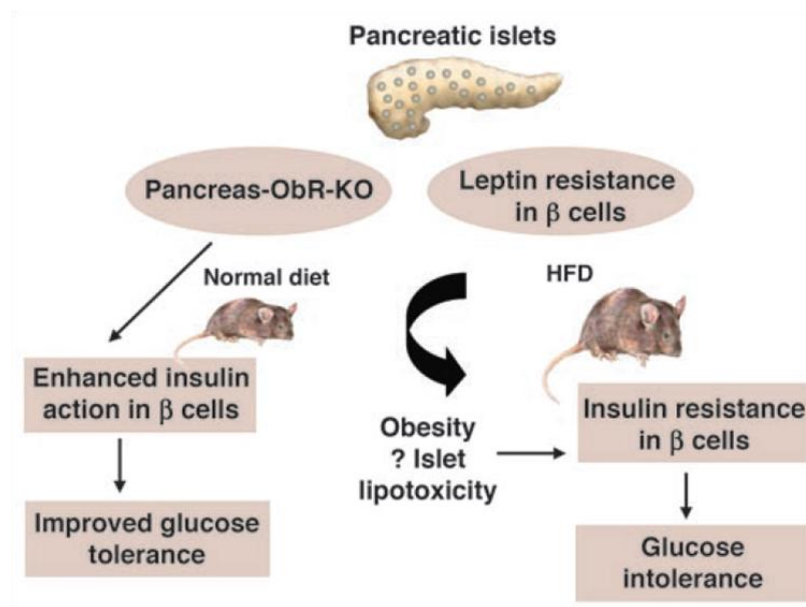
Figure 4.10. Proposed pathway for leptin signaling in the development of diabetes. Reproduced from reference 94.

Further experiments probing mechanisms behind leptin action on islets were performed by observing insulin release stimulated with sulfonylurea and GLP-1. Sulfonylurea, a class of drug that stimulates insulin release through the direct action of closing K_{ATP} channels, is commonly used to probe K_{ATP} channel-independent mechanisms of insulin release.[154,155] Results showed that while stimulation of both types of islets with glibenclamide and low levels of glucose yielded similar secretion rates (though slightly higher for KOs), addition of higher levels of glucose elicited significantly more secretion from KO islets compared to ObRlox controls. These results are consistent with the coupling of leptin signaling pathways with glucose dependent, K_{ATP} channel-independent mechanisms of insulin release. However, further biochemical analyses probing regulation of known signaling intermediates are warranted.

The incretin hormone GLP-1 is known to be a potent regulator of glucose-stimulated insulin secretion,[147] though the precise mechanism of action has yet to be defined.[156] Recent studies aimed at elucidating GLP-1 action on β-cells have revealed multiple potential signaling pathways,[157] with one report describing the possibility of GLP-1 signaling having the ability to overcome leptin-inhibited insulin secretion in islets.[158] This report suggests the role of leptin is primarily a dampener of basal insulin release during fasting and not an acute governor of insulin secretion. In this model, the amounts of inhibition that leptin produces can be easily overcome by nutrient and incretin signals (e.g. GLP-1) accompanying feeding. Results presented in this chapter correlate with this model by illustrating a reversal of the effects of leptin on glucose-stimulated insulin release by the addition of GLP-1 (Figure 4.6).

High Throughput Single Islet Analysis on a Microchip. The 15-islet microchip described in Chapter 3, which allowed for fast and high throughput monitoring of insulin release (assays every 10 s) on the single islet level, was used to collect all insulin secretion data presented here. The chip allowed for faster collection of islet data (compared to single- and four-sample devices) and ease of use for islet stimulation with a variety of insulin secretagogues and drugs of interest. Specifically, islets were perfused with combinations of glucose, leptin, palmitic acid, glibenclamide, and GLP-1 in BSS. Rate of experiment competition was maximized through the simultaneous collection of multiple data sets by loading the chip with two different types of islets (e.g. one set of n = 7 ObRlox and another of n = 8 KO) and treating all of them with the same perfusion buffer. The collected single islet insulin secretion traces could be averaged together to produce the types of plots shown throughout this chapter (typically used for islet type and treatment comparisons) and also used for direct comparison of single islet behavior.

Single islet comparisons allow additional information to be extracted from experiments through observations of the insulin release dynamics of single islets. While traditional batch islet experiments hinder this type of evaluation, monitoring single islet insulin release in parallel allows these comparisons to be made. As an example of this type of analysis, the individual islet traces that comprise KO averaged data in Figure 4.4 (8 mM glucose stimulation, FFA versus BSA, no leptin) are shown in Figure 4.11. After 48 hr treatment with cell media supplemented with BSA, 60% of KO islets showed pulsatile insulin release after stimulation with 8 mM glucose. In contrast, no islets treated with palmitic acid showed an oscillatory response. These data suggest that lipotoxic

effects on islets may inhibit mechanisms controlling pulsatile insulin release (shown to be important in insulin action on target tissues),[159,160] in the absence of leptin signaling.
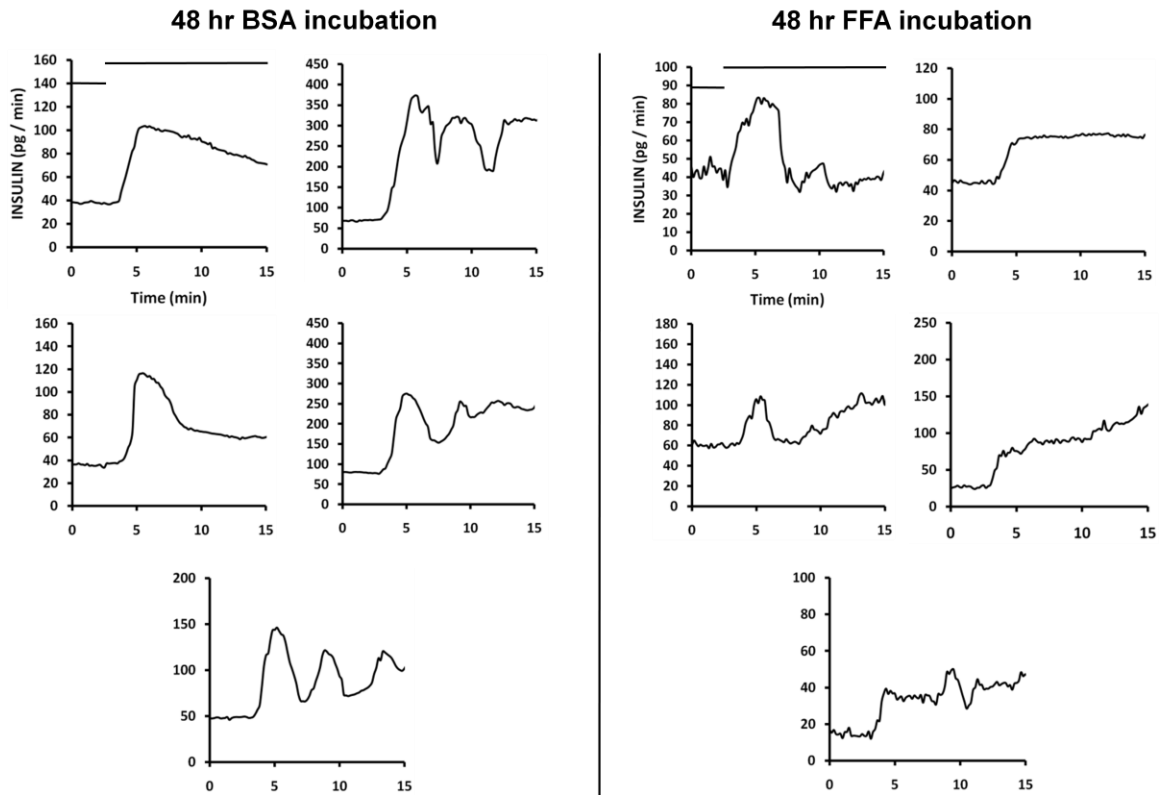
Figure 4.11. Insulin secretion traces from individual KO islets after incubation in fatty acid-free BSA (BSA) or 0.5 mM palmitic acid (FFA). Bars over plots (only in top left of each group) indicate perfused glucose concentration (low bar = 3 mM, high bar = 8 mM).

A total of 28 data sets consisting of 153 single islet experiments were collected with an over 25,000 insulin assays performed (a cost of over \$125,000 using traditional ELISA kits). A total of 14 non-consecutive days were spent running experiments (not including preparation, islet isolations, data analysis, etc.). In contrast, using a single-sample microchip to perform these studies would have required 53 days of experiments (assuming the completion of 3 islets a day which may not always be possible). These time savings further illustrate the advantages in using this device for high-throughput single islet studies.

Conclusions

A developed tool for monitoring insulin release from 15 single islets in parallel was used to investigate the effects of leptin signaling in islets. Experiments involved monitoring insulin release from single islets exposed to glucose, leptin, palmitic acid, glibenclamide, and GLP-1. An advantage in using the 15-sample device for islet studies was illustrated by the comparison of single islet secretion dynamics (Figure 4.11), an evaluation that cannot be performed with typical batch islet experiments in which secretion is measured from 20 or more islets grouped together. The results presented in this chapter suggest interaction of leptin signaling with FFA, glibenclamide, and GLP-1 stimulation of islets; however, further studies are needed to elucidate pathways responsible for the observed effects.

CHAPTER 5

IMPROVED QUANTIFICATION IN ON-CHIP INSULIN SAMPLING USED FOR
MONITORING PULSATILE INSULIN RELEASE FROM SINGLE ISLETS

Introduction

The ability to monitor insulin release from single islets holds potential to be a valuable tool in diabetes research.[49,87,92,93,125] In techniques for single islet secretion analysis, islets are commonly perfused with stimulant followed by offline analysis of perfusate for cellular secretions. Islet analysis microchips,[49,92,93] including the device presented in Chapter 3, offer an integrated online method for measuring insulin release. On these chips, an electrophoresis-based immunoassay for insulin is coupled to hydrodynamic perfusion flow for islet stimulation. Individual islets loaded into these chips were perfused by passing flow through a perfusion chamber that was open to atmosphere. The majority of sampled insulin would flow out of the chamber while only a small portion of insulin from the side of the chamber was sampled by electroosmotic flow (EOF), as illustrated by Figure 5.1A & B. With this type of perfusion, obtaining a representative sample depends on the ability to extract insulin from a localized region of the islet that is representative of total insulin released. An additional disadvantage to sampling controlled by EOF is that changes in sampling buffer composition (e.g., ionic strength or other additives) could result in changed sampling rate and non-optimized assay conditions.
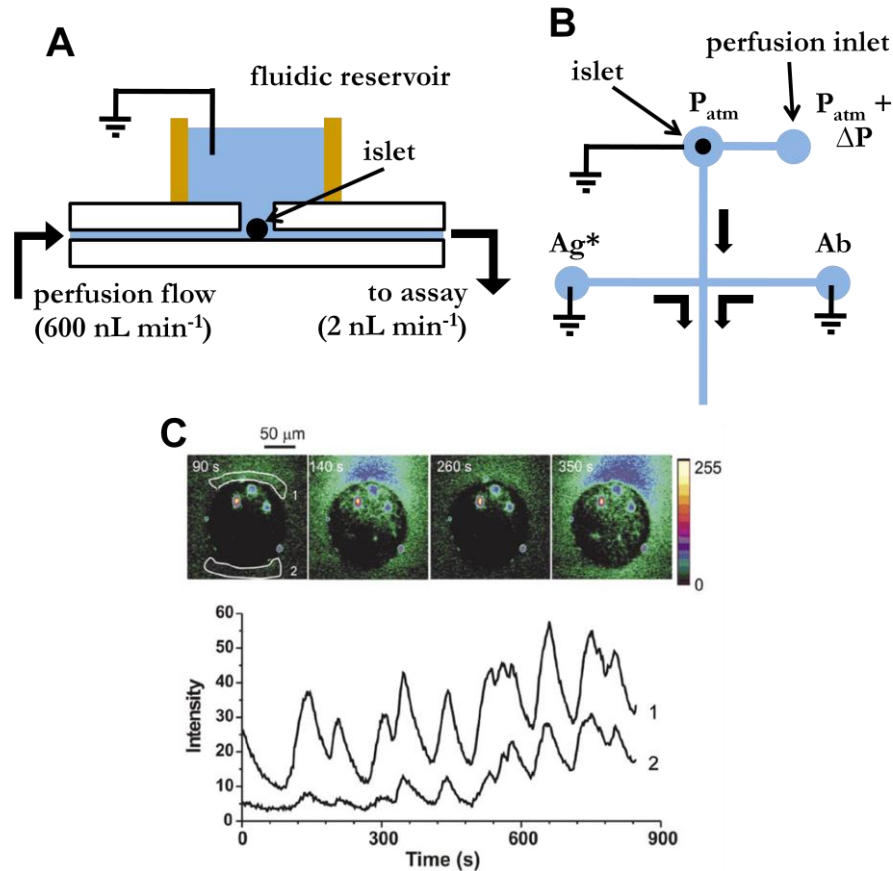
Figure 5.1. Illustrations of EOF-based islet sampling and heterogeneous insulin secretion from an islet. (A) Side-view of islet perfusion chamber holding an islet (not to scale). The majority of perfusion flow and secreted insulin flows into the fluidic reservoir positioned above the islet. Grounding of the reservoir and application of a negative potential downstream on the chip allows EOF to be used to sample released insulin. (B) Top-view of EOF-based insulin sampling. Sampled perfusate is mixed with antibody and labeled-antigen (also controlled by EOF). (C) Imaging analysis of Zn^{2+} release (co-secreted with insulin) from an islet. In the series of pseudocolor images, higher local intensity indicates an increase in Zn^{2+} concentration. Comparison of release from the regions of interest outlined in the far left image show different intensities indicative of different localized insulin release rates (lower plot). (C) is reproduced from reference 162.

Characterization of flow through this type of sampling chamber has suggested the potential for non-uniform insulin sampling. In these experiments (presented later in this chapter), confocal fluorescence images of an islet in a sample chamber perfused with fluorescein showed nonuniformity in concentration of perfused agent during the steady state. These results suggest that there may be variations in the concentration of stimulant around the islet during an experiment, in turn causing variation in the amounts of insulin

85

release from local sites on the islet surface. (A recent study showed localized Ca^{2+} flux, a precursor to insulin release, resulting from a partially stimulated islet).[161] Though this pattern of perfusion flow around the islet (and variation of stimulant) is likely to be observed in many cell perfusion apparatuses, the sampling of insulin from only one area or side of the islet may not yield a representative sample of total insulin release. Furthermore, there is evidence to suggest that that insulin release from islets incubating in glucose is not spatially homogenous as shown by Figure 5.1C in which a Zn^{2+} reactive dye is used to indirectly measure insulin release around and islet.[162] A system in which all cellular secretions are collected will yield a more quantitative sample representative of single islet secretion and also maintains the potential to be applied to other cells-on-chip systems.

Work presented here is aimed at redesigning portions of the 15-islet chip presented in Chapter 3 to allow collection of all insulin released by islets for more uniform sampling. In this chip design, islets are housed in reversibly sealed chambers (facilitating addition and removal of samples) through which perfusion flow is passed. All of the stimulated insulin release from the islet is then pushed out of the chamber and through a channel leading to the assay portion of the chip. The capillary electrophoresis (CE)-based immunoassay for insulin[90,91] demonstrated with other islet microchips was used for quantification of insulin.

The new chip was tested by quantitatively monitoring single islet secretion dynamics, specifically biphasic and pulsatile insulin release from islets in parallel. After successful characterization and testing, preliminary experiments investigating pulsatile insulin release[163,164] were performed. Studies included characterizing oscillation

frequencies of islets from individual animals, complementing a prior study showing that individual outbred mice have an intrinsic Ca^{2+} flux oscillatory frequency (e.g. islets from a single animal show Ca^{2+} flux with the same period).[126] Additionally, preliminary experiments probing the effects of free fatty acid (FFA) induced lipotoxicity on pulsatile insulin release were performed. Results from these studies illustrate the usefulness of high throughput methods for collecting single islet data.

Experimental Section

Chemicals and Reagents. Unless otherwise noted, all reagents were from Fisher. Tricine was from MP Biomedicals (Aurora, OH). Collagenase type XI, insulin, EDTA, fluorescein, and Tween 20 were from Sigma (St. Louis, MO). Cell culture reagents were purchased from Invitrogen (Carlsbad, CA). Fluorescein isothiocyanate-labeled insulin (FITC-ins) was obtained from Molecular Probes (Eugene, OR), and monoclonal antibody (Ab) to human insulin was from Biodesign International (Saco, ME). Poly(dimethylsiloxane) (PDMS) was purchased from G.E. Silicones (Waterford, NY). All solutions were made with 18-MΩ deionized water from a Millipore (Bedford, MA) Milli-Q filtration system and filtered with 0.2 μm nylon syringe filters.

Buffer for immunoassay reagents was 50 mM NaCl, 1 mM ethylenediaminetetraacetic acid (EDTA), 20 mM tricine, 0.1% (w/v) Tween 20, and 0.7 mg mL^{-1} BSA, adjusted to pH 7.4. Balanced salt solution (BSS) used as a physiological buffer for islets experiments consisted of 125 mM NaCl, 5.9 mM KCl, 1.2 mM $MgCl_2$, 2.4 mM $CaCl_2$, 25 mM tricine, and 0.7 mg mL^{-1} bovine serum albumin (BSA), adjusted

to pH 7.4 with NaOH. Separation buffer consisted of 20 mM NaCl and 150 mM tricine, adjusted to pH 7.4.

Microfluidic Chip Fabrication. The microchip design illustrated in Figure 5.2A was fabricated using previously described wet-chemical etching techniques.[49] Channels were etched to 15 μm deep in borofloat glass with hydrofluoric acid solution. Access holes to channels were drilled with 360 μm diameter (Tartan Tool Co., Troy, MI) and 1 mm diameter drill bits (Euro Tool Inc., Grandview, MO). The four perfusion inlet connectors were from Upchurch Scientific (Oak Harbor, WA) and the remaining fluidic reservoirs were made in-house from polytetrafluoroethylene (PTFE) tubing cut to length. PTFE reservoirs were attached to the chip with epoxy (E-6000, Eclectic Products, Inc., Pineville, LA) and allowed to cure for 24 hours.
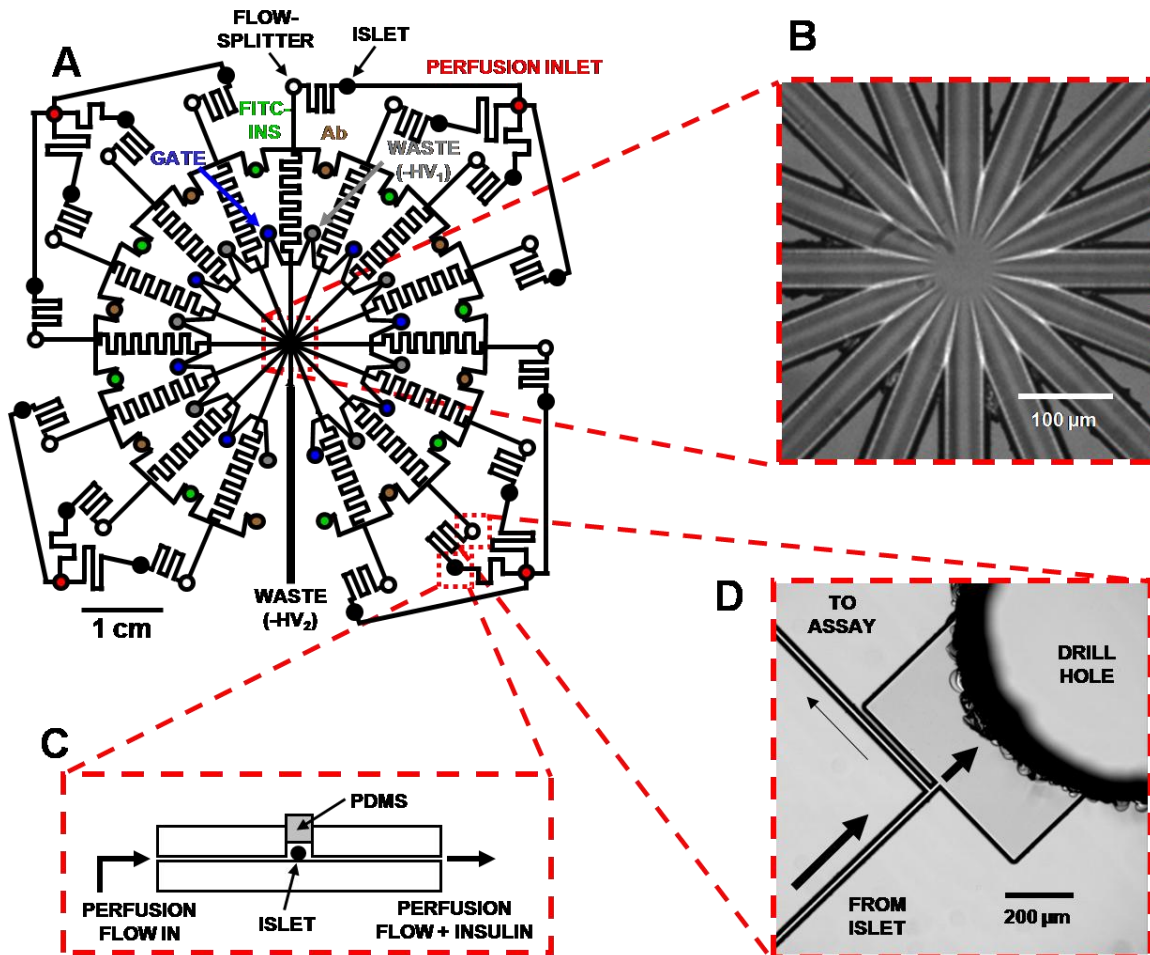
Figure 5.2. Channel design, images, and illustrations of key portions of a microfluidic chip for monitoring insulin secretion from 15 pancreatic islets. (A) The channel network of the entire device. Black lines represent 15 μm deep microfluidic channels, and fluidic reservoirs are depicted with circles (color coded for clarity). Operation of the chip is described in the Experimental section. **(B)** Brightfield image of the detection area taken with a CCD camera. Imaged area was 400 x 400 μm². Flow from 15 separation channels enter the center portion of the chip before flowing out through a single waste channel. **(C)** Side-view representation (not to scale) of an islet perfusion chamber. Islets are loaded into the islet chamber with physiological buffer and then sealed with a PDMS plug under a stereomicroscope. Perfusion buffer flows over the entire islet and pushes all secreted insulin into the sampling channel. **(D)** CCD image of an on-chip flow-split that allows the fast flowing insulin sampling stream to be compatible with the slower flow of EOF-driven immunoassay reagents. Arrows indicate direction and relative magnitude of flow.

Microfluidic Chip Operation. The microchip consists of 15 channel manifolds capable of CE-based immunoassays for continuous monitoring of insulin release from pancreatic islets. Flow through the radially designed separation channels converges at a common point to facilitate parallel fluorescence imaging detection (described later).

Electrical connections to the chip were made with a chip-electrode interface built in-house. Two separate high voltage power supplies (CZE1000R, Spellman High Voltage Electronics, Hauppauge, NY) were used to apply potential to the waste reservoirs (-HV$_1$ and -HV$_2$) and a single high-voltage relay (Kilovac, Santa Barbara, CA), controlled by a LabVIEW program, connected the gate reservoirs to ground.

Pancreatic Islet Loading and Sampling of Insulin. In contrast with previous immunoassay chips,[49,93] the device presented here performs islet perfusion, sampling, and introduction of secreted insulin to the on-chip assay entirely with hydrodynamic flow. The use of hydrodynamic flow for these functions was found to improve insulin sampling efficiency and microchip reproducibility when used with various perfusion buffer compositions. Flow from a pressurized vial of perfusion buffer was split four ways with a five-port manifold before entering the chip where each stream was split again before reaching perfusion chambers. Chambers on the chip were heated to 37 ℃ by a heating strip (Minco, Minneapolis, MN) positioned beneath the chip.

For analysis, islets were housed in perfusion chambers on the chip that were sealed with PDMS plugs (Figure 5.2C). PDMS plugs could be removed so that islets could be taken out after experimentation and the chip could be reused. Care was taken to not damage the islets when sealing the chamber, and islets were checked for visible damage after every experiment. Plugs were fabricated by puncturing a thin slab of PDMS with small bore blunted-tip stainless steel tubing (20 gauge). The resulting plugs were cut to length with a scalpel under a stereomicroscope.

Islets were perfused at 500 nL min^{-1} with buffer that could be switched to apply different glucose concentrations or test compounds as desired. The pressure at the islet

chamber associated with this low flow rate was not sufficient to break the reversible PDMS-glass seal. A low pressure drop in the islet chamber is also advantageous for maintaining islet heath. A perfusion flow rate of 500 nL min^{-1} is too high for downstream operations such as mixing with immunoassay reagents; therefore, a flow-split was added to the design (Figure 5.2D) so that only ~3.5 nL min^{-1} was passed to the assay region on the chip.

Insulin Secretion Assay and Calibration. The inclusion of hydrodynamic sampling to the 15-islet chip did not produce significant changes in performance compared to the chip presented in Chapter 3, and thus no major changes were made to the previously described immunoassay operation. Briefly, FITC-ins and Ab reservoirs (filled with FITC-ins and Ab in immunoreagent buffer, respectively) were grounded while -4 kV was applied to the waste (-HV$_2$) reservoir allowing the sampled insulin stream to mix and react with the immunoassay reagents while flowing through the serpentine-shaped reaction channels. 0.5 s injections onto the radially-aligned separation channels were made at 9.5 s intervals using an on-chip flow-gating injector. Injected plugs were separated by CE while traveling towards the center portion of the chip where fluorescence detection was performed.

Fluorescence Detection and Data Analysis. Multiplexed fluorescence detection was performed as previously described in Chapter 3. Briefly, fluorescence imaging of the detection area was performed with a 20x objective lens on an inverted epi-fluorescence microscope (IX71, Olympus America, Inc., Melville, NY) with a Xe arc lamp (Sutter Instrument Company, Novato, CA) and electron-multiplying CCD camera (Hamamatsu Photonic Systems, Bridgewater, NJ). A sample brightfield image of the

detection area taken using this setup (Figure 5.2B) shows all 15 separation channels and the common waste channel within the imaged region.

Series of images capturing the fluorescent migrating bands were collected ~28 Hz, stored, and analyzed with SlideBook software (Intelligent Imaging Innovations, Inc., Denver, CO). After the collection of images, fluorescence intensities from regions of interest drawn within each separation channel were used to produce parallel electropherograms. Comparison of peak heights from separated FITC-ins:Ab and free FITC-ins was used to quantify the amount of insulin introduced to each channel network. Calibration was performed by monitoring bound-to-free ratios (B/F) of separated fluorescent products while introducing insulin standards into the chip without the presence of islets, allowing B/F values to be assigned to specific insulin concentrations. Limits of detection (LODs) down to 0.5 nM insulin were calculated, which was sufficient for single islet studies.

Isolation of Murine Islets. Pancreatic islets were isolated from 20 to 30 g male CD-1 mice as previously described.[108] After isolation, islets were incubated at 37 °C and 5% CO_2 in RPMI cell culture media supplemented with 10% fetal bovine serum, 100 units mL^{-1} penicillin, and 100 μg mL^{-1} streptomycin. Islets were used 1 − 6 days after isolation. Islets chosen for experiments were of average size (100 − 200 μm diameter) and with an intact membrane. For studies involving monitoring islet oscillations from individual animals, male Swiss-Webster mice were used in place of CD-1 mice.

Results and Discussion

Characterization of Islet Perfusion. In previously used chips, individual islets were perfused by passing flow through an islet chamber that was open to the atmosphere and continuously sampled by EOF. To evaluate the perfusion system, step changes of fluorescein were made in the perfusion line while monitoring the islet chamber with scanning confocal fluorescence microscopy. Figure 5.3A shows a confocal image of an islet being perfused at 600 nL min^{-1} with 500 nM fluorescein in BSS. Panels B and C in Figure 5.3 demonstrate the time scale on which fluorescein is washed into and out of the islet chamber, respectively. With the islet present, some nonuniformity in concentration of perfused agent is observed during the steady state (see Figure 5.3A and different curves in B and C). Similar experiments in which no islet was present in the islet chamber showed no change in fluorescence intensity throughout the entire access hole (data not shown). The "shadowing" effect of the islet is likely to occur with most perfusion systems (i.e., cells in a tube or on a plate) with flow from one direction. This suggests that there may be variations in the concentration of stimulant around the islet that may cause dissimilarities in the amounts of insulin released into local areas around the islet. Furthermore, sampling from only one side or area around an islet may yield a biased sample.
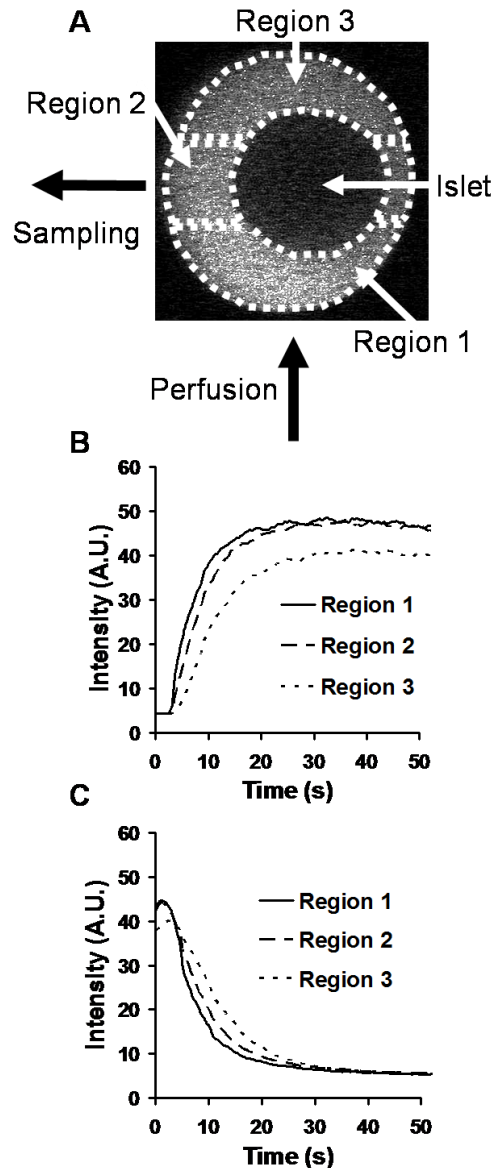
Figure 5.3. Confocal imaging analysis of islet perfusion. **(A)** Confocal image of islet during the perfusion of 500 nM fluorescein into the access hole. Black arrows indicate direction of perfusion and sampling fluid flow. Regions of interest described in parts **(B)** and **(C)** are indicated with broken lines. **(B)** Plots of fluorescence intensity versus time for each of the outlined regions of interest during the introduction of fluorescein into islet access hole. The start of the pressure driven perfusion was at t = 0 min. Data were collected at 2 Hz. **(C)** Fluorescence intensity for each region of interest during the perfusion of non-fluorescent BSS, flushing out the previously used fluorescein. Reproduced from reference **49**.

Improved Sampling of Secreted Insulin. While electrophoretic sampling of insulin was found to be useful with single, four-, and 15-islet chip designs, the disadvantages associated with potential biased insulin sampling justified redesigning of

94

islet perfusion. When sampling insulin electrophoretically, the majority of islet perfusate and secreted insulin flows into a fluidic reservoir positioned above the islet and only a small portion of insulin near the sampling channel continues towards the assay portion of the chip. Depending on the exact location of the islet within the chamber, its proximity to the sampling channel, and variation in insulin release across its surface, there is potential for sampling different amounts of insulin from islets that have the same overall secretion rate. Although islets used in experiments are size-matched (and should thus secrete insulin at similar rates), these factors will increase variability across islets.

The redesigned sampling portion of the chip, shown in Figures 5.2C and D, consists of islets sealed into chambers using removable PDMS plugs. By sealing islets into the chambers while perfusing them with glucose, all of the insulin released from the islet is pushed out of the chamber and moved towards the assay. However, as sampling flow coming from the islet chamber is flowing too fast (500 nL min^{-1}) to be appropriately mixed with immunoassay reagents controlled by EOF, an on-chip flow-split was incorporated into the design (Figure 5.2D) to pass only ~3.5 nL min^{-1} of perfusion to the assay.

Before the insulin sampling stream enters the flow-split (with the sampling channel emerging from one side as shown in Figure 5.2D) it was imperative that perfusate be adequately mixed to avoid bias from laminar flow segregation of secreted insulin (i.e., sampled insulin needs to be of uniform concentration across the channel before being split). To determine the appropriate length of channel between islet chamber and flow-split that allowed for complete mixing of sample by lateral diffusion, the distribution of FITC-ins across two laminar streams was imaged at various points on a

straight microchannel with the same dimensions as those used on the 15-islet chip (summarized in Figure 5.4). It was found that laminar flows of 50% FITC-ins solution and 50% buffer flowing at a combined rate of 500 nL min^{-1} mixed completely via diffusion at a point ~0.6 cm downstream of the convergence point. To allow mixing of insulin leaving the islet chamber, 2.4 cm (a length four-times what was needed for two-stream mixing) of channel was used to link the islet and flow-split portions of the chip.
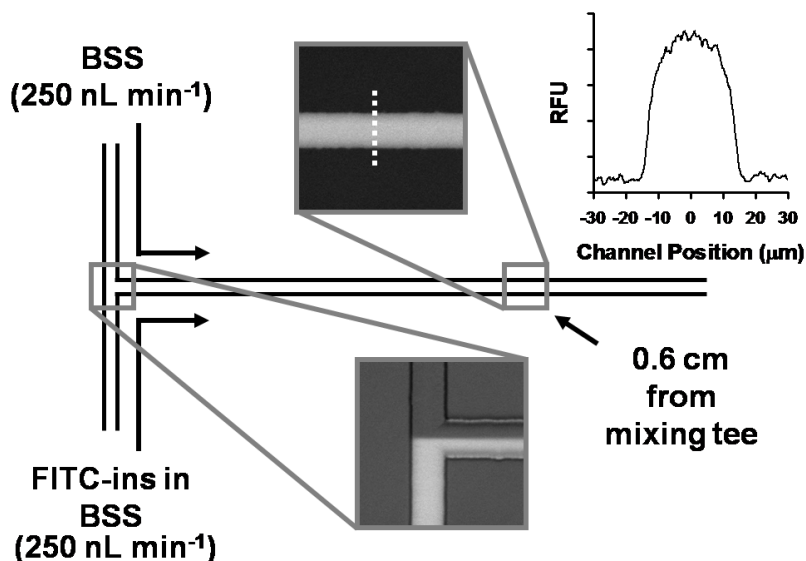
Figure 5.4. Summarized setup and results for determining appropriate length of channel between islet and flow-split allowing adequate sample mixing. Black lines in the figure represent a microfluidic channel design (mixing tee) and arrows indicate direction of flow. Solutions of BSS and FITC-ins in BSS were mixed on the chip (shown by the lower fluorescence CCD image) by flowing both solutions at 250 nL min^{-1} with a syringe pump. An image taken 0.6 cm from the mixing tee (upper expansion) shows complete mixing of the two streams. Line-scan data (upper right) taken from the dotted line drawn on this image confirms complete mixing.

Another advantage of using hydrodynamic flow for sampling is that it allows assay performance to be independent of buffer compositions (e.g. ion concentration or other additives) that may affect EOF. The use of different buffers may be of interest for performing experiments using various islet treatments or different biological samples. When sample flow is controlled by EOF, a change in sample buffer composition may result in different sample/reagent mixing ratios on the chip, potentially requiring reagent

concentrations to be modified with every buffer for an optimized assay. A chip that uses hydrodynamic sample introduction would be able to maintain a constant sample/reagent mixing ratio regardless of buffer composition. This ability was demonstrated by comparing observed mixing ratios in both an EOF-controlled sampling chip and a pressure-controlled sampling chip using a variety of perfusion buffers. For this experiment, each buffer was spiked with FITC-ins and perfused into an operating chip while the mixing point was monitored with fluorescence imaging. Mixing ratios were determined using fluorescence intensity of the perfused buffer before and after it was mixed with immunoassay reagent buffer. Results are shown in Figure 5.5. As indicated in panel A, mixing varied significantly across the tested buffers for EOF-controlled sampling. Results from the pressure-driven sampling chip (Figure 5.5B), however, show uniform mixing ratios regardless of buffer composition.
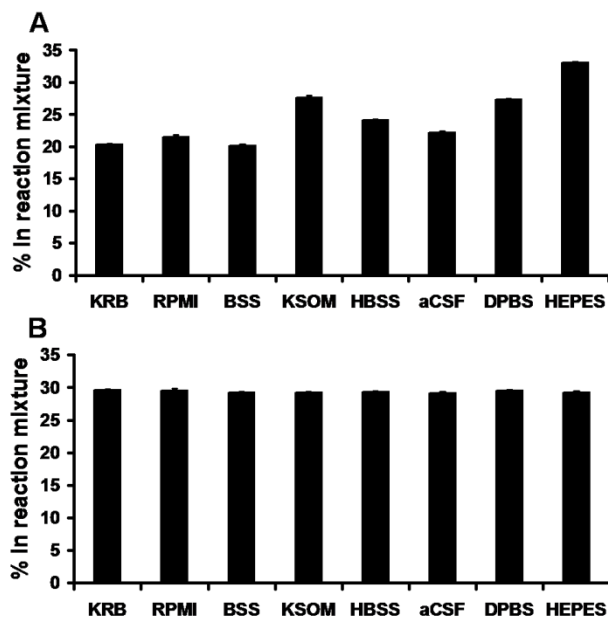
Figure 5.5. Comparison of online reagent mixing ratios on electrophoretic- and pressure-sampling chips with varying perfusion buffer compositions. Abbreviations are as follows: KRB, krebs ringer buffer; RPMI, RPMI cell media (from Invitrogen); BSS, balanced salt solution; HBSS, Hank's balanced salt solution; aCSF, artificial cerebrospinal fluid; DPBS, Dulbecco's phosphate buffered saline; HEPES, HEPES buffered saline. Data are averages of the measured mixing ratio at three time points, measured 2 min apart from one another. Error bars are ± 1 standard deviation. (A) Plot comparing sample/reagent mixing ratios obtained using electrophoretic sampling. (B) Plot showing mixing ratios obtained with the same buffers as in (A) using pressure-driven sampling.

Characterization of Hydrodynamic Sampling Chip Performance.

Characterization of islet perfusion and sample transport across the device was performed by perfusing BSS spiked with 100 nM FITC-ins into an operating device and taking fluorescence images at various positions of interest. These experiments are important as a potential disadvantage of using hydrodynamic flow (vs. EOF) for sampling is the increased dispersion of sample as it is transported across the device causing a decrease in effective temporal resolution. Results from these experiments are shown in Figure 5.6. The upper plot, produced by monitoring the fluorescence intensity of an islet chamber (with a loaded islet), shows a rise time (10% - 90%) of 3.5 s. This suggests the capability of fluid exchange and sampling of all insulin secreted by an islet within this time. The

98

bottom plot was produced from images taken at the injection cross and shows an overall delay time of 153 s and a maximum response time of 22 s for the chip (this analysis included perfusion dispersion prior to reaching the islet chamber). These times were verified by monitoring B/F on the device after a step-change in perfused insulin standard concentrations (data not shown). This response time is similar to what was observed with electrophoretic sampling (~25 s).[49] With the electrophoretic sampling design, however, the rise time was mostly a result of slower fluid exchange in the islet chamber rather than dispersion of sample in transit. A response time of 22 s was adequate for monitoring insulin secretion dynamics and oscillations from islets.
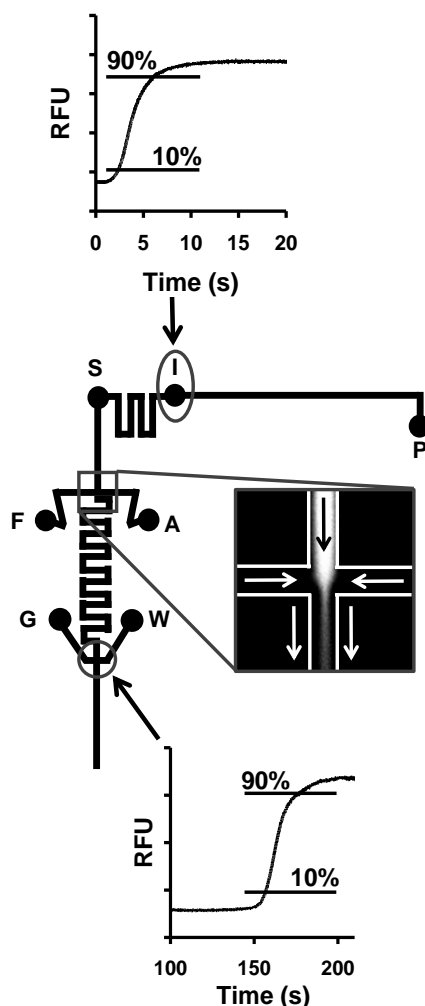
Figure 5.6. Illustration of a single network of the 15-sample chip with flow characterization plots from throughout the device. Fluidic reservoir abbreviations as follows: P, perfusion inlet; I, islet chamber; S, flow-split; F, FITC-ins; A, Ab; G, gate; W, waste (-HV$_1$). The upper plot shows fluorescence intensity vs. time produced from images of the islet chamber (with a loaded islet) while perfusing FITC-ins in BSS at 500 nL min^{-1}. A CCD image of the point of reagent mixing (middle expansion) shows perfusate and immunoassay reagent flows entering the reaction channel (FITC-ins is only present in the BSS; FITC-ins and Ab reservoirs contain only immunoassay reagent buffer). White lines represent channel walls, and arrows indicate direction of flow. The lower plot, produced from images of the injection cross, shows the delay and response time (10% - 90%) for the device up to the separation channel.

Parallel Immunoassay Performance. Before using the device for islet studies, the system was tested with the collection of serial immunoassays with online reagent mixing. Serial electropherograms from single channels on the 15-islet chip collected with online mixing of immunoassay reagents and insulin standards are shown in Figure

5.7A and B. Each separation (five per panel) shows two separated immunoassay products: FITC-ins:Ab (bound) and FITC-ins (free). The change in peak heights observed between the two panels was caused by an increase in insulin (5 nM in panel A, 100 nM in panel B) which shifted the immunoassay product ratio through a competitive binding reaction. Good reproducibility of migration times were observed on a single channel (relative standard deviation (RSD) of less than 1% for 5 separations). Low RSDs were also observed for single channel B/F (less than 2.5% for 5 separations).
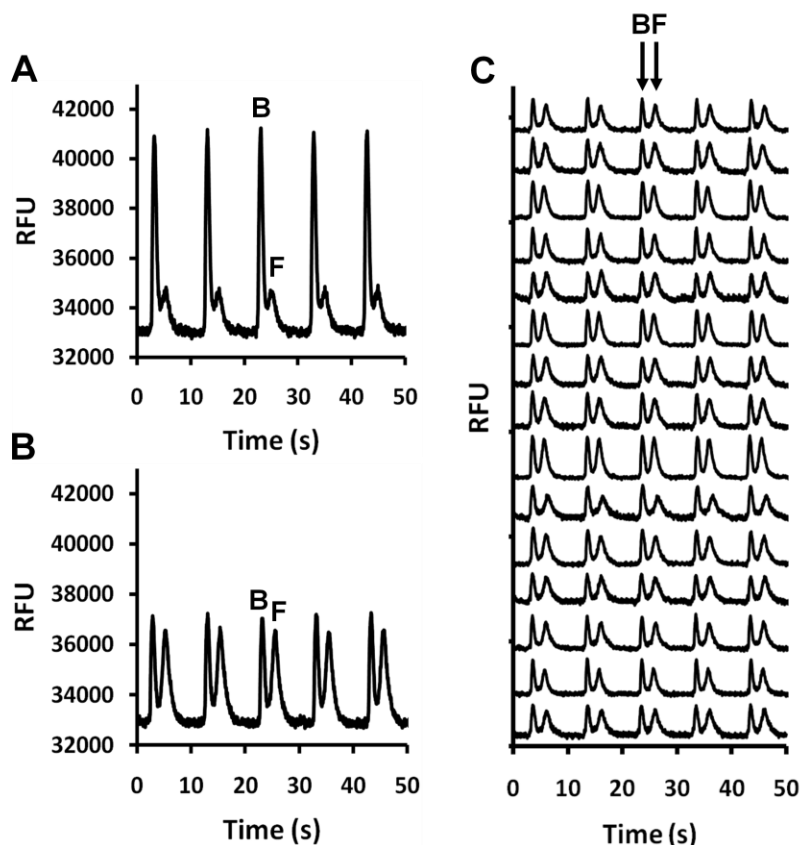
Figure 5.7. Typical serial and parallel electropherograms obtained with online mixing of immunoassay reagents. Injections were made every 10 s. FITC-ins bound complex [B] and free FITC-ins [F] are labeled accordingly. (A) Serial electropherograms collected when mixing 50 nM FITC-ins, 40 nM Ab, and 5 nM insulin standard. (B) Electropherograms collected after the introduction of 100 nM insulin standard into the same channel used in (A). RFU values are shown in (A) and (B) to allow peak height comparisons. (C) Serial electropherograms collected in parallel after introduction of 100 nM insulin standard using all 15 channel networks. Traces are offset for clarity.

Serial electropherograms collected in parallel with all channels on the 15-islet chip are shown in Figure 5.7C. Migration time RSD across the entire chip (< 4%) was larger than observed for a single channel, but still acceptable for parallel separations controlled by a single injection trigger. Small migration time variation is important in this case since parallel separations can only by performed as fast as they occur on the slowest channel. Averaged B/F RSD across all 15 channels (9.6%) was also larger than observed for single channel studies.

An unexpected advantage of using hydrodynamic sampling can be seen by minor improvements in chip performance and assay stability compared to parallel separations performed with the 15-islet chip with electrophoretic sampling (Chapter 3, Figure 3.3). Lower B/F RSDs for both analyses in a single channel as well as across all 15 channels were observed. Specifically, single channel B/F RSD decreased from ~3.5% to 2.5% for 5 serial assays and from 6% to 5% for 20 minutes of continuous operation when using hydrodynamic sampling. Additionally, the averaged B/F RSD across all 15 channels was reduced from 11.7 % to 9.6 %. Though minor, it is possible the improvements in assay stability are a result of more stable sample introduction flows that are not affected by factors such as non uniform channel surface properties or sample and protein adsorption. However, as flow through the rest of the chip is still partially controlled by EOF, it is enticing to think that a parallel device controlled entirely by hydrodynamic flow may show little to no variation between channel networks.

Parallel Measurement of Insulin Secretion from Pancreatic Islets. Functionality of the parallel microchip was tested by simultaneously monitoring insulin secretion from multiple individual islets stimulated with glucose. Two types of secretion

experiments were performed: stimulation with a 3 mM to 11 mM glucose step change to yield a biphasic response,[103,165] and continual stimulation of islets with 10 mM glucose to elicit oscillatory secretion.[126,166,167] These types of secretion characteristics have been suggested to be critical in governing insulin action on target tissues,[159,160] and methods that can monitor these dynamics hold potential to be valuable tools in diabetes research.

Insulin secretion plots shown in Figure 5.8A were from islets treated with a step change in perfused glucose concentration (3 mM to 11 mM) at t = 3 min. The figure presents plots from 13 islets (from a total of 15) that showed an increased rate of release after glucose stimulation from a single experiment with the microchip. The majority of plots show pronounced 1st phase release of insulin followed by a 2nd phase of sustained release; however, several islets show oscillatory release or a continual increase in release rate. An average of these plots (panel B) shows a biphasic insulin release profile that is characteristic of pancreatic endocrine tissue stimulated with elevated glucose.[103,121] The averaged basal rate of insulin secretion from Figure 5.8B (46 pg min^{-1} at 3 mM glucose) is slightly higher than values obtained using the previous 15-islet chip (34 pg min^{-1}) as well as the four-islet chip (27 pg min^{-1}). The secretion rate after glucose stimulation (160 pg min^{-1} peak) is also higher than what was observed with electrophoretic sampling, but still similar to what other studies using islet perfusion techniques have reported (showing a first phase peak between 100 and 200 pg min^{-1} islet^{-1}).[116,168]
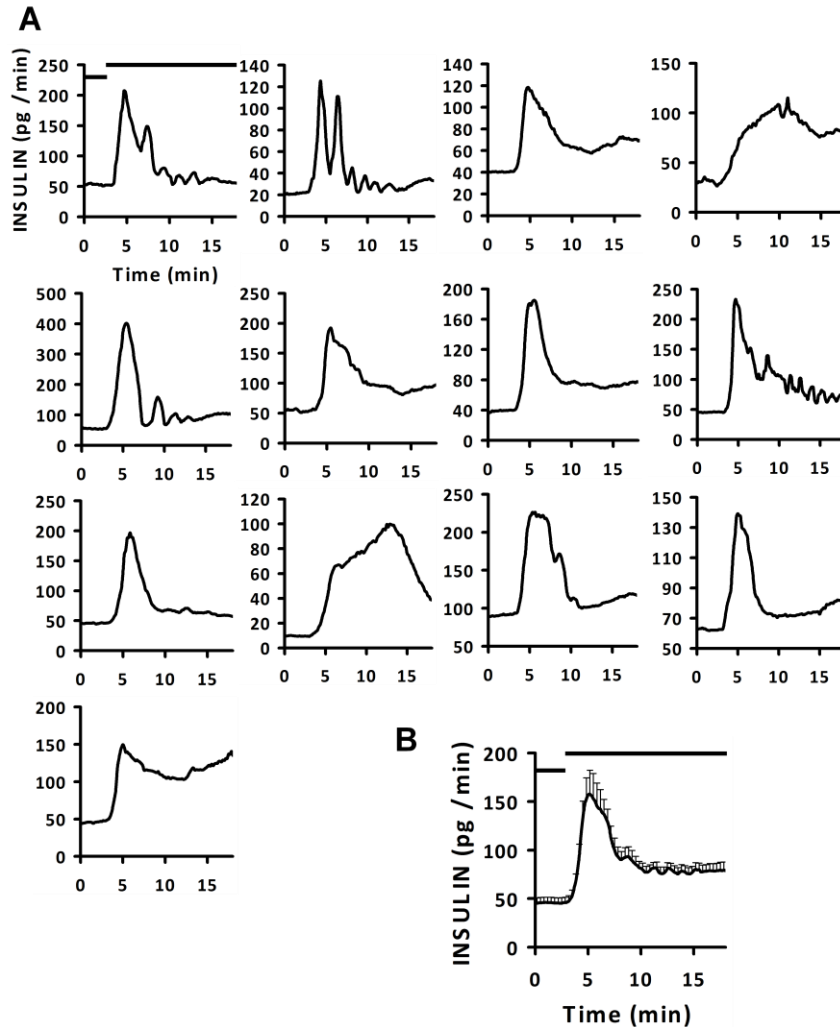
Figure 5.8. (A) 13 secretion plots from islets stimulated with a step change in glucose concentration. Two islets showed no increase in secretion rate after stimulation with high levels of glucose. Bars, shown only in the upper left plot, indicate glucose concentration (low bar = 3 mM glucose, high bar = 11 mM glucose). (B) Averaged plot from 13 single islet traces collected simultaneously with the 15-sample device. Average bars, placed every other data point for clarity, are ±1 SEM (standard error of the mean).

Results from continual exposure to 10 mM glucose are shown in Figure 5.9. The insulin secretion plots in panel A are from six individual islets showing expected pulsatile responses, with oscillation periods between one and three minutes. The distribution of oscillation periods from a total of 25 islets treated with 10 mM glucose is shown in Figure 5.9B (data taken from two experiments with the 15-islet chip). Observed secretion periods from these islets ranged from 1.25 to 3.25 minutes. Additionally,

104

several islets showed no oscillations suggesting that pulsatile behavior was either absent

or too fast to be adequately sampled with the temporal resolution of the device. Indeed,

metabolic and intracellular Ca^{2+} oscillations (driving factors in insulin exocytosis) with

periods less than 10 s have been monitored in islets.[169] Of the islets studied here, 24%

either did not oscillate or had oscillations faster than the measured temporal resolution of

22 s. The distribution of oscillation frequencies displayed in Figure 5.9B shows a

bimodal distribution that may suggest the presence of "fast" and "slow" oscillations[163,164]

(although fast oscillations were not directly observed).
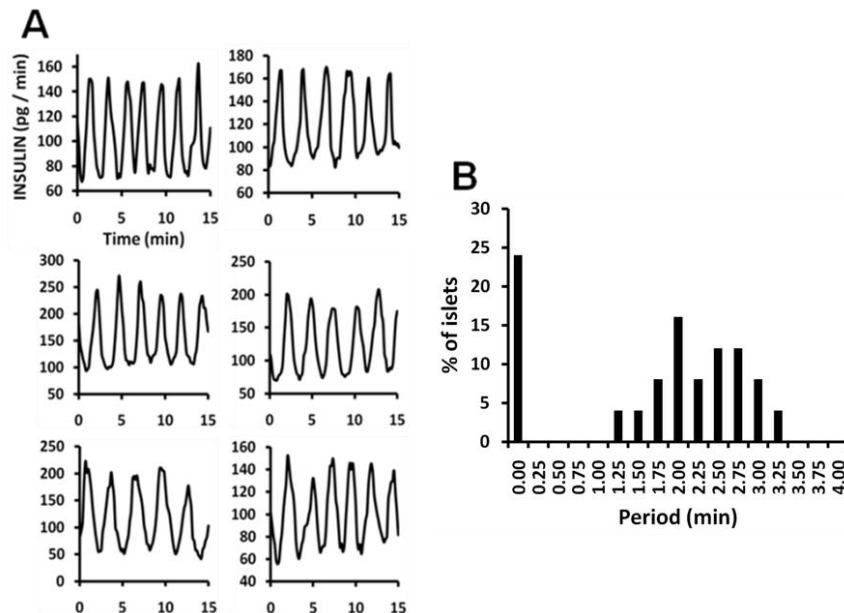
Figure 5.9. (A) Plots from six of 15 islets run simultaneously on the 15-islet chip showing oscillatory insulin release. Islets were stimulated with continuous flow of 10 mM glucose. (B) Plot comparing oscillation periods from a group of 25 islets from 2 mice tested with the 15-sample device over two experimental periods. These data show a bimodal distribution of periods including islets that showed no oscillations and islets that oscillated with periods of 1.25 – 3.25 min.

Both of the islet studies presented here demonstrate the usefulness of a high

throughput single islet monitoring system by showing the capability of obtaining

information on the single entity level as well as data that can be made into averaged plots.

Single islet data is important because it gives information pertaining to the dynamics of insulin secretion, which can be just as critical as the amount of insulin released.[122] Underlying mechanisms behind specific patterns of secretion have not been firmly identified and there is much interest in the development of theories explaining the fundamental causes of these dynamics and their potential involvement in diabetes.

Characterization of Pulsatile Insulin Release Frequencies from Individual Animals. To demonstrate the potential utility of the chip for characterizing insulin secretion dynamics, pulsatile release from islets from individual mice were examined. A recent study showed that isolated islets from individual outbred mice have a characteristic Ca^{2+} flux oscillatory frequency (i.e., islets from one mouse oscillate at specific period while islets from another mouse pulsed either faster or slower).[126] Though mechanisms behind oscillating islet behavior are not well defined, these results suggest that mice have an intrinsic drive in vivo that maintains similar Ca^{2+} flux oscillations within islets from a particular animal. Studies have shown reduction in amplitude and possibly frequency of secretion pulses in diabetic patients,[170,171] and it is possible that this observed imprinting could potentially influence the vulnerability of individuals to developing diabetes.[126]

However, a direct link between insulin secretion frequency in isolated islets and individual mice has not yet been observed (primarily due to insufficient islet secretion analysis methods). Using the redesigned 15-islet microchip, we tested islets from 6 individual mice for Ca^{2+} flux and insulin release oscillation periods during continual stimulation with 11.1 mM glucose. Ca^{2+} and insulin oscillations were observed under conditions reproduced from the previously described study to: i) establish the variability observed between animals was real and ii) show these variations in insulin secretion

mirrored the individual differences in Ca^{2+} at the single islet level. Oscillations from three mice used in the study are shown in Figure 5.10A, illustrating similar frequencies coming from particular mice. Results summarized by plotting the average of observed Ca^{2+} flux and insulin release periods from each mouse (Figure 5.10B and C) show two interesting trends: i) islets from single mice showed similar Ca^{2+} and insulin secretion frequencies and ii) oscillation periods are noticeably different from mouse to mouse. These results agree with the previous Ca^{2+} flux study, and confirm that insulin release from isolated islets is subject to the same intrinsic patterning as Ca^{2+} flux.
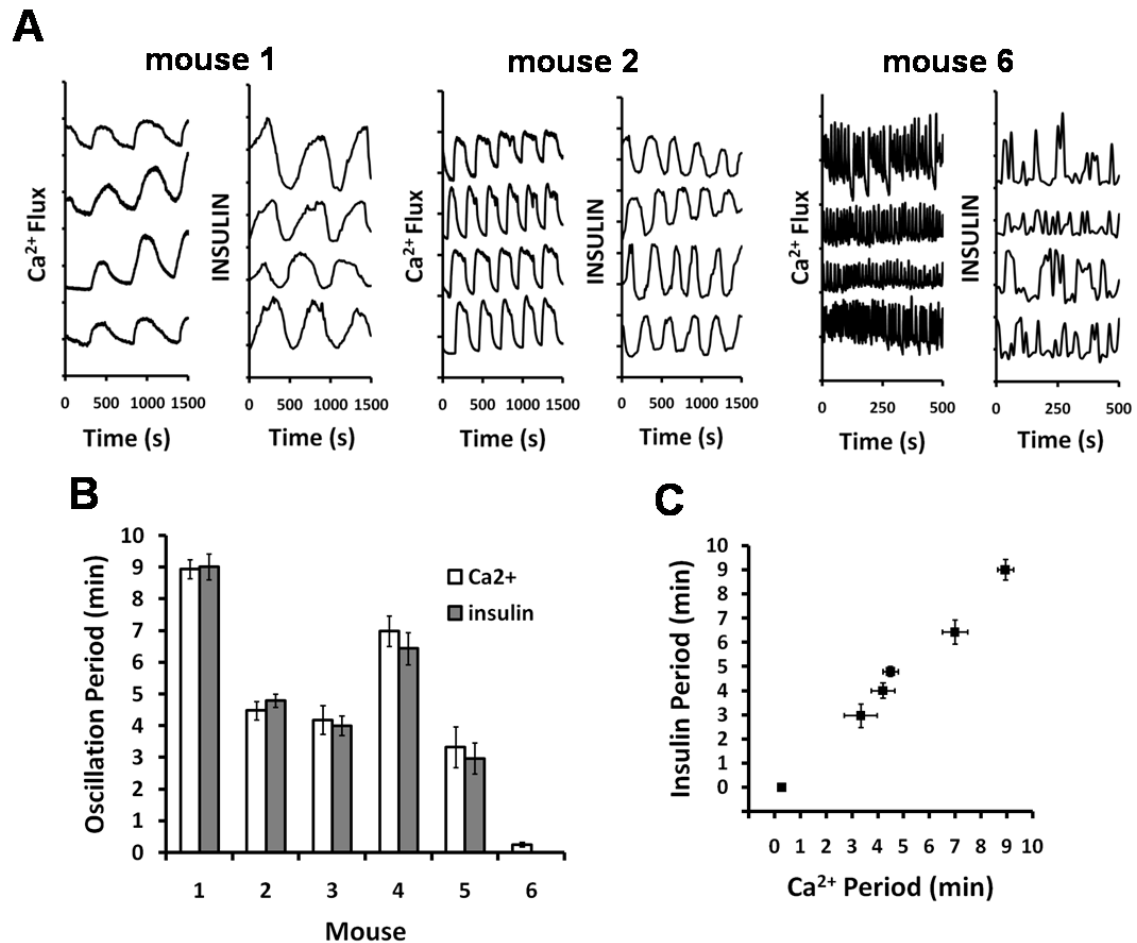
Figure 5.10. Ca^{2+} flux and insulin release profiles showing oscillatory frequencies that are characteristic of individual animals. (A) Ca^{2+} flux and insulin release traces from islets taken from three different mice (labeled accordingly). Displayed oscillation frequency averages are 9 min (mouse 1), 4.5 min (mouse 2), and 15 s (mouse 3). Periods were calculated using local minimum values. Insulin oscillations from mouse 6 were faster than the measured temporal resolution (22 s) of the chip, causing undersampling of secretion dynamics. (B) Comparison of average Ca^{2+} and insulin oscillation periods from each animal. Data sets are n ≥ 6 islets and error bars are ± 1 standard deviation. (C) Plot of average Ca^{2+} versus insulin for each mouse. The linear relationship of data points suggests good agreement of oscillation frequencies.

Preliminary Investigations into the Effects of Chronic FFA Exposure on Pulsatile Secretion. Experiments probing how long-term exposure to fatty acid influences secretory dynamics were performed by monitoring release from islets after being exposed to high concentrations of palmitic acid for 48 hours. Such incubations have previously been shown to cause impaired islet functioning including disturbed

metabolism[172] and inhibited glucose-stimulated insulin secretion.[144] This effect of fatty acids is considered a model of lipotoxicity, a potential mechanism of islet functional degradation in type 2 diabetes.[173] Although chronic exposure to fatty acids has been shown to cause a blunted first phase response from islets,[174] its effects on single islet oscillations are not well studied.

After incubation, islets were subjected to continuous perfusion with 10 mM glucose to induce oscillatory behavior while either intracellular Ca^{2+} levels or insulin release was monitored. Results showing three single islet plots from each data set in Figure 5.11 (A, Ca^{2+} flux from islets incubated in control media; B, Ca^{2+} flux from islets incubated in FFA; C, insulin release from islets incubated in control media; D, insulin release from islets incubated in FFA) illustrate that overall Ca^{2+} flux and insulin release rates were lower from islets treated with palmitic acid incubation, in agreement with previous studies. However, comparison of averaged insulin secretion (control: 148.72 pg min^{-1} ± 26.99; FFA: 112.91 pg min^{-1} ± 33.51) and Ca^{2+} flux (control: 202.14 nM ± 24.77; FFA: 167.48 nM ± 20.86) across all islets tested between the two groups did not yield a significant difference for either experiment ($P \geq 0.07$). The dynamic recordings shown here, however, offer more information regarding the impaired release and show association with suppression of oscillatory behavior. The islets affected by FFA incubation (panels B & D) show decreased oscillation amplitude as well as perturbed periods (either lacking oscillations completely or having potentially much slower oscillations than observed in panels A & C). These data suggest that FFA-induced lipotoxicity in islets can potentially affect mechanisms that control pulsatile secretion, possibly including oscillatory glycolysis[175] or membrane potential and ATP/ADP ratio.[176]

Furthermore, these results demonstrate the utility of the 15-islet chip for comparing single islet pulsatile release and highlight the potential importance of this type of data in diabetes research.
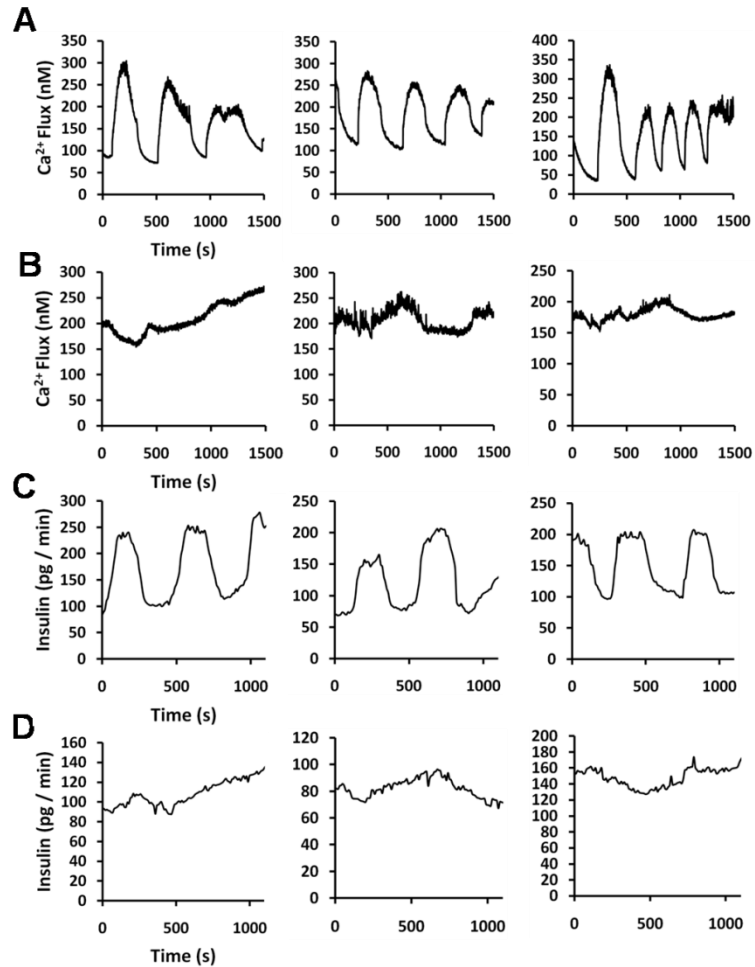
Figure 5.11. Effects of long-term FFA islet exposure on pulsatile Ca^{2+} flux and insulin release. Single islet insulin secretion and Ca^{2+} flux were monitored during continuous perfusion of 10 mM glucose after 48-hour incubation in RPMI media supplemented with either FFA-free BSA (A & C) or 0.5 mM palmitic acid (B & D). Islets incubated in FFA showed little to no oscillatory behavior, while those treated with BSA showed typical response. Only three islets from each data set (n ≥ 6) are shown.

Conclusions

A microfluidic chip for measuring insulin release from 15 isolated pancreatic islets with improved sampling was presented. Characterization of microchip

performance showed a delay time of 153 s and an expected rise time of 22 s for changes in insulin levels in the device. The chip was used to monitor biphasic and pulsatile insulin release from islets in parallel. Additionally, single islet data gathered with the device was used to characterize oscillatory secretion frequencies of islets from individual animals, showing that pulsatile release was similar between islets from a single animal, but different across multiple animals. Finally, studies aimed at investigating the effects of chronic FFA exposure on pulsatile insulin release showed an inhibition of secretion dynamics in islets treated with FFA incubation.

The microchip presented here allowed collection of high-throughput single islet secretion data for investigations of pulsatile insulin release. Previously reported methods of single islet analysis have offered the collection of data in lower throughput formats, and are thus not amenable for fast collection the data sets presented here. For example, the insulin secretion data from each mouse presented in Figure 5.10 were collected in a single experiment with the parallel chip. The use of a single sample method to collect these results would have required multiple experiments possibly performed over several days.

CHAPTER 6

SUMMARY AND FUTURE DIRECTIONS

Summary

Microfluidic devices for parallel analysis of insulin release from single islets of Langerhans were developed. These chips showed a marked improvement over single-sample devices through the collection of high throughput single islet secretion data while minimizing time, effort, and animal sacrifices needed for experiments. Analyses for insulin on chips housing four and 15 islets were made every 6 – 10 s allowing for characterization of islet secretion with high temporal resolution. The increases in islet throughput were accomplished by developing chips with multiple microfluidic channel manifolds, each capable of performing CE-based immunoassays. Additionally, these chips incorporated multiple CE separation channels, necessitating the use of methods for multiplexed fluorescence detection. Additional advantages over single sample devices are found in cost savings. The cost of reagents used with the 15-islet chip was as low as ~\$0.01 per assay, a substantial improvement over typical ELISA kits that may cost over \$5 an assay.

The first parallel islet microchip was designed for analyzing four samples simultaneously. Separations of immunoassay products were performed on microfluidic channels aligned parallel to one another, with multiplexed fluorescence detection being performed with a commercial scanning confocal microscope operated in line scan mode

(raster scanning a laser spot across the channels). Assays on this chip were performed every 6.25 s, yielding an overall rate of ~38 per minute. Assay LODs were roughly 10-fold worse than reported with single sample devices, ranging from 7 – 10 nM insulin. Although not as sensitive as previous chips, the 4-islet device was successfully used to monitor insulin release from islets in parallel.

Improvements in assay sensitivity and throughput were made with a second parallel islet chip capable of monitoring 15 islets. The use of a radial design of microfluidic channel networks (separation channels in the center portion of the chip with islet perfusion and immunoassay reagent mixing along the outer edges) facilitated this increase in performance. In this design, flow through the separation channels converged at a common point in the center of the chip where multiplexed detection was performed via fluorescence imaging. Separations on this chip were performed every 10 s, giving an overall immunoassay completion rate of 90 per minute. This chip was successfully used to monitor biphasic insulin release from 15 islets in parallel with reported LODs of 0.5 – 1 nM insulin (improved over results from the 4-islet chip).

After successful testing of the 15-islet microchip, it was used in a collaborative study investigating leptin signaling in islets. The expression of leptin receptors on cells in the endocrine pancreas suggests leptin may have direct interactions with islets in addition to its well characterized effects on the hypothalamus. In order to investigate the direct effects of leptin on islets, the 15-islet chip was used to monitor insulin release from islets from mice modified to lack leptin receptors in only the pancreas. Experiments involved characterizing insulin release under various conditions, including stimulation islets with glucose, leptin, glibenclamide, GLP-1, and palmitic acid. Additionally, the

effects of long-term fatty acid incubation on knockout islets were studied. It was found that inhibition of leptin signaling in islets from lean animals enhanced glucose-stimulated insulin secretion. Additionally, an inhibiting effect of leptin on insulin release was observed.

Further improvements made to the 15-islet chip design were aimed at optimizing sampling of insulin released from islets. In previous assays, insulin was sampled from a localized portion of the islet chamber, potentially resulting in variation in the amount of measured insulin. The addition of a sealed islet perfusion chamber allowed all of the insulin released by an islet to be pushed out of the chamber and towards the on-chip assay. Modifications of islet perfusion and sampling did not result in any significant changes in microchip performance; however, minor improvements over previous 15-iselt chip channel-to-channel reproducibility were observed. It is hypothesized that the ability to continuously introduce sample to the assay in a way that is independent of channel surface properties yields more stable assay operation. The improved 15-islet design was used to monitor biphasic and pulsatile insulin release from islets in parallel.

Studies investigating pulsatile insulin release and Ca^{2+} flux oscillations in islets from individual mice were performed. Results illustrated characteristic oscillation frequencies from specific mice, showing that pulsatile release was similar between islets from a single animal, but different across multiple animals. Additionally, preliminary experiments investigating the effects of chronic fatty acid exposure on pulsatile insulin release showed an inhibition of secretion dynamics in islets treated with FFA incubation. These studies, performed with the 15-islet chip, demonstrate the utility of high throughput single islet analysis through the observation of islet secretion dynamics.

Future Directions

Multiplexed Single Islet Assay. The microchips presented in this dissertation demonstrated the monitoring of insulin release form multiple islets using parallel microfluidic networks for performing assays for insulin. An additional application for parallel separations on a microchip would be a device that performs several different assays with perfusate from a single islet. This would be useful in monitoring other indicators of islet behavior besides insulin release, for example, the secretion of additional hormones such as glucagon and somatostatin. Also, amino acid secretions and interactions are thought to be involved in islet functions. Recently, there has been specific interest in GABA, glutamate, taurine, and glycine secretions from islets.[177-180] The ability to measure amino acids in conjunction with insulin and other hormones would provide more thorough characterization of islet behavior.

The basis for a multiplexed islet analysis chip would be on-chip islet perfusion coupled to several online assays, one for each secretion of interest. In a possible chip design presented in Figure 6.1, islet perfusate is split between two networks for immunoassay(insulin and glucagon) and a third network for amino acid characterization.
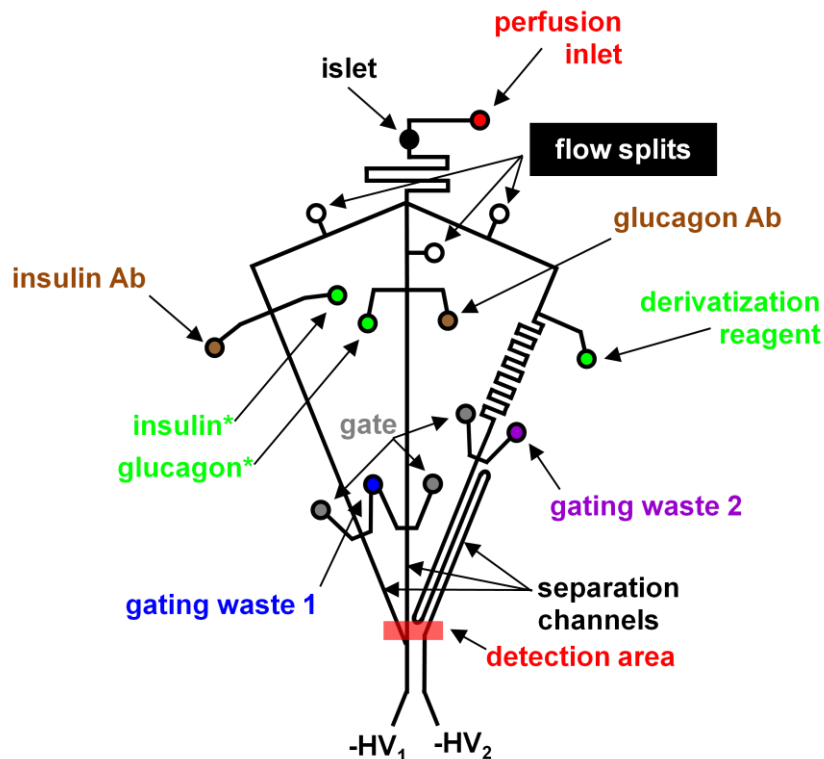
Figure 6.1 Possible chip design for simultaneous analysis of secretions from a single islet. Solid lines are channels, and circles (color coded for clarity) are fluidic reservoirs. On this chip, pressure-driven islet perfusion and sampling as described in Chapter 5 is used to introduce perfusate into assays for insulin, glucagon, and amino acids. Flow splits illustrated in the design will be designed independently to ensure proper sample/reagent mixing for each assay. Reagent flow will be controlled by EOF. The amino acid analysis will most likely require different reaction time, gating flow, and separation potential, and will thus be controlled with separate power supplies.

On this device, the assay for insulin would remain largely unchanged from methods described throughout this dissertation. The presented assay for glucagon would also function similarly. Flow from the islet will mix with fluorescent-labeled glucagon and anti-glucagon antibody for a competitive immunoassay. Assuming separation times for this assay are similar to what can be obtained with the insulin assay, injections onto separation channels in both assays could be controlled by a single injection trigger (as shown in Figure 6.1). However, since glucagon secretion rates are much lower compared to insulin (reports have shown about ten-fold lower),[102,181] it may be necessary to reduce the rate of islet perfusion to allow higher concentrations of glucagon to be introduced into

the assay. Additionally, precise control of pressure-driven sample introduction will allow optimization of sample/reagent mixing that is independent of flow leading to other assays.

The on-chip assay for amino acids will be accomplished through online derivatization with an amine-reactive fluorescent dye and subsequent analysis with CE. With this type of assay there is the potential for needing longer reaction and separation times compared to immunoassays, necessitating that flow be controlled by an independent injection trigger and power supply. Previously measured release of amino acids from islets measured in our lab yielded concentrations ranging from 2 to 100 nM. Online derivatization of analyte concentrations this low may be difficult to perform, as methods that report LODs at this level often utilize serial dilutions post-reaction.[182] Though OPA derivatization has been shown to be capable of producing LODs for amino acids down to 40 nM on a microchip,[183] the use of this reaction would require detection optics not compatible with the fluorescent tags used in the immunoassay (typically FITC). Amine-reactive dyes that excite and emit at similar wavelengths as FITC could provide an alternative for single wavelength detection.[184] Also, it may be possible to couple methods for preconcentration of analyte onto the chip design that have been shown to increase the concentration of biomolecules by up to 600-fold before injection onto a separation channel.[185] However, these concentration effects have been observed after a process time that lasts several minutes, and thus may significantly decrease temporal resolution.

All of the separation channels for the parallel assays would pass through a single detection area for multiplexed fluorescence detection. Detection would be performed

117

using the inverted epi-fluorescence microscope with EMCCD camera that has been used for detection with the 15-islet chip. As mentioned previously, it would be useful for all fluorescent probes used in these assays to have similar excitation and emission wavelengths to simplify detection optics. However, if derivatization components that fluoresce at different wavelengths are found necessary to obtain required LODs for the amino acid assay, options for dual-wavelength excitation and emission can be explored.

Integration of Additional Functions onto Parallel Islet Microchip. Further development of the 15-islet analysis chips towards a true lab-on-a-chip device would include the integration of fluorescence detection, on-chip pumping, and islet heating.

Fluorescence detection on the 15-islet chip was performed using light from an arc lamp for excitation. Though this proved useful for the developed assays, the integration of LIF detection onto the device could potentially increase sensitivity and allow the chip to be used for additional functions. Integration of LIF detection into microchips has been previously demonstrated through the use of optical fibers and liquid-core optical waveguides.[186] With these chips, laser light is introduced into the device with embedded fiber optics and then channeled towards a specific channel for fluorescence excitation. Though shown on single-channel devices, parallel on-chip fiber optic LIF detection as would be necessary for use with a parallel islet chip has not yet been demonstrated. Multiplexed detection using a single laser source would require the splitting of light into multiple pathways for parallel fluorescence excitation. It is possible that a radial design of separation channels may not be amenable with this type of excitation given the difficulty in directing light between adjacent channels. However, the collection of fluorescence emission from separation channels using fiber optics and waveguides rather

than a single objective lens would not necessitate the close proximity of detection points on a chip, allowing a redesigned device to include detection points spatially separate and more amenable for parallel fiber optic LIF detection.

The inclusion of pressure-driven flow for perfusion, sampling, and sample introduction into the 15-islet chip design yielded channel-to-channel assays that were slightly more reproducible compared to EOF islet sampling (Chapter 5). It is possible that this observed improvement in reproducibility was a result of using a type of flow that is not dependent on channel surface properties that may vary across a device.[26] It is possible that using hydrodynamic flow to control all sample and reagent movement and mixing could improve assay reproducibility even further. The introduction of hydrodynamic flow driven by on-chip pumps would accomplish this goal while also producing a more integrated device. One method of producing integrated microfluidic flow control involves creating peristaltic-style pumps using multi-layer soft lithography.[187] Modified designs of this type of pump have demonstrated flow rates up to 800 nL min^{-1},[183] adequate for islet perfusion. A possible chip design using these pumps for islet perfusion and immunoassay reagent flow is shown in Figure 6.2. It will be necessary to create a glass/PDMS hybrid chip as the flexibility of PDMS is required for proper functioning of the pumps while glass would still be needed for good CE separations. Alternatively, fluid pumping could be performed on a separate layer of PDMS through which flow is channeled for pumping before being introduced into the glass channels. CE separations and fluorescence detection would be performed as before, though gating of reaction fluid may also require hydrodynamic flow.
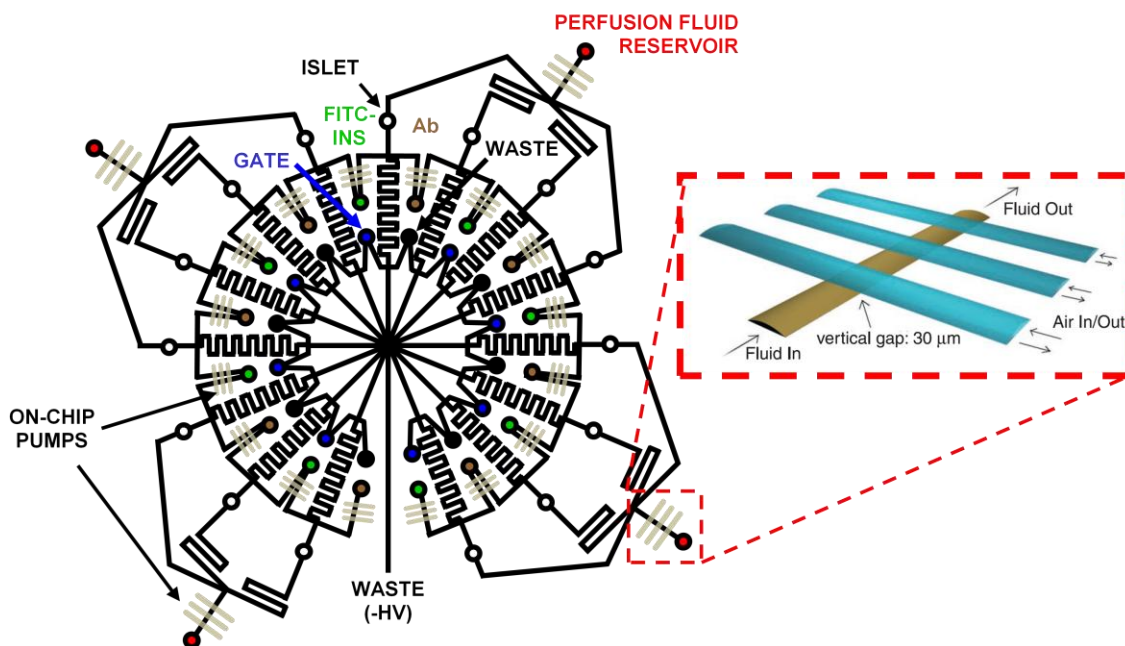
Figure 6.2. Possible chip design for integration of on-chip pumps for control of immunoassay reagent and sample flow. On this chip, fluid from perfusion buffer reservoirs would pass through integrated pumps before passing over islets sealed into chambers as described in Chapter 5. Additionally, flow of immunoassay reagents would be controlled by on-chip pumps. The ability to control perfusion and reagent flow rates with these pumps will allow direct missing of islet perfusate, eliminating the need for previously used flow splits. Functioning of the pumps, illustrated in the expansion on the right, is based on peristaltic-style pumping creating by timed inflation of control channels placed over the flow channel. It is likely that methods for pressure-driven flow-gating will be needed for injections on the device. Expansion in the figure is reproduced from reference 187.

A final improvement to chip design discussed here is the integration of islet chamber temperature control. Currently, heating of islets is performed using an external thin film heating strip attached to the underside of the chip. The use of this type of heater presents opportunities for uneven heating across the chip caused by variation in manual placement from experiment-to-experiment. Additionally, this heater does not use a feedback loop for temperature control, thus variations in ambient temperature may cause fluctuations in islet heating. Integrating controllable islet chamber heating into the device could decrease islet-to-islet heating variation as well as allow for monitoring of islet temperature. Integrated resistive heaters have been used with much success for on-chip PCR thermocycling, which requires precise control of fluid temperature.[188,189] The

functioning of these heaters is based on the patterning of conductive heating elements onto the device. Electrical current passed through the elements produces heat, and monitoring of temperature can be performed by measuring the resistance of additional circuits fabricated into the device that are also heated by the elements.[44,63] Integration of these tools onto a parallel islet chip would require the fabrication of multiple circuits of resistive heaters and temperature sensors passing under and around islet chambers to allow for heating of the perfusion flow and the islet to 37ºC.

Parallel Islet Analysis with Segmented Flow. Limitations of the temporal resolution of the 15-islet chip were demonstrated in Chapter 5 through the inability to reproducibly monitor 15 s secretion events. The development of a method for improved temporal resolution in islet analysis would be a useful improvement enabling the observation of fast oscillatory events. Recently, devices utilizing segmented flow for droplet-based assays have shown potential for improvements in temporal resolution.[190] In these assays, analyte and assay reagents are mixed in aqueous droplets suspended in a mobile oil phase. The reagents are allowed to react while traveling via pressure-driven flow to a detector without dispersion. The generation of droplets at a frequency of less than one second has been demonstrated, suggesting the potential for high temporal resolution of islet secretions.

A potential chip design for parallel droplet-based islet monitoring is shown in Figure 6.3. In this design, perfusate from islets is mixed with reagents for an insulin immunoassay and then split into aqueous droplets by forces from a flowing oil phase (commonly perfluorodecalin). Flows of perfusate, antigen, and antibody will be rapidly mixed when forming a droplet.[191] Droplets are pushed through microchannels by

pressure-driven flow of oil and the competitive binding reactions are allowed to proceed while flowing towards a detector.
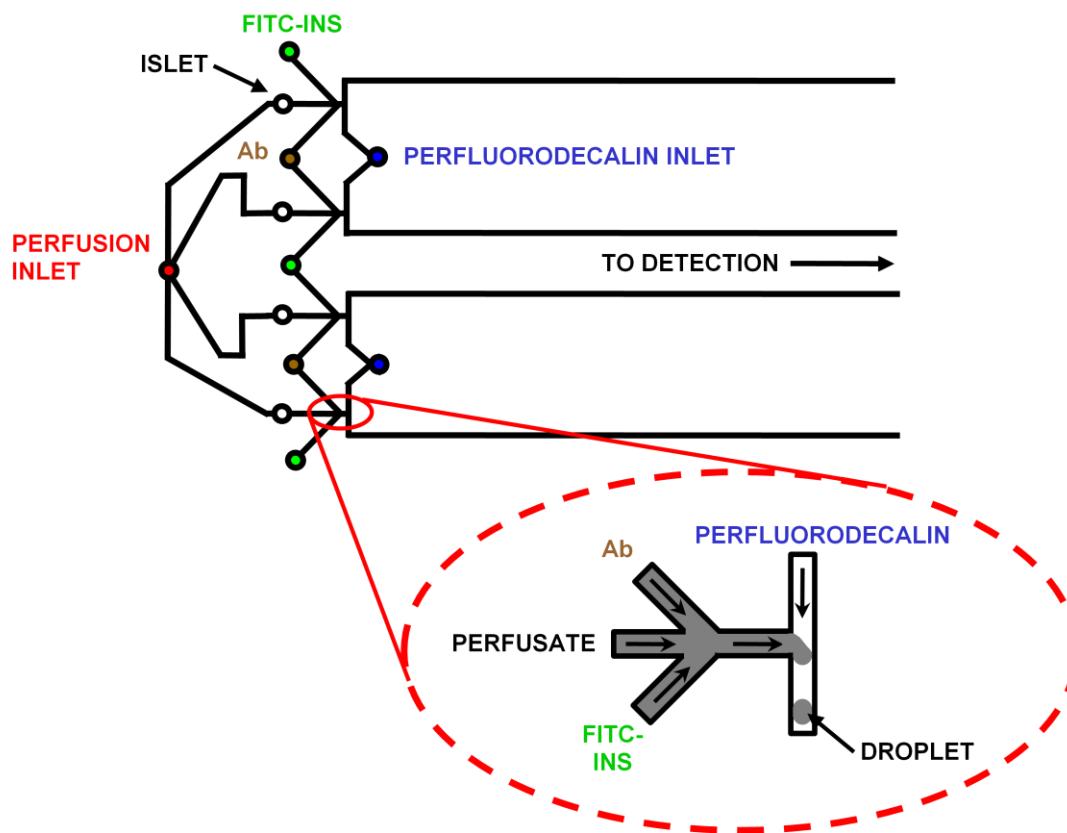
Figure 6.3. Possible chip design for droplet-based insulin assays for four islets in parallel. Black lines indicate microfluidic channels, fluidic inlets are color coded for clarity. Perfusion flow from islets sealed into chambers will mix with FITC-ins and Ab before intersecting a stream of perfluorodecalin. Shear forces at this intersection will create aqueous droplets containing perfusate and immunoassay reagents suspended in oil. Reactions between immunoassay reagents is allowed to occur during transit to a detection zone.

Current work in single-channel droplet-based islet assays in our lab has demonstrated fluorescence anisotropy as a potential detection technique. In this method, rotational diffusion of immunoassay products is determined by comparing polarization of emission light with that of excitation light. An advantage to this technique is that no separation step is required, and detection can be performed on intact droplets. However, difficulty in developing multiplexed chip-based fluorescence anisotropy may necessitate

122

alternative detection methods. Additional work in our lab has shown the ability to fuse droplets to an aqueous stream for CE separations, allowing a portion sample in the droplets to be analyzed by CE-LIF. Previous work presented in this dissertation has shown the capability for fluorescence detection of multiple CE separation microchannels, suggesting this method as a possible technique for parallel droplet-based assay detection.

Development of Data Analysis Software for Parallel Separations. The creation of a microchip for parallel separations greatly increases the rate at which data is collected, resulting in a larger total number of electropherograms to be analyzed. Although experimental data is collected in parallel, current limitations in data analysis software allow separations to be analyzed in a serial nature only (the currently used program was developed for a single channel device).[107] This requires peak high comparisons and B/F values to be calculated individually for each separation requiring a large amount of time to produce final insulin secretion plots. A reduction of time needed for parallel islet experiments could be made through the development of software capable of analyzing and organizing batches of separation data collected in parallel.

Ideally, the developed software would have several basic requirements. Parallel information exported by imaging analysis software must be imported and displayed for the user. Additionally, analysis time could be greatly reduced through batching of serial data to allow the user to define peak characteristics only once for each parallel channel. Ideal output from the program would be a list of calculated B/F values for each parallel channel that would be easily imported into Microsoft Excel for conversion into secretion rates. These advancements would greatly decrease the time needed for data analysis which can sometimes take multiple days.

123

APPENDIX A

CONSIDERATIONS IN MICROCHIP DESIGN AND FABRICATION

The design and fabrication of a functional microfluidic chip is dependent upon several critical factors. Primarily, fluidic channels and microfabricated structures must be designed with the appropriate properties to ensure proper performance (e.g. proper fluid mixing, reaction times, separation properties) for a particular application. These designs vary a great deal depending upon the intended function. There are, however, additional factors which can be influential in any chip design that can influence fabrication and functioning of microchips. This appendix will discuss several considerations aimed at facilitating chip fabrication that should be made when designing a microfluidic chip. The points discussed will generally pertain to glass chip fabrication using standard wet-chemical etching techniques as used to create chips described throughout this dissertation.

Channel Etching

When designing a photomask to be used for patterning a channel design onto a glass substrate (photoresist), it is critical to take the etching properties of glass into consideration for proper channel placement. As illustrated in Figure A.1, the isotropic etching properties of wet-chemical fabrication steps produce final channel

124

widths that are wider than what were originally designed on the mask. Thus, it is important to place channels on the mask with enough space between them to ensure that they remain independent structures after etching. Additionally, it is possible that the channel width patterned onto the glass substrate (photoresist) will be slightly larger than that on the photomask after broadening through UV exposure and photoresist/metal layer removal steps. However, these effects are typically minor in comparison to channel etching.
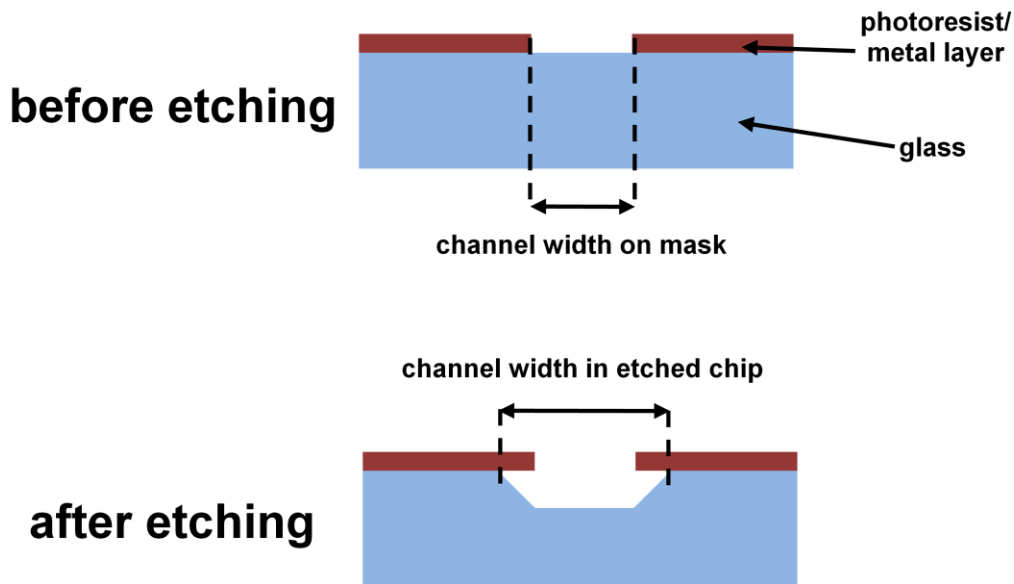
Figure A.1. Illustration of expansion of channel width upon etching. The isotropic etching produced when using wet chemical etching techniques produces trapezoid-shaped channels. During etching, total channel width is increased by a distance equal to two-times the depth of the channel. It is important to remember this channel-widening effect and plan accordingly when designing a photomask for microchip fabrication.

Access Hole Fabrication

Microfluidic chips consisting of enclosed channel networks typically require the fabrication of access holes to allow control of fluid within the device. There are several methods for fabricating these access points, including ultrasonic and laser drilling techniques that can create holes down to 50 μm in diameter. However, as these processes

can be expensive, it is common in our lab to use a drill press and small diameter diamond-tipped drill bit for the manual drilling of holes. In addition to costing less, this method can be less time consuming as it does not require microchips to be shipped to and from a service provider. However, since manual drilling is performed by hand with no available micromanipulation for hole positioning, care must be taken in planning for adequate space on a chip design to facilitate drilling. It is advisable that channels on the chip are placed far enough away from a drilling point to ensure they are not unintentionally damaged in the hole drilling process. Drilling into glass can occasionally cause chipping and cratering of the glass surface. Thus, it is important that channels positioned adjacent to access holes be spaced by an appropriate distance to be protected from potential damage. This appropriate distance is dependent upon the skill of the student fabricating the chip, but is typically around several millimeters.

Additionally, when drilling access holes by hand it is important to design a microchip that allows hole placement to be reproducible. For example, it may be difficult to manually drill a hole at a specified position on a straight channel with no markers or visual cues for drill bit alignment. It is often useful to design a chip so that holes are drilled at channel intersections (bends, etc.) to allow reproducible alignment and drilling. Alternatively, the inclusion of visual markers on a photomask that are nearby to channels can serve as a reference point for hole drilling.

Fluidic Reservoir Placement

Once access hole drilling and the remainder of microchip fabrication is completed, fluidic reservoirs are often placed on the chip surface. These reservoirs are

typically needed for a supply of fluid, collection of flow, or as a flow inlet from another device (e.g. syringe pump). Commercially available reservoirs obtained from Upchurch Scientific (NanoPort™) having diameters of nine and 10 mm are typically used in our lab. It is helpful to take desired reservoir position into account when designing a photomask by planning for enough space on the chip surface for placement of the required number of reservoirs. This process can be facilitated by drawing circles with the same diameters as fluidic reservoirs over a mask design created using AutoCAD to ensure there is no overlapping. Additionally, if high electrical potentials will be applied to reservoirs on a chip surface for electrokinetic flow, it is suggested that reservoirs be completely separated and have no parts touching to assist with electrical isolation.

If reservoir sizes other than those available with commercial pieces are required, it is possible to manually create reservoirs in-house from a variety of materials. Numerous vendors can supply glass or plastic tubing of varying inner and outer diameters that can be cut to length and affixed onto a chip surface with epoxy. This option is also more cost effective, as commercial reservoirs can cost up to $6 each while PTFE tubing costs about $1.60 per foot (enough for 48 reservoirs).

On-Chip Detection Area

As our lab typically utilizes fluorescence detection, this section will pertain to considerations for designing a microfluidic chip for use with optical detection. If fluorescence point detection is being performed on a chip, it is helpful to design the width of a channel at the detection point to be compatible with the diameter of the excitation laser spot to maximize fluorescence excitation and emission. It may also be useful to

include a visual marker in the chip design (close to the detection point) to help with reproducible positioning of the laser spot on the chip.

One important consideration, especially if developing a parallel chip with multiple fluorescence detection points, is ensuring that channel and detection area sizes are comparable with the field of view of optics used for detection. If imaging detection is used, optics must be able to produce an image of the entire on-chip detection zone on the detector. Though seemingly straightforward, this can be an important consideration as the field of view observed through a fluorescence microscope eyepiece is not necessarily the same size as the image collected on a CCD chip though a side port on the same microscope. Also, the etching of glass channels will increase the size of the detection area on a chip, possibly affecting the field of view needed for detection.

An additional consideration in optical detection with microchips is compatibility between chip thickness and working distance of a required objective lens. Generally, higher magnification lenses have shorter working distances (aside from special long working distance (LWD) objective lenses). If a certain magnification is required for detection, it is advisable to ensure the thickness of the device allows for proper objective lens proximity to the microchannels.

REFERENCES

(1)   Manz, A.; Graber, N.; Widmer, H. M. *Sens. Actuat. B 1* **1990**, 224 - 248.

(2)   Harrison, D. J.; Manz, A.; Fan, Z.; Ludi, H.; Widmer, H. M. *Anal. Chem.* **1992**, *64*, 1926 - 1932.

(3)   Effenhauser, C. S.; Bruin, G. J. M.; Paulus *Electrophoresis* **1997**, *18*, 2203 - 2213.

(4)   Jacobson, S. C.; Hergenroder, R.; Koutny, L. B.; Ramsey, J. M. *Anal. Chem.* **1994**, *66*, 1114 - 1118.

(5)   Dolnik, V.; Liu, S.; Jovanovich, S. B. *Electrophoresis* **2000**, *21*, 41 - 54.

(6)   McDonald, J. C.; Duffy, D. C.; Anderson, J. R.; Chiu, D. T.; Wu, H.; Schueller, O. J. A.; Whitesides, G. M. *Electrophoresis* **2000**, *21*, 27 - 40.

(7)   Jacobson, S. C.; Koutny, L. B.; Hergenroder, R.; Moore, A. W.; Ramsey, J. M. *Anal. Chem.* **1994**, *66*, 3472 - 3476.

(8)   Woolley, A. T.; Hadley, D.; Landre, P.; deMello, A. J.; Mathies, R. A.; Northrup, M. A. *Anal. Chem.* **1996**, *68*, 4081 - 4086.

(9)   Jacobson, S. C.; Hergenroder, R.; Moore, A. W.; Ramsey, J. M. *Anal. Chem.* **1994**, *66*, 4127 - 4132.

(10)   Panaro, N. J.; Yuen, P. K.; Sakazume, T.; Fortina, P.; Kricka, L. J.; Wilding, P. *Clin. Chem.* **2000**, *46*, 1851 - 1853.

(11)   Yin, H.; Killeen, K. *J. Sep. Sci.* **2007**, *30*, 1427 - 1434.

(12)   Yin, H.; Killeen, K.; Brennen, R.; Sobek, D.; Werlich, M.; van de Goor, T. *Anal. Chem.* **2005**, *77*, 527 - 533.

(13)   Wan, H.; Bergstrom, F. *J. Liq. Chromatogr. R T* **2007**, *30*, 681 - 700.

(14)   Ducret, A.; Van Oostveen, I.; Eng, J. K.; Yates, J. R.; Aebersold, R. *Protein Sci.* **1998**, *7*, 706 - 719.

(15)   Huang, H. C.; Quesada, M. A.; Mathies, R. A. *Anal. Chem.* **1992**, *64*, 967 - 972.

(16)   Dittrich, P. S.; Tachikawa, K.; Manz, A. *Anal. Chem.* **2006**, *78*, 3887 - 3907.

(17)   Roman, G. T.; Kennedy, R. T. *J. Chromatogr. A* **2007**, *1168*, 170 - 188.

(18)   Tao, L.; Kennedy, R. T. *TrAC - Trend. Anal. Chem.* **1998**, *17*, 484 - 491.

(19)   Mathies, R. A.; Huang, X. C. *Nature* **1992**, *359*, 167 - 169.

(20)   Woolley, A. T.; Sensabaugh, G. F.; Mathies, R. A. *Anal. Chem.* **1997**, *69*, 2181 - 2186.

(21)   Xu, H.; Roddy, T. P.; Lapos, J. A.; Ewing, A. G. *Anal. Chem.* **2002**, *74*, 5517 - 5522.

(22)   Lapos, J. A.; Ewing, A. G. *Anal. Chem.* **2000**, *72*, 4598 - 4602.

(23)   Pawley, J. B. *Handbook of Biological Confocal Microscopy*; 2nd Edition ed.; Plenum Press: New York, 1995.

(24)   Simpson, P. C.; Roach, D. J.; Woolley, A. T.; Thorsen, T.; Johnston, R.; Sensabaugh, G. F.; Mathies, R. A. *Proc. Natl. Acad. Sci.* **1998**, *95*, 2256 - 2261.
(25)   Liu, S.; Ren, H.; Gao, Q.; Roach, D. J.; Loder, R. T.; Armstrong, T. M.; Mao, Q.; Blaga, I.; Barker, D. L.; Jovanovich, S. B. *Proc. Natl. Acad. Sci.* **2000**, *97*, 5369 - 5374.
(26)   Cheng, S. B.; Skinner, C. D.; Taylor, J.; Attiya, S.; Lee, W. E.; Picelli, G.; Harrison, D. J. *Anal. Chem.* **2001**, *73*, 1472 - 1479.
(27)   Huang, Z.; Munro, N.; Huhmer, A. F. R.; Landers, J. P. *Anal. Chem.* **1999**, *71*, 5309 - 5314.
(28)   Sanders, J. C.; Huang, Z.; Landers, J. P. *Lab Chip* **2001**, *1*, 167 - 172.
(29)   Huang, Z.; Jin, L.; Sanders, J. C.; Zheng, Y.; Dunsmoor, C.; Tian, H.; Landers, J. P. *IEEE T Bio-med. Eng.* **2002**, *49*, 859 - 866.
(30)   Shi, Y.; Simpson, P. C.; Scherer, J. R.; Wexler, D.; Skibola, C.; Smith, M. T.; Mathies, R. A. *Anal. Chem.* **1999**, *71*, 5354 - 5361.
(31)   Emrich, C. A.; Tian, H.; Medintz, I. L.; Mathies, R. A. *Anal. Chem.* **2002**, *74*, 5076 - 5083.
(32)   Medintz, I. L.; Paegel, B. M.; Blazej, R. G.; Emrich, C. A.; Berti, L.; Scherer, J. R.; Mathies, R. A. *Electrophoresis* **2001**, *22*, 3845 - 3856.
(33)   Shackman, J. G.; Munson, M. S.; Ross, D. *Anal. Chem.* **2007**, *79*, 565 - 571.
(34)   Inoue, A.; Ito, T.; Makino, K.; Hosokawa, K.; Maeda, M. *Anal. Chem.* **2007**, *79*, 2168 - 2173.
(35)   Roddy, E. S.; Price, M.; Ewing, A. G. *Anal. Chem.* **2003**, *75*, 3704 - 3711.
(36)   Dang, F.; Tabata, O.; Kurosawa, M.; Ewis, A. A.; Zhang, L.; Yamaoka, Y.; Shinohara, S.; Shinohara, Y.; Ishikawa, M.; Baba, Y. *Anal. Chem.* **2005**, *77*, 2140 - 2146.
(37)   Zhang, L.; Yin, X. *Electrophoresis* **2007**, *28*, 1281 - 1288.
(38)   Gao, Y.; Shen, Z.; Wang, H.; Dai, Z.; Lin, B. *Electrophoresis* **2005**, *26*, 4774 - 4779.
(39)   Smith, E. M.; Xu, H.; Ewing, A. G. *Electrophoresis* **2001**, *22*, 363 - 370.
(40)   Simpson, J. W.; Ruiz-Martinez, M. C.; Mulhern, G. T.; Berka, J.; Latimer, D. R.; Ball, J. A.; Rothberg, J. M.; Went, G. T. *Electrophoresis* **2000**, *21*, 135 - 149.
(41)   Shadpour, H.; Hupert, M. L.; Patterson, D.; Liu, C.; Galloway, M.; Stryjewski, W.; Goettert, J.; Soper, S. A. *Anal. Chem.* **2007**, *79*, 870 - 878.
(42)   Solinova, V.; Kasicka, V. *J. Sep. Sci.* **2006**, *29*, 1743 - 1762.
(43)   Munce, N. R.; Li, J.; Herman, P. R.; Lilge, L. *Anal. Chem.* **2004**, *76*, 4983 - 4989.
(44)   Liu, C. N.; Toriello, N. M.; Mathies, R. A. *Anal. Chem.* **2006**, *78*, 5474 - 5479.
(45)   Xu, H.; Roddy, E. S.; Roddy, T. P.; Lapos, J. A.; Ewing, A. G. *J. Sep. Sci.* **2004**, *27*, 7 - 12.
(46)   Shen, Z.; Liu, X.; Long, Z.; Liu, D.; Ye, N.; Qin, J.; Dia, Z.; Lin, B. *Electrophoresis* **2006**, *27*, 1084 - 1092.

(47)   Bilitewski, U.; Genrich, M.; Kadow, S.; Mersal, G. *Anal. Bioanal. Chem.* **2003**, *377*, 556 - 569.

(48)   Bromberg, A.; Mathies, R. A. *Electrophoresis* **2004**, *25*, 1895 - 1900.

(49)   Dishinger, J. F.; Kennedy, R. T. *Anal. Chem.* **2007**, *79*, 947 - 954.

(50)   Honda, H.; Lindberg, U.; Andersson, P.; Hoffmann, S.; Takei, H. *Clin. Chem.* **2005**, *51*, 1955 - 1961.

(51)   Herrmann, M.; Veres, T.; Tabrizian, M. *Lab Chip* **2006**, *6*, 555 - 560.

(52)   Xu, H.; Ewing, A. G. *Electrophoresis* **2005**, *26*, 4711 - 4717.

(53)   Pei, J.; Dishinger, J. F.; Roman, D. L.; Rungwanitcha, C.; Neubig, R. R.; Kennedy, R. T. *Anal Chem* **2008**, *80*, 5225-31.

(54)   Carrilho, E. *Electrophoresis* **2000**, *21*, 55 - 65.

(55)   Kan, C.-W.; Fredlake, C. P.; Doherty, E. A. S.; Barron, A. E. *Electrophoresis* **2004**, *25*, 3564 - 3588.

(56)   Zhang, L.; Dang, F.; Baba, Y. *J. Pharmaceut. Biomed.* **2003**, *30*, 1645 - 1654.

(57)   Paegel, B. M.; Emrich, C. A.; Wedemayer, G. J.; Scherer, J.; Mathies, R. A. *Proc. Natl. Acad. Sci.* **2002**, *99*, 574 - 579.

(58)   Medintz, I. L.; Wong, W. W.; Sensabaugh, G.; Mathies, R. A. *Electrophoresis* **2000**, *21*, 2352 - 2358.

(59)   Mendintz, I.; Wong, W. W.; Berti, L.; Shiow, L.; Tom, J.; Scherer, J.; Sensabaugh, G.; Mathies, R. A. *Genome Res.* **2001**, *11*, 413 - 421.

(60)   Tian, H.; Emrich, C. A.; Scherer, J. R.; Mathies, R. A.; Andersen, P. S.; Larsen, L. A.; Christiansen, M. *Electrophoresis* **2005**, *26*, 1834 - 1842.

(61)   Yeung, S. H. I.; Greenspoon, S. A.; McGuckian, A.; Crouse, C. A.; Emrich, C. A.; Ban, J.; Mathies, R. A. *J. Forensic Sci.* **2006**, *51*, 740 - 747.

(62)   Aborn, J. H.; El-Difrawy, S. A.; Novotny, M.; Gismondi, E. A.; Lam, R.; Matsudaira, P.; Mckenna, B. K.; O'Neil, T.; Streechon, P.; Ehrlich, D. J. *Lab Chip* **2005**, *5*, 669 - 674.

(63)   Toriello, N. M.; Liu, C. N.; Mathies, R. A. *Anal. Chem.* **2006**, *78*, 7997 - 8003.

(64)   Fiedler, S.; Shirley, S. G.; Schnelle, T.; Fuhr, G. *Analytical Chemistry* **1998**, *70*, 1909-1915.

(65)   Fu, A. Y.; Spence, C.; Scherer, A.; Arnold, F. H.; Quake, S. R. *Nature Biotechnology* **1999**, *17*, 1109-1111.

(66)   Schrum, D. P.; Culbertson, C. T.; Jacobson, S. C.; Ramsey, J. M. *Analytical Chemistry* **1999**, *71*, 4173-4177.

(67)   McClain, M. A.; Culbertson, C. T.; Jacobson, S. C.; Ramsey, J. M. *Analytical Chemistry* **2001**, *73*, 5334-5338.

(68)   Wilding, P.; Kricka, L. J.; Cheng, J.; Hvichia, G.; Shoffner, M. A.; Fortina, P. *Analytical Biochemistry* **1998**, *257*, 95-100.

(69)   Gao, J.; Yin, X. F.; Fang, Z. L. *Lab on a Chip* **2004**, *4*, 47-52.

(70)   Takayama, S.; McDonald, J. C.; Ostuni, E.; Liang, M. N.; Kenis, P. J. A.; Ismagilov, R. F.; Whitesides, G. M. *Proceedings of the National Academy of Sciences of the United States of America* **1999**, *96*, 5545-5548.

(71)   Sato, K.; Egami, A.; Odake, T.; Tokeshi, M.; Aihara, M.; Kitamori, T. *Journal of Chromatography A* **2006**, *1111*, 228-232.

(72)   Ionescu-Zanetti, C.; Shaw, R. M.; Seo, J. G.; Jan, Y. N.; Jan, L. Y.; Lee, L. P. *Proceedings of the National Academy of Sciences of the United States of America* **2005**, *102*, 9112-9117.

(73)   Lau, A. Y.; Hung, P. J.; Wu, A. R.; Lee, L. P. *Lab on a Chip* **2006**, *6*, 1510-1515.

(74)   Huang, W. H.; Cheng, W.; Zhang, Z.; Pang, D. W.; Wang, Z. L.; Cheng, J. K.; Cui, D. F. *Analytical Chemistry* **2004**, *76*, 483-488.

(75)   Wheeler, A. R.; Throndset, W. R.; Whelan, R. J.; Leach, A. M.; Zare, R. N.; Liao, Y. H.; Farrell, K.; Manger, I. D.; Daridon, A. *Anal. Chem.* **2003**, *75*, 3581 - 3586.

(76)   Lee, P. J.; Hung, P. J.; Shaw, R.; Jan, L.; Lee, L. P. *Applied Physics Letters* **2005**, *86*.

(77)   Gould, J. L.; Keeton, W. T. *Biological Science*; 6th edition ed.; W. W Norton & Co.: New York, 1996.

(78)   Nadal, A.; Quesada, I.; Soria, B. *Journal of Physiology-London* **1999**, *517*, 85-93.

(79)   Voet, D.; Voet, J. G.; Pratt, C. W. *Fundamentals of Biochemistry*; John Wiley & Sons, Inc.: New York, 2002.

(80)   Nugent, D. A.; Smith, D. M.; Jones, H. B. *Toxicol. Pathol.* **2008**, *published online May 8, 2008*.

(81)   U.S. Department of Health and Human Services: Atlanta, GA, 2007.

(82)   Kahn, C. R. *Diabetes* **1994**, *43*, 1066-1084.

(83)   Jun, H. S.; Yoon, J. W. *Current Gene Therapy* **2005**, *5*, 249-262.

(84)   Treutelaar, M. K.; Skidmore, J. M.; Dias-Leme, C. L.; Hara, M.; Zhang, L.; Simeone, D.; Martin, D. M.; Burant, C. F. *Diabetes* **2003**, *52*, 2503 - 2512.

(85)   Narushima, M.; Kobayashi, N.; Okitsu, T.; Tanaka, Y.; Li, S. A.; Chen, Y.; Miki, A.; Tanaka, K.; Nakaji, S.; Takei, K.; Gutierrez, A. S.; Rivas-Carrillo, J. D.; Navarro-Alvarez, N.; Jun, H. S.; Westerman, K. A.; Noguchi, H.; Lakey, J. R. T.; Leboulch, P.; Tanaka, N.; Yoon, J. W. *Nature Biotechnology* **2005**, *23*, 1274-1282.

(86)   Ryan, E. A.; Lakey, J. R. T.; Paty, B. W.; Imes, S.; Korbutt, G. S.; Kneteman, N. M.; Bigam, D.; Rajotte, R. V.; Shapiro, A. M. J. *Diabetes* **2002**, *51*, 2148 - 2157.

(87)   Gilon, P.; Shepherd, R. M.; Henquin, J.-C. *J. Biol. Chem.* **1993**, *268*, 22265 - 22268.

(88)   Street, C. N.; Lakey, J. R. T.; Shapiro, A. M. J.; Imes, S.; Rajotte, R. V.; Ryan, E. A.; Lyon, J. G.; Kin, T.; Avila, J.; Tsujimura, T.; Korbutt, G. S. *Diabetes* **2004**, *53*, 3107 - 3114.

(89)   Tao, L.; Aspinwall, C. A.; Kennedy, R. T. *Electrophoresis* **1998**, *19*, 403 - 408.

(90)   Schultz, N. M.; Huang, L.; Kennedy, R. T. *Anal. Chem.* **1995**, *67*, 924 - 929.

(91)   Schultz, N. M.; Kennedy, R. T. *Anal. Chem.* **1993**, *65*, 3161 - 3165.

(92)   Roper, M. G.; Shackman, J. G.; Dahlgren, G. M.; Kennedy, R. T. *Anal. Chem.* **2003**, *75*, 4711 - 4717.

(93)   Shackman, J. G.; Dahlgren, G. M.; Peters, J. L.; Kennedy, R. T. *Lab Chip* **2005**, *5*, 56 - 63.

(94)   Morioka, T.; Asilmaz, E.; Hu, J.; Dishinger, J. F.; Kurpad, A. J.; Elias, C. F.; Li, H.; Elmquist, J. K.; Kennedy, R. T.; Kulkarni, R. N. *J. Clin. Invest.* **2007**, *117*, 2860 - 2868.

(95)   McClain, M. A.; Culbertson, C. T.; Jacobson, S. C.; Allbritton, N. L.; Sims, C. E.; Ramsey, J. M. *Analytical Chemistry* **2003**, *75*, 5646-5655.

(96)   Ocvirk, G.; Salimi-Moosavi, H.; Szarka, R. J.; Arriaga, E. A.; Andersson, P. E.; Smith, R.; Dovichi, N. J.; Harrison, D. J. *P. IEEE* **2004**, *92*, 115 - 125.

(97)   Sin, A.; Chin, K. C.; Jamil, M. F.; Kostov, Y.; Rao, G.; Shuler, M. L. *Biotechnology Progress* **2004**, *20*, 338-345.

(98)   Ionescu-Zanetti, C.; Shaw, R. M.; Seo, J. G.; Jan, Y. N.; Jan, L. Y.; Lee, L. P. *Proc. Natl. Acad. Sci.* **2005**, *102*, 9112-9117.

(99)   Toriello, N. M.; Douglas, E. S.; Mathies, R. A. *Anal. Chem.* **2005**, *77*, 6935 - 6941.

(100)   Kulkarni, R. N. *Int. J. Biochem. Cell B.* **2004**, *36*, 365 - 371.

(101)   Henquin, J. C. *Diabetes* **2000**, *49*, 1751-1760.

(102)   Henquin, J. C.; Ishiyama, N.; Nenquin, M.; Ravier, M. A.; Jonas, J. C. *Diabetes* **2002**, *51*, S60-S67.

(103)   Nesher, R.; Cerasi, E. *Diabetes* **2002**, *51*, S53 - S59.

(104)   O'Rahilly, S.; Turner, R. C.; Matthews, D. R. *N. Engl. J. Med.* **1988**, *318*, 1225 - 1230.

(105)   Ueki, K.; Okada, T.; Hu, J.; Liew, C. W.; Assmann, A.; Dahlgren, G. M.; Peters, J. L.; Shackman, J. G.; Zhang, M.; Artner, I.; Satin, L. S.; Stein, R.; Holzenberger, M.; Kennedy, R. T.; Kahn, C. R.; Kulkarni, R. N. *Nat. Biotechnol.* **2006**, *38*, 583 - 588.

(106)   Sandlin, Z. D.; Shou, M.; Shackman, J. G.; Kennedy, R. T. *Anal. Chem.* **2005**, *77*, 7702 - 7708.

(107)   Shackman, J. G.; Watson, C. J.; Kennedy, R. T. *J. Chromatogr. A* **2004**, *1040*, 273 - 282.

(108)   Pralong, W. F.; Bartley, C.; Wollheim, C. B. *EMBO J.* **1990**, *9*, 53-60.

(109)   Tao, L.; Kennedy, R. T. *Anal. Chem.* **1996**, *68*, 3899 - 3906.

(110)   Effenhauser, C. S.; Paulus, A.; Manz, A.; Widmer, H. M. *Anal. Chem.* **1994**, *66*, 2949-2953.

(111)   Jacobson, S. C.; Hergenroder, R.; Koutny, L. B.; Warmack, R. J.; Ramsey, J. M. *Anal. Chem.* **1994**, *66*, 1107-1113.

(112)   Thomas, C. D.; Jacobson, S. C.; Ramsey, J. M. *Anal. Chem.* **2004**, *76*, 6053 - 6057.

(113)   Taylor, J.; Picelli, G.; Harrison, D. J. *Electrophoresis* **2001**, *22*, 3699 - 3708.

(114)   Westerlund, J.; Bergsten, P. *Diabetes* **2001**, *50*, 1785 - 1790.

(115)   Maki, L. W.; Keizer, J. *Am. J. Physiol.* **1995**, *268*, C780-C791.

(116) Zawalich, W. S.; Yamazaki, H.; Zawalich, K. C.; Cline, G. *J. Endocrinol.* **2004**, *183*, 309 - 319.

(117) White, M. F.; Kahn, C. R. *J. Biol. Chem.* **1994**, *269*, 1 - 4.

(118) Allen, R. D. M.; Nankivell, B. J.; Hawthorne, W. J.; O'Connell, P. J.; Chapman, J. R. *Transplant. Proc.* **2001**, *33*, 3485 - 3488.

(119) Jacobson, S. C.; Ermakov, S. V.; Ramsey, J. M. *Anal. Chem.* **1999**, *71*, 3273 - 3276.

(120) Gilon, P.; Ravier, M. A.; Jonas, J.-C.; Henquin, J.-C. *Diabetes* **2002**, *51*, S144 - S151.

(121) Henquin, J.-C.; Nenquin, M.; Stiernet, P.; Ahren, B. *Diabetes* **2006**, *55*, 441 - 451.

(122) Nunemaker, C. S.; Wasserman, D. H.; McGuinness, O. P.; Sweet, I. R.; Teague, J. C.; Satin, L. S. *Am. J. Physiol. Endocrinol. Metab.* **2006**, *209*, E523 - E529.

(123) Zawalich, W. S.; Zawalich, K. C.; Tesz, G. J.; Taketo, M. M.; Sterpka, J.; Philbrick, W.; Matsui, M. *Biochem. Bioph. Res. Co.* **2004**, *315*, 872 - 876.

(124) Newgard, C. B.; McGarry, J. D. *Annu. Rev. Biochem.* **1995**, *64*, 689 - 719.

(125) Bergsten, P. *Am. J. Physiol. Endocrinol. Metab.* **1998**, *274*, E796 - E800.

(126) Nunemaker, C. S.; Zhang, M.; Wasserman, D. H.; McGinness, O. P.; Powers, A. C.; Bertram, R.; Sherman, A.; Satin, L. S. *Diabetes* **2005**, *54*, 3517 - 3522.

(127) Pelleymounter, M. A.; Cullen, M. J.; Baker, M. B.; Hecht, R.; Winters, D.; Boone, T.; Collins, F. *Science* **1995**, *269*, 540-543.

(128) Campfield, L. A.; Smith, F. J.; Guisez, Y.; Devos, R.; Burn, P. *Science* **1995**, *269*, 546-549.

(129) Tartaglia, L. A.; Dembski, M.; Weng, X.; Deng, N. H.; Culpepper, J.; Devos, R.; Richards, G. J.; Campfield, L. A.; Clark, F. T.; Deeds, J.; Muir, C.; Sanker, S.; Moriarty, A.; Moore, K. J.; Smutko, J. S.; Mays, G. G.; Woolf, E. A.; Monroe, C. A.; Tepper, R. I. *Cell* **1995**, *83*, 1263-1271.

(130) Seufert, J.; Kieffer, T. J.; Habener, J. F. *Proc. Natl. Acad. Sci.* **1999**, *96*, 674 - 679.

(131) Kieffer, T. J.; Heller, R. S.; Habener, J. F. *Biochem. Bioph. Res. Co.* **1996**, *224*, 522-527.

(132) Emilsson, V.; Liu, Y. L.; Cawthorne, M. A.; Morton, N. M.; Davenport, M. *Diabetes* **1997**, *46*, 313-316.

(133) Kulkarni, R. N.; Wang, Z.-L.; Wang, R.-M.; Hurley, J. D.; Smith, D. M.; Ghatei, M. A.; Withers, D. J.; Gardiner, J. V.; Bailey, C. J.; Bloom, S. R. *J. Clin. Invest.* **1997**, *100*, 2729 - 2736.

(134) Poitout, V.; Rouault, C.; Guerre-Millo, M.; Reach, G. *Diabetes Metab.* **1998**, *24*, 321-326.

(135) Kieffer, T. J.; Habener, J. F. *Am. J. Physiol. Endocrinol. Metab.* **2000**, *278*, E1 - E14.

(136) Tanizawa, Y.; Okuya, S.; Ishihara, H.; Asano, T.; Yada, T.; Oka, Y. *Endocrinology* **1997**, *138*, 4513-4516.

(137) Leclercq-Meyer, V.; Considine, R. V.; Sener, A.; Malaisse, W. J. *Biochem. Bioph. Res. Co.* **1996**, *229*, 794 - 798.

(138) Gu, H.; Marth, J. D.; Orban, P. C.; Mossmann, H.; Rajewsky, K. *Science* **1994**, *265*, 103-106.

(139) Grynkiewicz, G.; Poenie, M.; Tsein, R. Y. *J. Biol. Chem.* **1985**, *260*, 3440-3450.

(140) Kulkarni, R. N.; Roper, M. G.; Dahlgren, G. M.; Shih, D. Q.; Kauri, L. M.; Peters, J. L.; Stoffel, M.; Kennedy, R. T. *Diabetes* **2004**, *53*, 1517 - 1525.

(141) Sinha, M. K.; Opentanova, I.; Ohannesian, J. P.; Kolaczynski, J. W.; Heiman, M. L.; Hale, J.; Becker, G. W.; Bowsher, R. R.; Stephens, T. W.; Caro, J. F. *Journal of Clinical Investigation* **1996**, *98*, 1277-1282.

(142) Grill, V.; Bjorklund, A. *Cellular and Molecular Life Sciences* **2000**, *57*, 429-440.

(143) Zhou, Y. P.; Grill, V. E. *Journal of Clinical Investigation* **1994**, *93*, 870-876.

(144) Biden, T. J.; Robinson, D.; Cordery, D.; Hughes, W. E.; Busch, A. K. *Diabetes* **2004**, *53*, S159-S165.

(145) Eto, K.; Yamashita, T.; Matsui, J.; Terauchi, Y.; Noda, M.; Kadowaki, T. *Diabetes* **2002**, *51*, S414-S420.

(146) Deeney, J. T.; Prentki, M.; Corkey, B. E. *Seminars in Cell & Developmental Biology* **2000**, *11*, 267-275.

(147) Perfetti, R.; Merkel, P. *Eur. J. Endocrinol.* **2000**, *143*, 717-725.

(148) Tuttle, R. L.; Gill, N. S.; Pugh, W.; Lee, J. P.; Koeberlein, B.; Furth, E. E.; Polonsky, K. S.; Naji, A.; Birnbaum, M. J. *Nature Medicine* **2001**, *7*, 1133-1137.

(149) Pende, M.; Kozma, S. C.; Jaquet, M.; Oorschot, V.; Burcelin, R.; Le Marchand-Brustel, Y.; Klumperman, J.; Thorens, B.; Thomas, G. *Nature* **2000**, *408*, 994-997.

(150) Bernal-Mizrachi, E.; Wen, W.; Stahlhut, S.; Welling, C. M.; Permutt, M. A. *Journal of Clinical Investigation* **2001**, *108*, 1631-1638.

(151) Ning, K.; Miller, L. C.; Laidlaw, H. A.; Burgess, L. A.; Perera, N. M.; Downes, C. P.; Leslie, N. R.; Ashford, M. L. J. *EMBO J.* **2006**, *25*, 2377 - 2387.

(152) Unger, R. H.; Zhou, Y. T. *Diabetes* **2001**, *50*, S118-S121.

(153) Poitout, V.; Robertson, R. P. *Endocrinology* **2002**, *143*, 339-342.

(154) Munoz, A.; Hu, M.; Hussain, K.; Bryan, J.; Aguilar-Bryan, L.; Rajan, A. S. *Endocrinology* **2005**, *146*, 5514-5521.

(155) McClenaghan, N. H.; Flatt, P. R.; Ball, A. J. *J. Endocrinol.* **2006**, *190*, 889-896.

(156) Tsuboi, T.; Xavier, G. D.; Holz, G. G.; Jouaville, L. S.; Thomas, A. P.; Rutter, G. A. *Biochem. J.* **2003**, *369*, 287-299.

(157) Holz, G. G. *Diabetes* **2004**, *53*, 5-13.

(158) Kieffer, T. J.; Heller, R. S.; Leech, C. A.; Holz, G. G.; Habener, J. F. *Diabetes* **1997**, *46*, 1087 - 1093.

(159) Matthews, D. R.; Naylor, B. A.; Jones, R. G.; Ward, G. M.; Turner, R. C. *Diabetes* **1983**, *32*, 617-621.

(160) Komjati, M.; Bratuschmarrain, P.; Waldhausl, W. *Endocrinology* **1986**, *118*, 312-319.

(161) Rocheleau, J. V.; Walker, G. M.; Head, W. S.; McGuinness, O. P.; Piston, D. W. *Proc. Natl. Acad. Sci.* **2004**, *101*, 12899 - 12903.

(162) Qian, W.-J.; Peters, J. L.; Dahlgren, G. M.; Gee, K. R.; Kennedy, R. T. *Biotechniques* **2004**, *37*, 922 - 933.

(163) Bergsten, P. *American Journal of Physiology-Endocrinology and Metabolism* **1995**, *268*, E282-E287.

(164) Liu, Y. J.; Tengholm, A.; Grapengiesser, E.; Hellman, B.; Gylfe, E. *Journal of Physiology-London* **1998**, *508*, 471-481.

(165) Straub, S. G.; Sharp, S. W. *Diabetes Metab. Res. Rev.* **2002**, *18*, 451-63.

(166) Luciani, D. S.; Misler, S.; Polonsky, K. S. *J. Physiol.* **2006**, *572*, 397-92.

(167) Porksen, N.; Hollingdal, M.; Juhl, C.; Butler, P.; Veldhuis, J. D.; Schmitz, O. *Diabetes* **2002**, *51*, S245-254.

(168) Cooksey, R. C.; Pusuluri, S.; Hazel, M.; McClain, D. A. *American Journal of Physiology-Endocrinology and Metabolism* **2006**, *290*, E334-E340.

(169) Dahlgren, G. M.; Kauri, L. M.; Kennedy, R. T. *Biochim. Biophys. Acta* **2005**, *1724*, 23 - 36.

(170) Polonsky, K. S.; Given, B. D.; Hirsch, L. J.; Tillil, H.; Shapiro, E. T.; Beebe, C.; Frank, B. H.; Galloway, J. A.; Vancauter, E. *New England Journal of Medicine* **1988**, *318*, 1231-1239.

(171) Ristow, M.; Carlqvist, H.; Hebinck, J.; Vorgerd, M.; Krone, W.; Pfeiffer, A.; Muller-Wieland, D.; Ostenson, C. G. *Diabetes* **1999**, *48*, 1557-1561.

(172) Kohnke, R.; Mei, J.; Park, M.; York, D. A.; Erlanson-Albertsson, C. *Nutritional Neuroscience* **2007**, *10*, 273-278.

(173) Cnop, M. *Biochemical Society Transactions* **2008**, *36*, 348-352.

(174) Ayvaz, G.; Toruner, F. B.; Karakoc, A.; Yetkin, I.; Cakir, N.; Arslan, M. *Diabetes & Metabolism* **2002**, *28*, S7-S12.

(175) Tornheim, K. *Diabetes* **1997**, *46*, 1375-1380.

(176) Detimary, P.; Gilon, P.; Henquin, J. C. *Biochemical Journal* **1998**, *333*, 269-274.

(177) Franklin, I. K.; Wollheim, C. B. *J. Gen. Physiol.* **2004**, *123*, 185 - 190.

(178) Hayashi, M.; Yamada, H.; Uehara, S.; Morimoto, R.; Muroyama, A.; Yatsushiro, S.; Takeda, J.; Yamamoto, A.; Moriyama, Y. *J. Biol. Chem.* **2003**, *278*, 1966 - 1974.

(179) Bustamante, J.; Lobo, M. V. T.; Alonso, F. J.; Mukala, N.-T. A.; Gine, E.; Solis, J. M.; Tamarit-Rodriguez, J.; Martin del Rio, R. *Am. J. Physiol. Endocrinol. Metab.* **2001**, *281*, E1275 - E1285.

(180) Gammelsaeter, R.; Froyland, M.; Aragon, C.; Danbolt, N. C.; Fortin, D.; Storm-Mathisen, J.; Davanger, S.; Gundersen, V. *Journal of Cell Science* **2004**, *117*, 3749-3758.

(181) Vieira, E.; Salehi, A.; Gylfe, E. *Diabetologia* **2007**, *50*, 370-379.

(182) Lau, S. K.; Zaccardo, F.; Little, M.; Banks, P. *Journal of Chromatography A* **1998**, *809*, 203-210.

(183) Cellar, N. A.; Kennedy, R. T. *Lab Chip* **2006**, *6*, 1205 - 1212.

(184) Banks, P. R.; Paquette, D. M. *Bioconjugate Chemistry* **1995**, *6*, 447-458.

(185) Foote, R. S.; Khandurina, J.; Jacobson, S. C.; Ramsey, J. M. *Analytical Chemistry* **2005**, *77*, 57-63.

(186) Bliss, C. L.; McMullin, J. N.; Backhouse, C. J. *Lab on a Chip* **2007**, *7*, 1280-1287.

(187) Unger, M. A.; Chou, H. P.; Thorsen, T.; Scherer, A.; Quake, S. R. *Science* **2000**, *288*, 113-116.

(188) Burns, M. A.; Johnson, B. N.; Brahmasandra, S. N.; Handique, K.; Webster, J. R.; Krishnan, M.; Sammarco, T. S.; Man, P. M.; Jones, D.; Heldsinger, D.; Mastrangelo, C. H.; Burke, D. T. *Science* **1998**, *282*, 484-487.

(189) Pal, R.; Yang, M.; Johnson, B. N.; Srivastava, N.; Razzacki, S. Z.; Chomistek, K. J.; Heldsinger, D. C.; Haque, R. M.; Ugaz, V. M.; Thwar, P. K.; Chen, Z.; Alfano, K.; Yim, M. B.; Krishnan, M.; Fuller, A. O.; Larson, R. G.; Burke, D. T.; Burns, M. A. *Lab Chip* **2005**, *5*, 1024 - 1032.

(190) Wang, M.; Roman, G. T.; Schultz, K. N.; Jennings, C.; Kennedy, R. T. *Anal. Chem.* **2008**, *80*, 5607 - 5815.

(191) Song, H.; Bringer, M. R.; Tice, J. D.; Gerdts, C. J.; Ismagilov, R. F. *Applied Physics Letters* **2003**, *83*, 4664-4666.